Anita Zvolinschi

On exergy analysis and entropy production minimisation in indutrial ecology

Doctoral thesis
for the degree of doktor engeniør

Trondheim, September 2006

Norwegian University of Science and Technology
Faculty of Natural Sciences and Technology
Department of Chemistry

NTNU
Innovation and Creativity

NTNU
Norwegian University of Science and Technology

Doctoral thesis
for the degree of doktor enginiør

Faculty of Natural Sciences and Technology
Department of Chemistry

ISBN 82-471-8068-5 (printed version)
ISBN 82-471-8067-7 (electronic version)
ISSN 1503-8181

Doctoral theses at NTNU, 2006:151

Printed by NTNU-trykk

Preface

The main part of the work on this thesis was carried out at the Department of Chemistry and the Industrial Ecology Programme, Norwegian University of Science and Technology (NTNU), Trondheim, Norway, within the "Industrial Ecology in the Energy-Intensive Industry" project. The inventory data acquisition (Chapter 4) and experimental work for measuring the paper sheet temperatures and moistures (Chapter 5) were carried out at Norske Skog's mill, at Skogn located about 80 km from Trondheim in central Norway.

When this work begun, there were several ideas available in literature about how the engineering thermodynamics, in particular, the exergy concept, should be applied into the field of industrial ecology. And, there were few ideas about how the irreversible thermodynamics, in particular, entropy production calculation and minimisation, should be introduced in this field. Therefore, this thesis originated from the well-known need to understand and increase the efficiency of (energy-intensive) industrial processes. Thermodynamics seemed indispensable to find one's solution in a multitude of resource and process alternatives. The emergence for sustainability developed this thesis towards factors other than efficiency in order to deal with the concept of sustainability.

Acknowledgements

First I wish to express my appreciation to Professor Signe Kjelstrup from Department of Chemistry, NTNU, for her painstaking efforts to convince me that I should trust my work and insight to write this thesis. I thank her for the constructive research suggestions and her never-ending support.

I acknowledge Professor Helge Brattebø from the NTNU's Industrial Ecology Programme for encouraging me to apply exergy analysis to a (partial) product life cycle. I thank him for the insight into life cycle analysis and system think-

ing. My interest in sustainability was triggered by Professor Hedzer van der Kooi, who introduced me into aspects of exergy-based indicators in sustainable development. I express my gratitude to him. The invaluable answers given by Professor Olav Bolland, Professor Ivar S. Ertesvåg, and Dr Göran Wall, helped me to the exergy analysis of power plants and the paper production mill. I thank them for providing me with their expertise on exergy analysis.

My colleagues from the Department of Chemistry and Industrial Ecology Programme provided me with a lot of professional assistance during the thesis work. Special thanks are given to Dr Eivind Johannessen, who allowed me to share his research experience on the state of minimum entropy production. Using Latex would not be possible without his help. I also thank Dr Lars Nummedal, Dr Audun Røsjorde and Einar Ryeng for their help with technical computing problems, and to Terje Bruvoll for his help with practical problems. I am grateful to Alfred Holmberg for his assistance during my technical visits to the Norske Skog ASA, at Skogn. I also acknowledge the assistance from Stewart Clark, NTNU for editing this thesis.

Finally, I wish to express my gratitude to my supportive and tolerant family. Their encouragement has been constant throughout my career. I thank them for their help and understanding during the time this thesis work was being done. I wish to dedicate this thesis to my son, Vasile Ioan.

21 August 2006, Trondheim *Anita Zvolinschi*

Summary

The objective of this thesis is to improve the basis for applying industrial ecology to the evaluation of material and energy resource use and transformation in industrial systems. The underlying hypothesis was that when the second law of thermodynamics is applied it improves the basis for using industrial ecology for the evaluation of the use and transformation of resources in industrial systems. Exergy analysis and entropy production calculation and minimisation of industrial processes are used as methods for analysis. Chapter 1 presents an introduction to the thesis, and describes why and how the second law of thermodynamics can be applied in industrial ecology. The status of the evaluation methods for resource use in industrial ecology is also reviewed. Chapter 2 gives a brief pedagogical introduction to the exergy analysis method, presenting its advantages and limitations. Several examples are illustrated in order to show how exergy analysis can be used. The following exergy indicators are introduced: exergy renewability (α), exergy efficiency (ϵ) and environmental compatibility (ζ).

In Chapter 3, the exergy indicators are applied to answer whether to build a natural gas-fired or hydrogen-fired combined cycle power plant to meet increased future needs for electricity in Norway. The results show that the two power plants with different degrees of CO_2 emission abatement are equivalent judged by their exergy renewability and environmental compatibility, but not judged by their exergy efficiencies. The exergy efficiency indicator favours the construction of the natural gas-fired combined cycle power plant in combination with CO_2 sequestration in a depleted gas reservoir.

In Chapter 4, the exergy indicators are determined to evaluate the resource use in a paper production and recycling system within three different wastepaper management scenarios. In addition, several indicators based on life cycle inventory analysis are calculated to evaluate the environmental performance

of the system. Two boundaries are set for the system to find what effect the change of the system boundary has on the indicators. In almost all cases, the exergy and life cycle inventory indicators favoured the system within the scenario with a high degree of wastepaper recycling.

Following the exergy loss distribution in the paper production chain analysed in Chapter 4, it was identified that the paper drying process is one of the most exergy-intensive process in that chain. Therefore, in Chapter 5, an industrial-scale Valmet paper drying machine is characterised and optimised by its actual and minimum entropy production rate. It is shown that the second law optimal operation path of the drying machine is very near to the actual operation path when only the steam temperatures are varied. When the inlet air humidity is increased we found that the total entropy production rate can be reduced by up to 35% compared to the reference system.

Given that many of single-process units can be characterised by the entropy production rate, the thesis proposes an indicator in Chapter 6 that enables industrial ecology to find how far a single-process unit in operation is from the state of minimum entropy production. The indicator is termed the process maturity indicator (π), and is calculated as the ratio between minimum entropy production and the actual entropy production of a single process unit. This indicator is suggested for use as a tool for industrial ecology because it gives a realistic limit for the improvement potential of resource use in industrial processes. The following industrial units were analysed by π: a co- and counter-current heat exchanger, two alternatives of SO_2 oxidation reactor, a distillation column and the paper drying machine from Chapter 5. It was found that the chemical reactors have the largest potential to be improved compared to the other process units discussed.

Nomenclature

List of abbreviations:

AC	air compressor
ADP	abiotic depletion potential
adt	air-dried tonne
ATR	auto-thermal reformer
BHP	boiler house plant
BOD	biological oxygen demand
BHP	boiler house plant
CHE	cross heat exchanger
COD	chemical oxygen demand
DIP	de-inking plant
EA	exergy analysis
FC	fuel compressor
FE	fuel expander
HE	heat exchanger
HTS	high-temperature shift-reactor
GDP	Gross Domestic Product
GT	gas turbine
LCA	life-cycle analysis
LCA	life-cycle inventory
LTS	low-temperature shift-reactor
MEA	mono-ethanol amine
MW	molecular weight
MWTP	municipal waste treatment plant
NGCCPP	natural gas-fired combined cycle power plant
N_t	total nitrogen
PMP	paper making plant
PRE	pre-reformer
P_t	total phosphorus

ST	steam turbine
T	transportation
TMP	thermo-mechanical pulping plant
W	woodyard
WPTP	waste paper treatment plant
WWTP	waste water treatment plant

List of Latin symbols:

A	area of transfer, [m^2]
b	width of paper sheet, [m]
B	basis weight of paper, [kg/ m^2]
c_i	mass composition of component i, [-]
C_p	specific heat capacity at constant pressure, [J/ kg K]
D_{cyl}	diameter of drying cylinders, [m]
E	exergy, [J]
$\Delta_{\mathrm{r}}G$	reaction Gibbs energy, [J/ mol]
h	overall heat transfer coefficient, [W/ m^2 K]
H	enthalpy, [J]
$\Delta_{\mathrm{vap}}H$	vaporisation enthalpy of the free water, [J/ kg]
$\Delta_{\mathrm{sor}}H$	sorption enthalpy of the water to paper, [J/ kg]
l	length of the paper sheet between two cylinders, [m]
L	total length of paper sheet in paper drying machine, [m]
L_{ij}	phenomenological coefficient for coupling of fluxes i and j
J	flux of the evaporated water, [kg/ m^2 s]
J_q	flux of total heat, [W/ m^2]
J_i	flux of component i, [mol/ m^2 s]
J_s	flux of entropy, [J/ m^2 K s]
m	mass flow rate, [kg/ s]
$M_{\mathrm{H_2O}}$	molecular weight of water, [kg/ mol]
n	factor in Eqs. (5.1), (5.2), (5.5), and (5.9)
p	pressure of the system, [bar]
$p^{\ominus}$	standard pressure, [bar]
p^*	equilibrium vapour pressure, [bar]
p^*_{p}	equilibrium vapour pressure over paper, [bar]
Pr	Prandtl number, [-]
R	gas constant, [J/ mol K]
Re	Reynolds number, [-]
Q	heat delivered to the system, [J]
S	entropy of the system, [J/ K]

$\left(\frac{dS}{dt}\right)_{\text{irr}}$	total entropy production rate, [W/ K]
$\Delta_{\text{vap}}S$	vaporisation entropy of the free water, [J/ kg K]
$\Delta_{\text{sor}}S$	sorption entropy of the water to paper, [J/ kg K]
T	temperature, [K] or [^{0}C]
U	internal energy, [J]
v	travelling speed of paper through the paper drying machine, [m/ s]
V	volume, [m^3]
W	work done on the system, [J]
x_i	molar composition of component i, [-]
X_i	thermodynamic driving force i
$X_{\text{in,air}}$	inlet air humidity, [kg H_2O/ kg dry air]
X^*	saturation humidity of air above the paper sheet, [kg H_2O/ kg dry air]
w	moisture content of paper, [kg H_2O/ kg dry paper]

List of Greek symbols:

α	exergy renewability indicator , [-]
β_1, β_2	coefficients in Eqs. (D-5) and (D-6)
ϵ	exergy efficiency indicator, [-]
ζ	environmental compatibility indicator, [-]
Θ	desorption isotherm in Eqs. (D-3) and (D-4)
κ	thermal conductivity, [W/ m K]
μ	dynamic viscosity, [kg/ m s]
ν	kinematic viscosity, [m^2/ s]
π	process maturity indicator, [-]
σ	local entropy production rate, [W/ m K]
ω	paper sheet wrap angle on cylinder, [^{o}]

Subscripts and superscripts:

cyl	cylinder
in	input
out	output
p	paper

List of Figures

List of Tables

Contents

Chapter 1

Introduction

1.1 Motivation

Not long ago, humankind has started to foresee and recognise that further uncontrolled growth of the population and its economy will threaten the environment for people, as well as for other species on Earth. The environment with its ozone layer protection, global carbon-oxygen cycle, biodiversity, and natural resources reservoirs is irreversibly damaged by one of the most influential economic activities, industry. Georgescu-Roegen (1971, 1976) pointed out that the entire economy is a large converter of an enormous quantity of low-entropy materials (fossil fuels, metal ores) into high-entropy materials (waste). The change of entropy is dictated by the second law of thermodynamics, which also gives us the direction of the change. Consequently, the quality and not the quantity of natural resources is depleted or lost. The second law of thermodynamics can realistically determine the magnitude, type, and location of the quality losses that result from the use and transformation of natural resources. Aside from the drastic measure to slow population growth and the economic growth by force, the most effective way to reduce these losses is to use and transform resources more efficiently.

Both quality and quantity of resources are needed for development, and a sustainable development requires their secure supply at reasonable cost and with minimal negative impacts. In 1987, the World Commission on Environment and Development (the Brundtland Commission) was the first that launched the meaning of sustainable development. Sustainable development was defined as the "development that meets the needs of the present without compromising

the ability of future generations to meet their own needs" (Brundtland 1990). The Commission noted that its definition contains two key components: *needs* and *limitations*. On the limitations component of sustainable development, OECD (1996) proposed that:

1. "The rates of use of renewable resources should not exceed their rates of regeneration";

2. "The rates of use of non-renewable resources should not exceed the rates at which renewable substitutes are developed"; and

3. "The rates of pollutant emissions should not exceed the corresponding assimilative capacity of the environment".

A secure supply of resources is generally agreed to be a necessary but not sufficient requirement for sustainable development. Furthermore, sustainable development has to follow sustainable paths of resource use and transformations, like those imposed by the three constrains mentioned by OECD (1996). A greater resource transformation efficiency allows such resources to contribute to development for a longer period of time. Even for resources that may eventually become inexpensive and widely available, an increase of this efficiency is likely to remain a sought solution to reduce the resource needs. Both simple and complex systems are then efficiently designed to harvest and transform resources, and abate the associated environmental impacts.

Learning about the paths of resource use and about the levers for lightening the impact of resource use and transformation on the environment is one role of industrial ecology. The term "industrial ecology" was proposed for the first time by Frosch and Gallopoulos (1989) in a paper published in September 1989 in *Scientific American*. Frosch and Gallopoulos (1989) embraced in their paper the concept of "industrial metabolism" which Ayres (1989) has developed to organise thinking about the massive, systematic transformation of material resources in economies. Following guidelines proposed by Frosch and Gallopoulos (1989) and Ayres (1989), industrial ecology takes a system view in developing strategies to facilitate more efficient use of materials and energy and to reduce the release of wastes to the environment. The ultimate objective of the field is the emergence of an economy that cycles all of materials that it uses, emitting

only few amounts of waste, while providing high quality services to the large population already here and still likely to grow.

The motivation for the thesis comes from the need where industrial ecology confronted with real problems can evaluate the use and transformation of resources in complex systems (e.g. a national economy or a firm) as well as in simple systems (e.g. an industrial plant or a single process unit). The systems studied in this thesis are of the latter types. An energy policy question relevant to Norway and a wastepaper recycling problem relevant to a pulp and paper mill and to solid waste planners from Trondheim city will be analysed. Instead of moving towards higher levels of organisation in the economy, the thesis applies industrial ecology towards single process units (i.e. a paper drying machine, single heat exchangers, distillation columns, chemical reactors). This may be unexpected, since industrial ecology mostly deals with higher levels than this. However, using this approach, the thesis will give a solution to the above-mentioned need. An entropy production minimisation method will be demonstrated to obtain optimal resource transformation of industrial processes from the perspective of the second law of thermodynamics.

An energy policy question in Norway: The case of two gas-fired combined cycle power plants

Energy policy in Norway continues to be an important subject of domestic political discussion with international consequences. Norway's fossil resource reservoirs contribute significantly to Europe's security of supply of energy resources. The energy sector in Norway is unique in Europe. Norway represents 1% of the population of Europe, and it has 75% of the oil resources, 45% of the natural gas resources and 30% of the hydropower resources (Statistics Norway 2003). Norway has also extensive access to own renewable resources so that which provides Norwegian society with hydropower. This covers almost 99% of the domestic electricity demand (considering that the electricity demand for pumping water back to the water reservoir is exclusively produced from renewable resources). Other renewable resources remain at a very low level, but account for an adjusted 5% of total energy supply.

Electricity is a major component of domestic primary energy supply, meeting as much as 45% of the domestic final energy demand. After a drop in the electricity demand in 2003 due to a significant increase in prices, the demand rose again in 2004 - by 6.5% to 110 TWh (Statistics Norway 2003). The highest rates of increase have been in the service and residential sectors. Though

industry accounted for 43% of national electricity demand in 2003, its rate of growth has been slower than in the service and residential sectors. The use of electricity in the energy-intensive industries accounts for about 24% of national electricity use in 2004 (Statistics Norway 2004).

Thus, Norway is now facing important challenges because it has the World's most intensive electricity demand per capita. In 2004, the net figure was 31.2 MWh electricity per capita (Statistics Norway 2004), and this figure is expected to grow. The electricity demand growth is outpacing onshore electricity generation, and CO_2 emissions are thus rising. Consequently, natural gas-fired power plants are seem to be the most appropriate way of increasing the domestic electric-power supply. This decision is supported by the huge national natural gas reserves, the relatively low impact on the environment if we ignore global warming, and the limited possibility to extend hydropower capacity.

Meeting its Kyoto target without compromising security of supply is however Norway's biggest energy policy challenge. This challenge is addressed in Chapter 3, which is a comprehensive study of two different gas-fired combined cycle power plants with two different options for abatement of CO_2 emissions. The options are the CO_2 sequestration and the CO_2 to methane conversion by means of photosynthetically fixation of carbon in biomass. A specific answer to a policy question of which type of power plant to be built in Norway is given from the perspective of the second law of thermodynamics, using exergy analysis and exergy-based indicators. The aim is to demonstrate that if industrial ecology adopts the exergy-based indicators it has the ability to aggregate the technical details of, for example, the two power plants, and communicate these details to politicians in their debate about which type of power plant to construct.

A wastepaper recycling problem: The case of a Norwegian pulp and paper mill

The pulp and paper industry is the fifth largest user of electricity and thermal energy in the World. In Norway, this industry is the third largest industrial electricity user after the basic metals industry and the petroleum and chemicals industry. This categorises the pulp and paper industry as an exergy-intensive one, which makes it an interesting case study for industrial ecology.

Here a parenthesis is given concerning the definition of the performance criteria that is called efficiency. When characterising a system as an energy-intensive

one, this first asks for a definition of efficiency; and then for a threshold over which that system is energy intensive according to the definition used. Efficiency is a key concept to assess the performance of a system at any level of organisation. It relates the effect obtained, or output, to the effect supplied, or input. The lack of a unified scientifically-based approach to the selection of values of a system's inputs and outputs leads to different treatments depending on the level of interest. For example, at a national economy level, efficiency has been defined as the ratio of energy "consumption" to GDP. At a down-scaled level, for instance at an individual industrial sector, energy efficiency has been defined as the ratio of energy "consumption" to gross output.

A proper definition of efficiency is relevant to industrial ecology in stimulating discussions on energy "consumption" and energy "savings", which in colloquial usage means exergy consumption and exergy savings, respectively. Decreasing exergy consumption and increasing exergy savings require first an accounting method for the (material and energy) inputs and outputs, and then a thorough determination of the efficiency of transformation of the inputs into the outputs (see Section 1.2 for further discussion). The case of the pulp and paper industry is discussed in the following.

Electricity and thermal energy demands for production of a square kilometre of different paper grades is usually presented in literature to characterise the performance of resource use in the pulp and paper industry. Figures 1.1 and 1.2 show the demand for electricity and thermal energy for different paper grades over a period of twenty five years. These figures can be used to characterise the industry, but cannot be used to understand and determine the specific reasons behind the exergy savings. The exergy consumption/savings mechanism is a feedback process, which is as much as a driver of economic growth as a consequence of economic growth (Ayres et al. 2002). Therefore, it is also important to know the potential for growth in a particular industry. The growth potential is commonly presented as a trend of annual use of a particular product. Figure 1.3 shows such a trend for paper and pulp use in the World and in different geographic regions.

Industrial ecology looks for a systematic way to deal with the exergy consumption and savings in industry because it is interested to build an interrelation between an efficient use of resources and a good environmental performance in industrial systems. Finding the way requires a thermodynamic approach, which enables us to properly and completely evaluate the use and transformation of resources in industrial systems. Given this background, Chapter 4

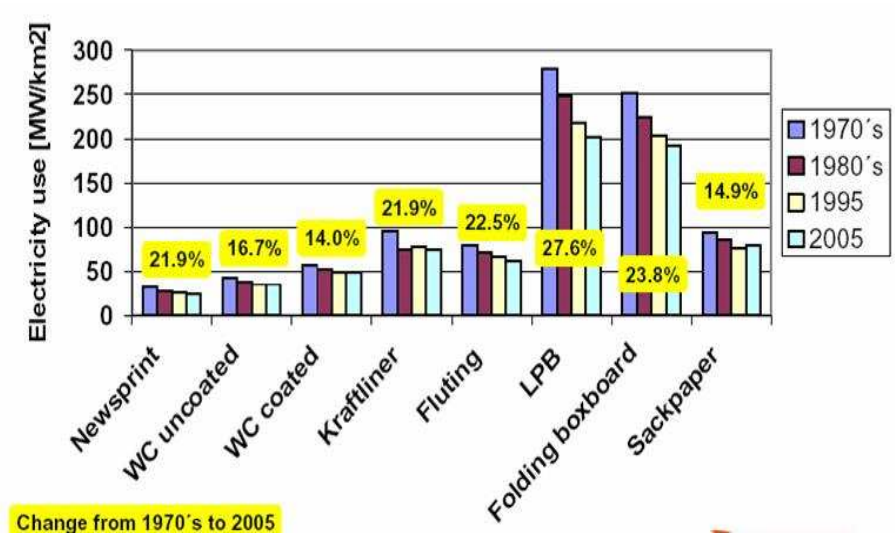

Figure 1.1. Electricity demand for the production of different paper grades. LPB = liquid packing board. (Source: Metso Corporation (2000)).

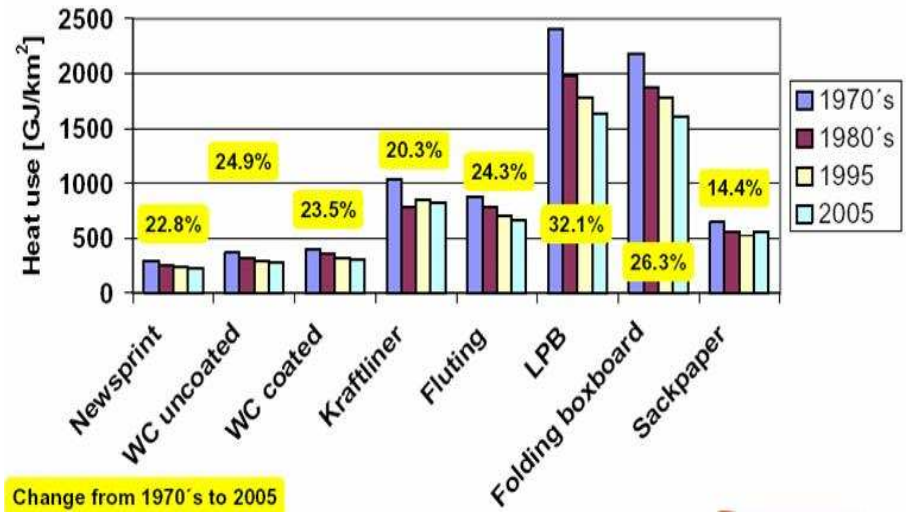

Figure 1.2. Thermal energy demand for the production of different paper grades. LPB = liquid packing board. (Source: Metso Corporation (2000)).

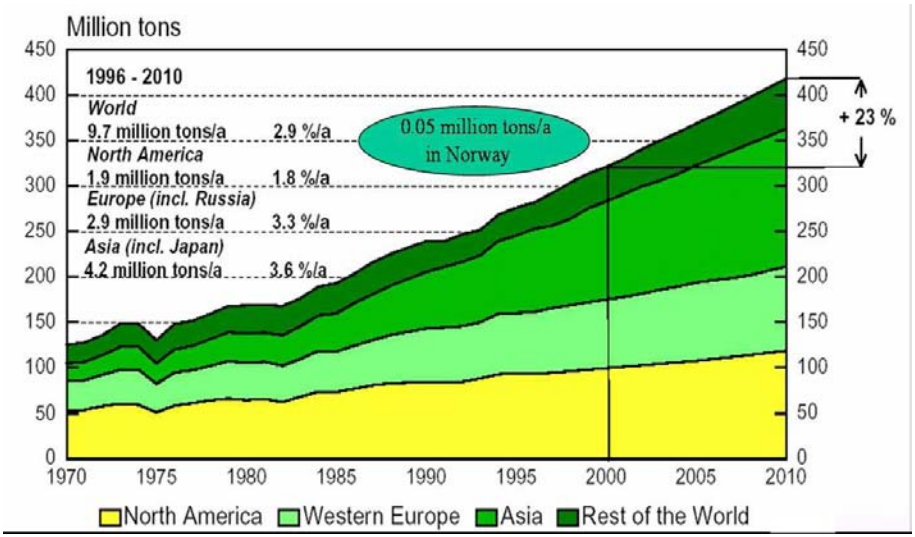

Figure 1.3. Trends of paper and board use in the World and different geographic regions. (Source: Metso Corporation (2000)).

presents an evaluation of the resource use performance and the environmental performance of a paper production and recycling system in Norway. Exergy analysis and life cycle inventory analysis are applied to find the answer to the following question: What is the best degree of paper recycling in relation to a specific pulp and paper production mill?

Earlier work on the entropy production minimisation at NTNU

Chapters 5 and 6 are a continuation of the work done on entropy production minimisation of single and connected process units by the group of Professor Signe Kjelstrup and her co-workers at the NTNU's Department of Chemistry in the last ten years. The research efforts done on the entropy production minimisation problem ought to be brought to industrial ecology, because the state of minimum entropy production might be seen as the most sustainable state of operating industrial processes. This state can be found by means of the irreversible thermodynamics.

Several outcomes have been asserted by this group. The first was the equipartition of the driving forces theorem (Sauar et al. 1996, 1997). This theorem was used as a design criteria for heat exchangers (Nummedal and Kjelstrup 2001), chemical reactors (Sauar et al. 1997, Kjelstrup et al. 1999, 2000, Røsjorde et

al. 2005a), and diabatic distillation columns (Sauar et al. 2001). The second result was the application of the theorem of equipartition of entropy production in chemical reactors (Kjelstrup and Island 1999, de Koeijer et al. 2004a, Johannessen and Kjelstrup 2004, 2005, Nummedal et al. 2005) and distillation columns (de Koeijer et al. 2004b, Røsjorde et al. 2005b). This theorem was first proved by Tondeur and Kvaalen (1987), who also proposed it as a design criterion in single process units. The third outcome was the discovery of a highway in state space for reactors with minimum entropy production (Johannessen and Kjelstrup 2005). The work showed that there is a collection of solutions for the entropy production minimisation problem in a reactor, and this collection looks like a highway with its connecting roads. The highway has been proved to be an energy-efficient way in order to operate the reactor in its state space (Johannessen and Kjelstrup 2005). This work gave several explanations why the highway is in agreement with the state-of-the-art operating conditions practised by chemical process engineers today in the following chemical reactors: sulphur dioxide oxidation, ammonia synthesis, methanol synthesis, propane dehydrogenation, and tubular steam reforming.

Entropy production minimisation in connected process units was the last outcome of the group. Røsjorde et al. (2005a) found the second-law optimal operating conditions of a propane dehydrogenation plant of twenty-six connected process units. These conditions gave the lowest total entropy production and the highest exergy efficiency of the whole plant.

Although this is very important, this thesis does not use the approach of the entropy production minimisation of connected process units. Instead, it uses the group's research efforts on the entropy production minimisation of single process units in order to define an indicator for industrial ecology. Because there is a little experience with the formulation, calculation and minimisation of entropy production in industrial ecology, Chapter 5 gives an example how to formulate, calculate and minimise the entropy production in an industrial paper drying machine. Then, Chapter 6 makes use of this insight to introduce and apply a new indicator to industrial ecology. The evaluation of the full range of implications that the application of this indicator may have at a process chain, a whole plant, or an industrial sector, is not yet defined in this thesis.

1.2 Why and how can we apply the second law of thermodynamics to industrial ecology?

White (1994) defined industrial ecology as a "study of the flows of material and energy in industrial and consumer activities, of the effects of these flows on the environment, and of the influence of economic, political, regulatory and social factors on the flows, use and transformation of resources". Graedel and Allenby (2003) proposed that all waste materials have to be seen as potential nutrients, and all industrial activities have to optimize their overall efficiency, and ultimately to eliminate all waste. This suggestion is an extension of what Ayres (1989) called *industrial metabolism* and characterised as "the energy-and-value-yielding process essential to economic development" (Ayres 1996).

Four areas of interest related to the use and transformation of resources and to the study of material and energy flows have been identified in industrial ecology. These ares are exergy accounting, analysis, measurement and optimisation.

In the area of accounting, the industrial ecology is concerned with comparing and accounting all kinds of resource stocks and flows for the purpose of resource availability and loss accounting. It also compares and accounts all kinds of production and consumption material wastes that are disposed into the environment for the purpose of measuring the environmental harm potential of these material wastes and of those processes that generate these wastes.

The first notion was proposed by Wall (1977, 1986). In his thesis he proposed exergy as an accounting measure of resource stocks and flows because exergy is definable and measurable for any material resource stock and flow whatsoever (contrary to the heat of combustion that is a measure of combustible materials only). Wall's proposal was based on the measure introduced in the 18th century by French academicians (Carnot, Navier, Poncelet). This measure was called *énergie utilisable* by French academicians, *availability* by American scientists and *exergy* by researchers in Europe.

The general definition of exergy is a quantity of work which can be extracted by an external consumer during a reversible interaction between a system and its surroundings until equilibrium is reached. Exergy depends on the relative states of a system and its surroundings, as defined by any relevant set of parameters. Under complete equilibrium, exergy is zero. According to this definition of exergy the problem considered includes first, the system or its material and energy input and output flows, then, the surroundings, and finally, the work transferred to the external consumer.

The latter notion, suggested more recently by Ayres et al. (1998), Rosen and Dincer (1999), regards exergy as a measure of potential harm from production and consumption material wastes which are disposed into the environment. The idea emerged from the fact that the chemical exergy in form of chemically and physically reactive material wastes (or external exergy losses) can be seen as a measure of potential environmental harm. This exergy is dissipated into the environment, and through its chemical potential can cause harm to the environment and living cells. Seager and Theis (2002a,b) illustrated several applications of chemical exergy as an alternative to industrial ecology to evaluate and assess the pollution potential of material wastes.

However, Ayres and Masini (2004) argued that if exergy is to be used as a measure of potential environmental harm the definition of the reference states that was proposed by Szargut et al. (1988) to compute the standard chemical exergy of any chemical compound should be replaced. The arguments enumerated by Ayres and Masini (2004) were that the definition of the reference states should be dependent on the environmental sink into which a chemical compound is disposed or released and they should be dependent on what specific reactions occur within that sink. Ayres and Masini (2004) proposed that the sink-specific reference species should be used instead of the standard reference species proposed by Szargut et al. (1988). A chemical substance with a long residence time in the atmosphere, lithosphere or hydrosphere may be a candidate for treatment as a sink-specific reference species. However, for the purpose of estimating the chemical exergy of chemical compounds in this thesis, the calculation approach given by Szargut et al. (1988) will be used.

In the area of analysis, industrial ecology is concerned with using methods to analyse any kind of material and energy resource and flow transformation in industrial systems. The second law of thermodynamics is fundamental since its exergy measure is connected to the correct accounting of the various kinds of material and energy flows and the correct analysis of their transformations, without exception (Rant 1956, Marchal 1956, Fratzcher 1962, Szargut and Petela 1965, Brodyansky 1973, Ahern 1980, Kenney 1984, Kotas 1985, Szargut et al. 1988). The exergy analysis method was developed to determine the exergy losses and the potential of reducing these losses in engineering systems. The total exergy loss (E_{loss}) can be found by subtracting the sum of all exergy flows coming into the system, E_{in}, from the sum of all exergy flows coming out from the system, E_{out}. The calculation of E_{in}, E_{out} and E_{loss} is referred to as

exergy analysis, and Eq. (1.1) gives the relation for the exergy balance.

$$\underbrace{E_{in} - E_{out} = E_{loss}}_{\text{Exergy balance}} \tag{1.1}$$

The exergy loss of a system can be found without making up an exergy balance if corresponding total entropy production is available. The Gouy-Stodola's theorem is useful here (Gouy 1889, Stodola 1898). The theorem is expressed as

$$\underbrace{E_{loss} = T_0 \left(\frac{dS}{dt}\right)_{irr} \Delta t}_{\text{Gouy-Stodola theorem}} \tag{1.2}$$

where E_{loss} is the exergy loss in the system, T_0 is the environment temperature ($T_0 = 298$ K), and $(dS/dt)_{irr}$ is the total entropy production rate as a result of the irreversibility of the processes that occur in the system over a given interval of time Δt.

There are two kinds of exergy losses in a system, namely the external and internal exergy losses. External exergy losses are related to the relative conditions of the system and its surroundings (i.e. non-ideal heat insulation, unused exergy that leaves a plant such as emissions in flue gases or emissions in water effluents, outflow cooling water, nitrogen in air-separation plants). The sum of external exergy losses over all units of the system is the total external exergy loss of that system.

Internal exergy losses are due to the irreversibility of processes taking place inside the system due to pressure drop, heat and mass transfer and transport. These losses are mainly related to the imperfections of the material and energy transformations in each individual unit of the system and the manner in which these units are integrated into the system. The sum of internal exergy losses over all units of the system is the total internal exergy loss of that system.

The distribution of the internal exergy losses over the units of the system can be obtained from the exergy analysis at the boundary of each unit, considered as a black box. The distribution of the internal exergy losses in each black box unit can be obtained from the entropy balance (the first equality of Eq. (1.3)) or from the integral of local entropy production rate over the volume V (the last equality of Eq. (1.3)), if a control surface is put in the appropriate place.

$$\underbrace{\left(\frac{dS}{dt}\right)_{irr} = A(J_s^{out} - J_s^{in})}_{\text{Entropy balance}} = \int_V \sigma dV > 0 \tag{1.3}$$

Here, $(dS/dt)_{irr}$ is the total entropy production rate of the system, J_s^{out} is the entropy flux out of the volume V of the system, J_s^{in} is the entropy flux into the volume V of the system, σ is the local entropy production rate, A is the surface area through which the fluxes enter and leave the volume V.

Irreversible thermodynamics offers a systematic way to derive the local entropy production rate, σ. This is referred to as the local entropy production calculation (Førland et al. 2001):

$$\underbrace{\sigma = \sum_{i=1}^{n} J_i X_i}_{\text{Local entropy production calculation}} \tag{1.4}$$

where J_i and X_i are conjugate flux-force pairs. Irreversible thermodynamics gives that each flux is a linear function of all forces, or in formula form:

$$J_i = \sum_{j=1}^{n} L_{ij} X_j \text{ where } i = 1, 2, ..., n \tag{1.5}$$

where L_{ij} are the phenomenological coefficients, and X_j are the thermodynamic driving forces of the system. Onsager prescribed that each flux is connected to its conjugate force via the phenomenological coefficients that are related by the following relation (Onsager 1931a,b):

$$L_{ij} = L_{ji} \text{ where } i, j = 1, 2, ..., n \tag{1.6}$$

It is important to know that the linear flux-force relations in Eq. (1.5) are local and pose few restrictions on their use. The phenomenological coefficients L_{ij} can be functions of the state variables and the global flux-force relations are therefore often non-linear. For this reason, irreversible thermodynamics theory today is a versatile theory that applies to many practical problems (Hafskjold

and Ratkje 1995, Røsjorde et al. 2000, Kjelstrup and Bedeaux 2001, Reguera and Rubi 2001, Vilar and Rubi 2001, Røsjorde et al. 2001).

The exergy balance, the entropy balance, and the integral of the local entropy production over the volume V can be calculated independently, and must give the same answer for the total entropy production rate of the system. Each of these methods has its own advantages and range of applicability. For example, it is possible to check the consistency of the mathematical models that are used to model and simulate processes of a single process unit. This is done by checking if the local entropy production rate is positive in all points of that unit.

It is thus possible to obtain the complete quantitative characteristics of exergy losses in a system. These losses are connected with the internal and external conditions of the system. Next to the locations where exergy losses occur, the reasons why they occur can be classified. This information is very important in all conception, design and operation stages of the system. According to Brodyansky et al. (1994), 40% of the exergy losses in a system can be attributed to the stage of process conception, and 40% to the engineering design stage. Thus, about 80% of the exergy losses in a system at the operating stage are not likely to be reduced.

To summarise, the main objectives of exergy analysis are:

1. To determine the possibility of realising a new process or designing a new system of any complexity without determination of the distribution of internal exergy losses. Such a determination is possible through the exergy balance at the boundary of the process or system and the subsequent determination of total exergy loss and of exergy efficiency.

2. To determine the exergy losses and the exergy efficiencies of all units of a system in operation. To determine the possibilities for increasing the exergy efficiency of the system as a whole by means of increasing the exergy efficiencies of the units in a system. To determine which units of the system are most influential on its exergy efficiency. To evaluate the limits of exergy efficiencies for the specific conditions of the units in the system.

In the area of measurement, industrial ecology is concerned with using indicators. One way to evaluate the performance of a system to transform resources

is the exergy efficiency. A fundamental role in determination of the exergy efficiency is played by the exergy losses that take place in every unit of the system. The exergy efficiency is defined as:

$$\epsilon = \frac{E_{out}}{E_{in}} = 1 - \frac{E_{loss}}{E_{in}} = 1 - \frac{T_0 \left(\frac{dS}{dt}\right)_{irr} \Delta t}{E_{out} + T_0 \left(\frac{dS}{dt}\right)_{irr} \Delta t} \tag{1.7}$$

Sorin and Brodyansky (1992) showed that the effect of exergy losses in different units of a system is unequal. The further the units are in the process chain of the system, the greater is the effect. The effect is closely related with the exergy efficiencies of the units. A change in exergy efficiency of one unit affects the consumption of exergy at the input of the entire system independently of the location of the unit in which this change occurs. A change in the exergy loss (or entropy production) of one unit differently and non-equivalently affects the total exergy efficiency of the system, with the condition that the exergy output of the system is the same.

This is the reason why an engineer should first try to decrease the exergy losses at the units located in the final stages of the process chain, and then those located in the other stages. In addition, the engineer should find the different contributions to the exergy loss or entropy production in each unit of the system. The entropy production calculation offers a systematic way to split the total entropy production rate between its different contributions (see the example of a paper drying machine in Chapter 5). As a result, the contributions due to different kinds of transport such as mass, heat and charge transport can be obtained. In such a way it is possible to quantify and localise the exergy loss due to different transport phenomena.

In addition, there is an interdependence between the structure of the system and its total exergy efficiency; the exergy efficiency decreases as the number of its units rises. In Chapters 2 and 3 it will be shown that the higher the complexity of the systems analysed (i.e. number of process units) the lower the exergy efficiency of those systems.

The exergy efficiency should be used as an indicator in industrial ecology because it has the advantage to be applicable equally well for simple systems (e.g. an industrial plant) and for complex systems (e.g. a national economy). Other indicators based on the exergy calculation can be complementarily used to indicate exergy efficiency. This thesis recommends two other exergy-based

indicators for industrial ecology, which were recently proposed in the literature (Dewulf et al. 2000). These indicators were termed by Dewulf et al. (2000) as exergy renewability and environmental compatibility.

In the area of optimisation, industrial ecology is concerned with formulating and optimising objective functions. The objective function that is proposed in this thesis is the total entropy production. The minimisation problem is formulated as

$$\underbrace{\text{Find minimum } \left(\frac{dS}{dt}\right)_{irr} = \int_V \sigma dV \quad \text{subject to given constraints.}}_{\text{Entropy production minimisation problem formulation}} \tag{1.8}$$

This entropy production minimisation problem posed in practice, where we deal with equipment of finite size which we wish to operate in finite time, can be used to answer the question which operation path has minimum internal exergy loss or minimum entropy production with given constraints.

Equation (1.7) shows that one strategy to develop exergy-efficient operation paths in industrial processes may be to reduce the total entropy production rate ($(dS/dt)_{irr}$), keeping the same exergy output (E_{out}) or the same exergy input (E_{in}) for a given environmental temperature (T_0) and a given period of time (Δt). When minimising the total entropy production rate of a system, it is then possible to distinguish between practical strategies to improve the problems related to the resource transformation of that system. Knowing the main sources of entropy production means knowing the major components of a system's irreversibility, and thus pinpoint a realistic thermodynamic improvement potential for that system to transform the resources. This potential is different than that obtained for the condition of maximum exergy efficiency, when all internal exergy losses are zero at the expense of an infinite area for the equipment and an infinite time for the processes that occur using that equipment.

It should be noted that the thermodynamic optimisation problem as defined above has conceptual limitations. These are due to the fact that entropy production minimisation deals only with the consumption and losses of exergy, whereas in practice, one must to take into account a wide variety of consumptions. Therefore, it is critical to carry out a techno-economic analysis and optimisation which involve estimates of necessary capital and social expenses,

and should lead, in the long run, to economy of natural resources. However, it is not possible to know if one can arrive at a truly techno-economic optimum without considering in addition the exergy analysis of the entire system.

In this direction, the joint application of exergy analysis and engineering economics was proposed under the name of Exergo-Economics by Schimdt (1953), Sorin and Brodyansky (1992), Brodyansky et al. (1994), Gaggioli (1980, 1983) in Europe, and under the name of Thermo-Economics by Tribus (1961), Evans (1969), El-Sayed and Aplec (1970), El-Sayed and Evans (1970) in the United States. In these two methods, the optimisation problem is similarly solved using a set of equations that combines the prices of the components of a system their operating parameters and their exergy efficiencies. The prices are not set by the unit mass, but by the specific exergy content of each material and energy stream. These methods have two advantages over the classical one (techno-economic analysis), even though it complements rather than substitutes it. The advantages of these methods are:

1. They directly reflect quality losses of all kinds of natural resources.

2. The effects of time-dependent factors (e.g. price policy) are excluded.

The development of these two methods has evolved in several directions in the last twenty five years (Moran 1982, Kotas 1985, von Spakowski et al. 1991, El-Sayed 1993, Valero et al. 1994, Sciubba 2004). For example, von Spakowski et al. (1991) proposed to extend the exergy accounting to include the environmental externalities, while Sciubba (2004) developed a method called the Extended Exergy Accounting, which takes into account labour, capital, and environmental remediation costs. Nevertheless, these methods can facilitate the incorporation of an optimisation approach in industrial ecology. However, the thesis does not make use of any of these methods. Instead, it will use a method to find minimum entropy production applying a method which has been recently proved to be a tool to achieve approachable and attainable solutions of the minimum exergy losses in the design and operation of individual process units.

1.3 The status of the evaluation tools for resource use and transformation in industrial ecology

To evaluate the performance of a systems for resource use and transformations, industrial ecology makes use of several physical methods and their associated indicators. The status of these methods and the indicators is presented in the following.

Mass-based methods have been popular to determine the physical basis of economic activity and its interaction with the ecosystem (Adriaanse et al. 1997, Matthews et al. 2000). These methods determine the mass of material flows that passes from the ecosystems to the economy and the emissions from the economy to the ecosystems. Most of the studies are at the level of the entire economy, but disaggregation to more detailed levels is being developed. For example, the Material Flow Analysis studies the use of materials in integrated industrial and consuming activities. Since mass does not capture many other properties of materials, such as their energy and exergy values, the MFA studies are limited by themselves.

Analysts at the Wuppertal Institute have developed an indicator called the *material input per service unit* (MIPS) (Bringezu et al. 1994, Schmidt-Bleek 1994, Hinterberger et al. 1994). This indicator measures the mass of resources moved from the environment for providing a unit mass of product or a unit service. Hertwich and co-workers, in their review (Hertwich et al. 1997), argued that this indicator is not a good tool for the evaluation of environmental impact associated with the resource use because each material in MIPS is not equally undesirable. For example, whether the mass throughput comes from the natural gas that fuels a power plant or the river water that cools it, the MIPS is not able to show which material is the most undesirable to generate electricity in a power plant. In addition, MIPS is not sufficient to evaluate the resource use because it does not take into account any energy resource transformation.

Energy-based methods such as net energy analysis and fuel cycle analysis determine the flow of energy through various economic activities (Hannon 1973, Constanza and Herendeen 1984, Spreng 1988). These methods consider the energy content of industrial inputs from ecosystems and industrial outputs from the economy. Klüppel et al. (1997) proposed the *cumulative energy demand* (CED) indicator based on the net energy analysis. This indicator measures in Joules the demand of primary energy for production of a mass unit of product

or a unit of service. It includes the energy requirements for transport, and the feedstock energy (i.e. the primary energy demand for the materials produced from oil, coal or wood) (Klöpffer 1997, Frischknech 1997, Frischknech et al. 1998). To account for all energy demands, Klöpffer (1997) proposed to use the calorific values or the *lower heating values* (LHVs) of all kinds of energy resources. Like mass, energy also does not capture the contribution of non-calorific materials, and ignores the second law of thermodynamics.

The *abiotic depletion potential* (ADP) is used in the standard LCA method to assess the impact of resource use of a product life cycle. According to Guinee and his colleagues (Guinee et al. 2002), the ADP is a measure of the decrease of the availability of abiotic resources in the natural environment. The method presented by Guinee et al. (2002) requires the division of ADP in two categories, one for materials such as ores and minerals, and one for fossil fuels such as oil, natural gas and coal. As described in the method for the calculation of abiotic depletion of resources two problems are defined, resulting in two different end-points: the loss of the availability of natural elements and the loss of the availability of fossil fuels. To find the amount of the loss of availability of fossil fuels, the lower heating values of fossil fuels are used. However, there are different alternatives to use same fossil resources. In the example of burning of a fossil resource, the exergy content of burnt fuel is lost entirely. The depletion of fossil fuels will also increase in the case of non-calorific use of fossil fuels, for example, in the production of plastics. The formula used to calculate the ADP gives the same value of ADP in both the burning and non-calorific use of the same fossil fuel, see Guinee et al. (2002). As stated by Cornelissen (1997) in his thesis, this fact makes the ADP indicator inappropriate as a measure for the evaluation of resource use and transformation.

Exergy-based methods take into account the first and second laws of thermodynamics, and they capture an array of material and energy flows under the same unit, Joule. These methods have long been use to determine the thermodynamic efficiency of industrial processes (Fratzscher 1961, Bosnjakovic 1965, Brodyansky 1973, Szargut et al. 1988, Kotas 1980, Fitzmorris and Mah 1980, Kotas 1985), to analyse the behaviour of ecosystems (Jorgensen 1997), and to account for all ecological products and services in the joint economic and ecological system as a single network of material and energy flows (Hau and Bakshi 2004, Ukidwe and Bakshi 2004, Yi et al. 2004). Various extensions of exergy analysis such as Industrial Cumulative Exergy Consumption Analysis (Szargut et al. 1988), Exergetic Life Cycle Analysis (Cornelissen 1997) and Life Cycle Exergy Analysis (Gong and Wall 2001) were developed to evaluate the

performance of industrial systems to use and transform resources.

The Industrial Cumulative Exergy Consumption method determines the cumulative exergy consumption of industrial production processes and chains. Szargut et al. (1988) proposed the *cumulative exergy consumption* as an indicator for resource depletion in industrial processes. This indicator aggregates all exergy requirements for the production of a specific unit product. However, this indicator does not take into account the exergy losses associated with the disposal of the product or the influence of recycling or reuse of products. Dewulf and Langenhove (2003) claimed a solution to this problem, and developed an indicator that was called the *exergetic material input per unit service*. This indicator takes into account the exergy requirements associated with the disposal and recycling of materials. In other work, these authors have integrated several industrial ecology principles into a set of indicators for environment assessment of technology (Dewulf and Langenhove 2005).

Sciubba (2004) proposed the Extended Exergy Accounting method to determine the cumulative exergy consumption associated with not only the material and energy inputs but also with the labour and capital inputs of non-exergetic externalities (Sciubba 2004).

The Exergetic Life Cycle Analysis and Life Cycle Exergy Analysis were elaborated for different purposes. The purpose of the first method is to incorporate the exergy concept in the standard LCA. This is why all the steps in LCA are the same as the steps in Exergetic LCA. The inventory step in the Exergetic LCA is more extensive than that of the standard LCA method, because it requires a complete flow-sheet of the mass and energy flows of all production steps. The impact assessment step consists of the calculation of the exergy of the flows and the determination of the exergy losses in all production steps. There is no classification step. The final result of this method is the sum of all exergy losses, which is defined as the life-cycle irreversibility.

The purpose of the Life Cycle Exergy Analysis method is to evaluate and measure the conditions of sustainability in the design phase of engineering systems (Gong and Wall 2001). This condition is characterised by the use of exergy resources in such a way that the input of exergy will be paid back during the life time of the system, and the used deposits must be completely restored.

To solve the imperfections provided by mass and energy as measures for the evaluation of material and energy resource use and transformation, Ayres et

al. (1998) and Finnveden (1994) independently proposed exergy as a better measure for resource use and depletion in the LCA method. Finnveden (1994), and later Finnveden and Östlund (1997), suggested a thermodynamic approach in which the use of material and energy resources in LCA are to be described as either consumption of exergy or production of entropy. Entropy production has also been considered as a measure of environmental pollution (Ayres and Martinas 1995), and as an ecosystem disturbance (Faber et al. 1995, Glasby 1988, Kuemmel 1989). Ayres et al. (1998) argued that exergy is an appropriate concept for statistical use, both as a measure of resource stocks and flows and as a measure of waste emissions and potential for causing environmental harm.

Ayres et al. (1998) stated that there are three advantages of using exergy in the LCA. The first advantage is that exergy allows the calculation of thermodynamic (exergetic) efficiency. This will tell us to what extent the process can be improved. This improvement will have an immediate impact on the amount of resources used and wastes and other emissions generated. The second advantage of exergy-enhanced LCA is the fact that it facilitates comparing very different items such as chemical products, utilities such as electricity and heat, and waste. The authors also stressed that monetary units are much less satisfactory because obviously they will be a function of time and of other political factors that in long term are not significant. The third advantage is the possibility to accomplish year-to-year auditing for large firms, industries, or even nations. The current approach of standard LCA is highly unsatisfactory, with a built-in incompetence to compare flows of different nature: like "apples" and "oranges" (Ayres et al. 1998). Exergy removes this important deficiency.

1.4 Aim of the thesis

The thesis aims to reinforce industrial ecology by theoretical input from both engineering thermodynamics and irreversible thermodynamics and to improve the application of industrial ecology for the evaluation of the resource use of industrial systems. The question that will specifically be addressed is: *How can resource use and transformation be evaluated by industrial ecology*? To answer this question, the thesis proposes to introduce several indicators, some of them proposed by others, one of them new. The concepts of the second law of thermodynamics, such as exergy flow, exergy loss and (minimum) entropy production, will be used throughout the thesis to build an understanding of resource use and transformation in industrial systems, in general, and in energy-intensive industry, in particular.

1.5 Outline of the thesis

Apart from Chapters 1 and 7 the thesis consists of chapters which all have been or are about to be published separately.

Chapter 1 presents why and how the second law of thermodynamics should be considered in industrial ecology. It also introduces the case studies in the thesis, and it gives the status of the evaluation tools for resource use and transformation in industrial ecology.

Chapter 2 presents the theoretical background of the thesis. Several examples with the applications of exergy analysis and entropy production minimisation are also presented.

Chapter 3 calculates in detail three exergy indicators to evaluate the sustainable power production paths in two gas-fired combined cycle power plants with different degrees of CO_2 abatement options. The same gas turbine combined cycle technology is used for the power production in both two power plants. The CO_2 emission abatement options are the sequestration of CO_2 in a depleted natural gas reservoir and the photosynthetic conversion of CO_2 to biomass and then of biomass to synthetic gas, a pipeline-quality methane-rich gas.

Chapter 4 presents the exergy analysis and life cycle inventory of a paper production and recycling system in Norway. Three paper recycling scenarios are considered in relation with an integrated pulp and paper mill in Norway. A set of indicators based on both exergy analysis and life cycle inventory analysis is proposed to be used in finding the best wastepaper recycling degree in the mill considered.

Chapter 5 shows how to formulate, calculate and minimise the total entropy production rate in a Valmet paper drying machine. The impacts of changing the inlet steam temperatures in the drying groups of the drying machine, and of changing the inlet air humidity in the drying machine on the total entropy production rate are studied.

Chapter 6 presents a new indicator that gives a realistic limit for the improvement potential of resource use performance of any individual process unit. This indicator, termed the process maturity indicator, is used to evaluate the distance between the actual and optimal operation in terms of entropy production for the heat exchangers, chemical reactors, distillation columns, and a paper

drying machine.

Chapter 7 concludes the main findings of the thesis and gives some directions for future research for industrial ecology in the context stated above.

For notations relevant to exergy analysis the thesis follows the recommendations given by Tsatsaronis (2005). Notations relevant to entropy production minimisation method follow de Groot and Mazur (1984). Other notations follow the IUPAC's recommended symbols. The abbreviations and symbols used in this thesis are defined in the Nomenclature.

Chapter 2

Energy flows in industrial ecology: The exergy method

Signe Kjelstrup[a] and Anita Zvolinschi[a,b]

[a]Department of Chemistry
[b]Industrial Ecology Programme
Norwegian University of Science and Technology
NO-7491 Trondheim, Norway

This chapter is adapted from Chapter 5.2.2 " Energy/exergy accounting and analysis"
in *Textbook of Industrial Ecology*
H. Brattebø, H. Opoku, K. Røine and M. Hermundsgård (eds)

Abstract

We explain how the exergy content of a resource can be calculated with respect to the environment and with respect to product states. Exergy calculations are now standard and can be done with good accuracy. Production and recycling of materials can be analysed, as well as power production. Economic gains or biological significance are not considered in exergy analysis. The method offers one of many ways to obtain more sustainable industrial processes. We suggest three exergy-based indicators that can be used to aggregate exergy calculations, and we present both examples and results of their applications in electricity generation and hydrogen production and use in fuel cell cars. The strengths and limitations of exergy analysis are also presented.

2.1 Introduction

The production of all materials, transport and public services - in fact all human activities - requires energy flux. Biological and industrial systems stop functioning without a supply of energy. The Earth obtains this energy flux from the Sun. The energy flux through a system is always conserved, according to the first law of thermodynamics, but energy can change into different forms. According to the second law of thermodynamics, there is a conversion of energy that is always from electrical, chemical, or potential energy to thermal energy.

The purpose of this chapter is to give the laws of thermodynamics for energy flow analysis, and introduce a convenient variable for second law analysis, the exergy function. The exergy function is, as we shall see, the energy available for work in a given environment, and only this function can give a fair comparison of the energy efficiency of different processes. Exergy analysis is a well-established branch of thermodynamics; it informs about the levels of exergy flows and the exergy losses during energy conversion in production processes. We need basic thermodynamics to show this (e.g., Atkins (1998)).

2.2 Energy is conserved

The systems of interest in industrial ecology are all *open*; i.e. they exchange heat, work and mass with the surroundings. We can examine a small system (i.e. a box of few molecules) or a large one (i.e. an oil reservoir). Thermodynamics deals with both types of systems equally well. We regard the system as a "black box". A thermodynamic system is characterised by its state variables;

the pressure, temperature and chemical potentials. It is of interest to compare the states of the black box before and after a process has taken place.

Energy is not an absolute quantity. We need a reference for its measurement. For instance, potential energy is measured with respect to a zero height level. Internal energy is measured with respect to a certain standard state. We can measure the *change in internal energy* from one state to another, $\Delta U = U_2 - U_1$, by measuring how much work (W') and heat (Q) need to be added to change the internal energy from the initial value U_1 to the final value U_2. According to the first law of thermodynamics, $\Delta U = Q + W'$, where Q is the added heat and W' is the work that is needed to take certain materials from state 1 to 2. The useful work is $W = W' - p_0 \Delta V$, see Eq. (2.2).

Conservation of energy then means that:

$$U_2 = U_1 + Q + W' \tag{2.1}$$

There are many processes that can bring about this particular change, but the first law of thermodynamics says that all of them are equivalent. In Fig. 2.1, we indicate paths a and b.

The first law of thermodynamics puts heat and work on the same basis. They are *equivalent*, meaning that they both can change the internal energy of a system. But, is heat always equivalent to work? Clearly, when it comes to heating a room, we obtain the same heating by burning wood in a fireplace, or by passing the same amount of Joules through an electric heater in the room. But, when it comes to doing work, heat is *inferior* to electric energy. In effect, electricity is "pure" work. We have to multiply Q by the efficiency of a Carnot machine in order to find the maximum work that can be obtained from

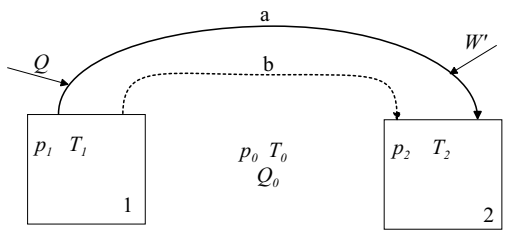

Figure 2.1. The transition of materials from state 1 (at p_1, T_1) to 2 (at p_2, T_2) requires input of heat (Q) and work (W'), from the surroundings (at p_0, T_0). The heat delivered to the surroundings is Q_0.

the heat source. In practice, the obtainable work is always smaller than the work from a Carnot machine because, among the other reasons, the Carnot efficiency is the limiting case of zero power production.

Work is an absolute quantity. The ability of a system to do work is then absolute, and it can be measured on a work scale. The ability of a system to do work gives a neutral basis for comparing different processes that may be natural or industrial. These arguments have lead to the introduction of the exergy function, something that measures the ability to do work in a given environment.

2.3 Exergy is not conserved

The exergy function was introduced to obtain an absolute measuring scale for energy, a scale that measures the ability to do useful work. One of the leading scientists in the previous century, Denbigh (1956) spelled this out in the 1950s. It was already mentioned under another name by Gibbs in 1888 (Gibbs 1961). The function is particularly useful in industrial ecology, because it is absolute and refers to *the environment*.

The exergy function is found by rewriting the first and second laws of thermodynamics. We follow Denbigh (1956), and consider a process that takes some materials from state 1 to state 2, during time Δt, along a certain path, say path a in Fig. 2.1. The process interacts with the environment, which has temperature T_0 and pressure p_0. Therefore, we introduce the variables of the environment into Eq. (2.1). The heat that brings the system from state 1 to 2, Q, leads to a change in the environment $Q_0 = -Q$. Not all of the work added to the system is useful; only W is. The useful work (W) is the total work minus the expansion work ($p_0 \Delta V$) done by the system. This gives

$$\Delta U = -Q_0 - p_0 \Delta V + W \tag{2.2}$$

There is an entropy change in the environment (ΔS_0) and in the system (ΔS) during the process. The environment has constant temperature, so $\Delta S_0 = Q_0 \,/\, T_0$. The total entropy change is

$$\Delta S + \Delta S_0 = \left(\frac{dS}{dt} \right)_{irr} \Delta t \geq 0 \tag{2.3}$$

The entropy production per unit time of system and environment is $(dS/dt)_{irr}$,

and this quantity is always positive or zero. This is the second law of thermodynamics. When these relations are introduced in Eq. (2.2), we obtain

$$W = T_0 \left(\frac{dS}{dt}\right)_{irr} \Delta t + \Delta U + p_0 \Delta V - T_0 \Delta S \tag{2.4}$$

This equation also gives the expression for maximum useful work (W_{max}). We find W_{max} when the process is reversible (like for instance a Carnot cycle), when $(dS/dt)_{irr} = 0$. The exergy function, or the exergy, is therefore defined as

$$E \equiv W_{max} = \Delta U + p_0 \Delta V - T_0 \Delta S \tag{2.5}$$

Exergy is a state function, it does not depend on the process. The lost work, or the *lost exergy*, is the difference between the maximum work (W_{max}) and the real work (W). This is the Guoy-Stodola's theorem (Gouy 1889, Stodola 1898)

$$E_{loss} \equiv W_{loss} = T_0 \left(\frac{dS}{dt}\right)_{irr} \Delta t = W_{max} - W \tag{2.6}$$

The lost work or lost exergy depends on the process. In popular terms, the lost work is the *friction* in a machine or a process. Imagine a person on a bicycle (Fig. 2.2 A and B).

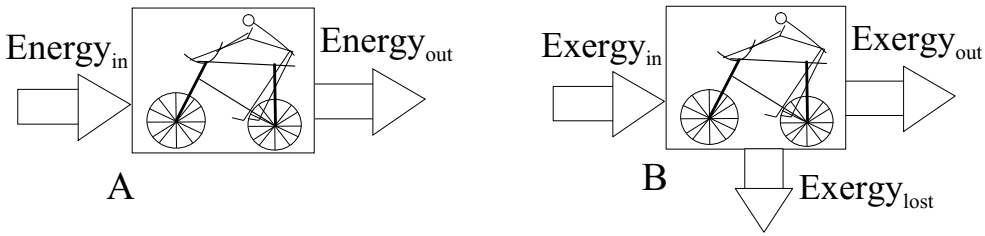

Figure 2.2. The energy (A) and exergy (B) balance of bicycling.

There is an energy input in terms of food for the person. This input is converted to heat and work; the energy is conserved (Fig. 2.2 A). Food can also be measured on an exergy scale. The person is doing work using the food exergy (Fig. 2.2 B). The work performed is the force times the travelled distance. But bicycling is not done without overcoming friction (that is, the entropy production of bicycling is positive). There is always lost work or lost exergy (Fig. 2.2 B), and Eq. (2.6) explains how to find it. The exergy loss may be relatively large, for relatively small periods of time. In second-law *optimisations*,

we are seeking to find a path of operation that has minimum entropy production rate, see Nummedal and Kjelstrup (2001), Johannessen and Kjelstrup (2005), Røsjorde et al. (2004).

With the picture of bicycling in mind, we can conclude as follows. The energy flow through an open system is constant (Fig. 2.2 A). The chemical energy input (e.g., food intake) will take different forms in the energy output (e.g., bicycling and heat). The flow of energy available for work, the exergy flow, through a system is not conserved; it is reduced by this conversion (Fig. 2.2 B). We obtain less work than the exergy input, because some exergy is lost. Energy conversion is always connected with lost exergy. Examples of lost work in the energy and chemical industries have been computed by de Swaan et al. (2004).

2.4 Calculating exergy

Exergy is defined with reference to the environment. The environment has temperature T_0, pressure p_0, and a certain chemical composition varying with the location on the Earth. The standard temperature T_0 is often set to 288 K, and the standard pressure p_0 to 1 atmosphere.

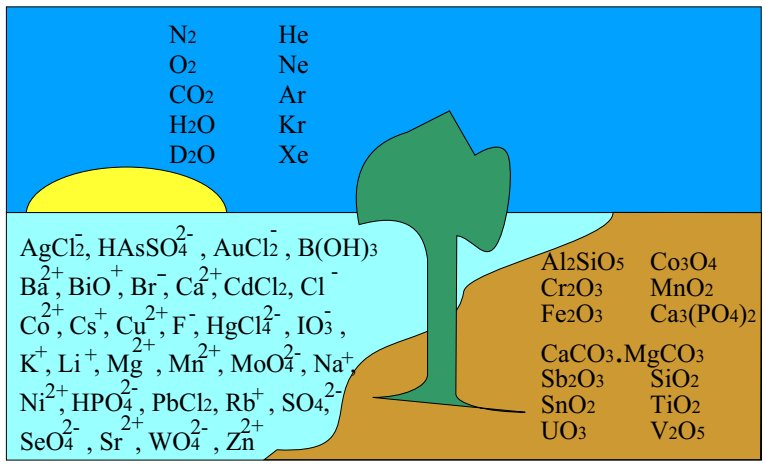

Figure 2.3. The three standard mixtures of air, ocean and Earth's crust with their reference substances.

The standard composition has been the subject of discussion, see for example Ahrendts (1980), Szargut et al. (1988), and Ayres and Masini (2004). The discussion has developed because the environment is normally not in equilibrium and because there are local variations in its composition.

In this thesis, we follow Szargut's approach in the definition of standard composition and reference states. The author defined three mixtures of the environment: one for the air, one for the ocean, and one for the Earth's crust (Szargut et al. 1988). The three standard mixtures of the environment are illustrated in Fig. 2.3. The numbers of reference substances in these mixtures are fixed to 10, 32, and 13, respectively. There is only one reference substance per chemical element, and each mixture has a certain average composition. For example, graphite has carbon dioxide as reference substance, and hydrogen has liquid water as reference. In this picture, an oil reservoir is not a part of the standard environment. It is a resource, because it does not have an average composition. Szargut's standard environment is composed of the most stable (or abundant) species available.

The standard exergy is now the exergy calculated for standard temperature, pressure and composition. Sets of standard exergies of reference components have been tabulated and discussed. Standard values of T (temperature), S (entropy), U (internal energy), and derived properties H (enthalpy) and G (Gibbs energy) are given subscripts *0*.

Exergy analysis concerns calculations of E_{in}, E_{out}, and E_{loss}. Expressions that can be used to calculate the exergy content of a heat reservoir at T_1, of one component, and of a chemical mixture, respectively, are given in Table 2.1.

Table 2.1. Exergy content of a flow in state 1 compared to the environment state 0.

Exergy content of an amount of heat, Q, at T_1:
$E_1^{heat} = Q((T_1 - T_0)/T_0)$
Exergy content of one component at p_1 and T_1:
$E_1^{tm} = (H_1 - H_0) - T_0(S_1 - S_0)$
Exergy content of an ideal mixture of substances at p_0 and T_0:
$E_1^{rx} = \Delta_{rx} G^0(T_0)$

Thermodynamic variables for the formulas in Table 2.1 can be found in several books, e.g. (Aylward and Findlay 1994). Extensive tables can be found in Wagman et al. (1968). Common programs for process modelling like Aspen Plus (2003) also contain databases for exergy calculations.

2.5 A scale to measure lost work in process analysis and design

Exergy analysis, or calculation of exergy input, output, and loss, can be used in industry, the public sector, and academia for several purposes. Questions

to be answered by exergy analysis can be:

• *How can we find the production process for a material that uses the smallest amount of work?* This problem concerns the route that takes some raw materials from state *1* to a wanted product in state *2*. Different routes are possible. They may need a varying degree of renewable resources. We can ask: *What are the exergy needs for using recycled compared to virgin materials?*

• *How can we obtain as much work as possible from an energy resource, given a particular purpose?* For instance, how does natural gas perform in fuel cell cars compared to other cars? The exergy loss may differ between the different routes, making some of them more efficient than others.

• *How can we improve the design or the operating conditions of a given process to save input of exergy?* This is an optimisation problem, where one seeks to find operating conditions for a single process that give minimum exergy loss.

• *How does a society use its resources in a region, in a country or in the world?* Such studies have been done for countries, among them Sweden (Wall 1986) and Norway (Ertesvåg 2000, 2005). Ertesvåg (2001) also did an exergy analysis for several countries.

Examples 1-4, below, are typical examples of exergy analysis of production processes in industry. We shall see that they are also all relevant for industrial ecology. In Section 2.6, we shall bring the analysis in Examples 1-4 to a more aggregated level, a level that may be useful for political discussions. Several indicators based on exergy calculations will be introduced.

Example 1 Evaluating chemical production routes

In order to evaluate different production routes for mono-propylene glycol, Tober (1997) calculated the associated exergy inputs and exergy losses. The results are given in Table 2.2. The commercial production route, route A, uses

Table 2.2. Exergy inputs, CO_2 emission and exergy loss for two mono-propylene glycol (MPG) production routes (Tober 1997). Values are given for the production of one tonne of mono-propylene glycol.

Route	Exergy input [GJ/t MPG]	Renewable exergy input [GJ/t MPG]	CO_2 [t/t MPG]	Exergy loss [GJ/t MPG]
A	34.7	0.0	0.5	14.2
B	40.6	33.5	-1.6	14.6

raw materials from crude oil. The other alternative, route B, uses biomass and solar energy as exergy inputs. A distinction was made between exergy inputs from renewable and non-renewable resources in the two routes. Emissions of CO_2 were also calculated.

Table 2.2 shows that the processes in routes A and B have similar exergy losses. There is thus no need to distinguish between the processes from the perspective of their exergy loss. Route A has a somewhat smaller exergy input requirement than route B has, but route B has most of its input from renewable resources. In route A, there are CO_2 emissions, while route B has CO_2 fixation. A choice can then be made between routes A and B on the basis of their different use of renewable exergy inputs and CO_2 emissions.

In most cases, weighting of variables is difficult, but necessary. One way to introduce weighting is to associate each important factor with a cost. Other factors than those considered here, are then relevant. For instance, route B needs a much larger area than route A. Investment costs are yet not known for route B, and such costs normally affect a decision.

Example 2 Improving a single process

By systematically calculating all exergy losses in a single process, targets for process improvements become visible. Take as an example, the calculation of contributions to E_{loss} for production of aluminium from aluminium oxide, see Kjelstrup and Bedeaux (2001). The results are given in Table 2.3.

Table 2.3. The type, location, and amount of exergy loss (in kWh/kg Al) in aluminium production. The exergy input was 13 kWh/kg Al (Kjelstrup and Bedeaux 2001).

Exergy loss by	Location of loss	Exergy loss [kWh/kg Al]
Charge transfer	In the electrolyte	1.3
	In diffusional layers	0.1
	At electrode surfaces	0.5
	In the bulk part of the cathode	0.3
	In the bulk part of the anodes	0.3
Hot products	Products leaving at $T > T_0$	0.3
Side reactions	At the anode	0.1
Thermal conduction	Through all side walls	4.8
Total exergy loss		7.7

The exergy input (electricity input from the grid) for the production is 13 kWh/kg aluminium. The sum of lost exergy is 7.7 kWh/kg. We see that losses are especially large in the walls of the cell, where they amount to 4.8 kWh/kg. This means that we should devote effort to a better (design) construction of the cell in the wall. The production of aluminium from aluminium cans can be analysed in the same manner. This has not been done so far.

Example 3 Comparing alternative production paths

The process industries are major energy converters in today's society. Separation methods are especially costly from an exergy perspective, and there are few alternative methods. When it comes to separation and purification of components, distillation is often unavoidable. New concepts are therefore being actively pursued, like diabatic distillation, heat pump assisted distillation and heat-integrated distillation. In the next example, we compare the last concept to a conventional adiabatic distillation column.

In conventional distillation, thermal energy is supplied in a reboiler at the bottom of the column at high temperature, and it is withdrawn in a condenser at the top of the column at a lower temperature (Fig. 2.4 A).

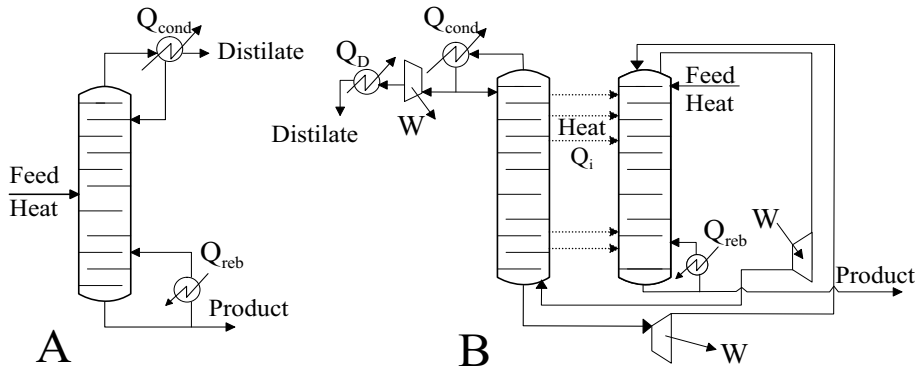

Figure 2.4. Conventional (A) and heat-integrated distillation column (B) (Røsjorde et al. 2004)

In the heat-integrated distillation column (Fig. 2.4 B), some (or all) of the heat released in the top section is transferred to trays in the bottom section at locations where it is needed. This design reduces the thermal energy needed in the reboiler. But extra work is needed to raise the pressure in the top part and accomplish the internal heat transfer. The two distillation columns can

be compared when they produce the same quality of products out of the same chemical mixture input. The exergy content of the material streams input and output are then the same in the two distillation columns, and therefore, we can compare the exergy losses. The calculation was done by Røsjorde et al. (2004). The results are shown in Table 2.4.

Table 2.4. The exergy input, exergy loss, and exergy saving (in kWh) of a conventional distillation column compared to an optimal heat-integrated distillation column (HIDiC), with a feed flow of an equimolar benzene-toluene mixture of 100 mol/s (Røsjorde et al. 2004)

	Conventional DiC	Optimal HIDiC
Reboiler exergy input	1492	105
Condenser exergy output	-462	-225
Net compressor work input	0	831
Extra heat exchanger input exergy	0	-37
Exergy loss	1025	673
Exergy savings		352

Table 2.4 shows that the more complicated heat-integrated distillation column (HIDiC) has the potential of saving a large amount of exergy loss (352 kWh) over the adiabatic distillation column for a feed flow rate of 100 mol/s. This example shows that the exergy analysis can be used to compare designs.

A complete comparison should also take into account the exergy input needed to construct and dismantle the systems. Experience shows that the exergy input required for the construction of the process equipment is often much smaller than the exergy input required for process operation in its entire life-cycle (Lombardi 2003).

Example 4 Energy resource utilization in the transport sector

The transport sector today is using a large part of the fossil fuel reservoirs. It is important to find alternatives to these resources and reduce the transport-related emissions. Wright (2004) calculated the exergy loss for an internal combustion engine and a fuel-cell car. The exergy losses were more than double in an ordinary car than in a fuel-cell car.

Kjelstrup and Møller-Holst (1993) calculated the location and magnitude of exergy losses at 1273 K in a solid oxide fuel cell (SOFC) that operated on methane, see Table 2.5. They found, with some simplifications, that 71% of

Table 2.5. The exergy loss (in kW) of an SOFC unit operated at a pressure of 1 bar. One mole of methane is completely converted, and the current density is 1 A cm^{-2} (Kjelstrup and Møller-Holst 1993).

Exergy input	772
Location of exergy losses	
in reforming reaction	106
by incomplete reactions	0
by cracks	7
due to overpotential	69
due to Joule heat	39
Work output	552
Exergy efficiency (in %)	71

the exergy input was used as work. Most of the exergy losses were associated with the production of hydrogen fuel from methane (106 kJ), and to the overpotential and Joule heat losses (69 and 39 kJ, respectively) of the electrochemical cell.

2.6 Making a process more sustainable

We have seen above that a process always leads to lost exergy. This dissipates energy quality as heat in the surroundings. In most cases, heat flow into the surroundings is not harmful. More important for the environment is therefore that reactants (E_{in}) have changed into products (E_{out}). Some resources have been depleted, and some unwanted by-products have probably been formed and discarded into the environment.

Many industrial processes are necessary because of their products and services. We must therefore find a way to deal with their unwanted by-products and products after use by society. In an ideal situation, we can bring these products back to their reactant state. An exergy supply is usually needed to make this process happen. In such a situation, industrial processes can be said to be *more sustainable* than in the situation when the products are disposed into the environment after use. The exergy supply can be termed the exergy needed for abatement, $E_{in,abatement}$, and it can be taken as the exergy to make a certain process more sustainable by abatement. However, the possible loss of natural capital in the form of exhaustible resources should be taken into account when calculating the exergy needed for abatement.

Another point to be taken into account is the exergy efficiency in the use

of the renewable and non-renewable resources, E_{out} compared to E_{in}. The closer the two values are, the longer we can keep the exergy of resources for the future. Furthermore, it is not arbitrarily which resource, E_{in}, we use in our production and abatement processes. Some resources are renewable with or without small abatement exergy needs, some are connected with large abatement exergy requirements. We present the exergy-based indicators that quantify these factors below.

2.7 Exergy analysis on an aggregated level: Exergy-based indicators

Exergy-based indicators were introduced by Dewulf et al. (2000) to address the points in Section 2.6 on an aggregated level. The authors made a distinction between exergy sources that were renewable without human work, and sources that were non-renewable. They defined the renewability fraction of the exergy inputs:

$$\alpha = \frac{E_{in,renewable}}{E_{in}} \tag{2.7}$$

Here, $E_{in,renewable}$ is the sum of all exergy supplied from renewable resources. Route B in Example 1 above has α near one; and a value of one helps define an ideal process.

The exergy efficiency (ϵ) was defined as (see Eq. (1.7), Chapter 1):

$$\epsilon = \frac{E_{out}}{E_{in}} = \frac{E_{in} - T_0(dS/dt)_{irr}\Delta t}{E_{in}} \tag{2.8}$$

The value of one represents a reversible process that has a zero entropy production rate ($(dS/dt)_{irr} = 0$). This process requires infinite amounts of time and/or area. We know that the limit 1 for ϵ is unrealistic because we demand products or services in a finite time. The indicator ϵ indicates how far we are from reversible operation. The absolute values of E_{out} and E_{in} are still important. A relatively small change in ϵ, i.e., in a distillation process, can still mean that a lot of exergy can be saved. Table 2.4 pointed out this fact.

The third indicator proposed by Dewulf et al. (2000) is environmental compatibility (ζ). It is the quotient of the exergy inputs for the production processes (E_{in}) and the sum of all exergy inputs necessary to abate the emissions and products at the end of their life ($E_{in,abatement}$) plus the exergy inputs for the

production processes (E_{in}):

$$\zeta = \frac{E_{in}}{E_{in} + E_{in,\ abatement}} \tag{2.9}$$

Equation (2.9) can show us whether or not products and production emissions need a large exergy input for their abatement to make them harmless in comparison with the exergy input for the production of products. Harmless does not mean that their exergy content is zero, it only states that, for example, there is no accumulation of carbon dioxide from fossil sources in the atmosphere, because it is for instance sequestrated into a depleted gas reservoir. Take again the example of natural gas (or methane) for electric power production; carbon dioxide is a product of natural gas oxidation with air. In the simplest regime possible one may consider an abatement process for carbon dioxide only. Since the product (i.e. electricity) does not need abatement, the environmental compatibility indicator is calculated as:

$$\zeta_c = \frac{E_{in}}{E_{in} + E_{in,abatement\ of\ CO_2}} \tag{2.10}$$

An extreme abatement may be to close the material cycle in a system. Closing the material cycle can be seen as one strategy for returning the final state of products and emissions in a system to its previous state. This strategy is not necessary the best one if the previous state is defined in macroscopic terms without taking into account the exergy depletion of exhaustible resources. In this context, the sink-specific definition of the reference states proposed by Ayres and Masini (2004), as discussed in Section 1.2, may be more appropriate than the "standard" reference states proposed by Szargut et al. (1988). However, for the purpose of estimating the exergy indicators in Chapters 3 and 4, the approach given by Szargut et al. (1988) will be used.

In the following, two applications of the exergy indicators are presented. Table 2.6 gives examples of two gas-fired combined cycle power plants (Zvolinschi et al. 2006b) and two hydrogen-based fuel-cell cars (Neelis et al. 2000), which were assessed by the three exergy-based indicators.

The study by Zvolinschi et al. (2006b) analysed two gas-fired combined cycle power plants, a standard power plant, which combusts directly natural gas in a gas turbine, and a new proposal that first converts the natural gas into hydrogen and then combusts the hydrogen in a gas turbine. The CO_2 emissions emerged from the power plants were subsequently abated by means of an amine absorption process, a photosynthetic conversion of CO_2 into biomass,

and a anaerobic gasification of biomass into methane. The values of the exergy indicators (first row in Table 2.6) show no a clear winner. Therefore, in this case, the indicators cannot give us the information so that one can decide which power plant should be constructed.

Table 2.6. Exergy-based indicators (α, ϵ and ζ_c) for two case studies. See text for explanations.

Case studies and processes to be compared	α	ϵ	ζ_c
400 MWh electricity generation[a] by:			
Natural gas-fired combined cycle power plant	0.43	0.22	0.95
Hydrogen-fired combined cycle power plant	0.43	0.21	0.94
Hydrogen for fuel-cell cars[b,c] produced by:			
Large-scale steam reforming	0.001	0.21	0.48
Retail-scale water electrolysis[c]	0.98	0.068[b]	0.99

[a] CO_2 abatement by means of CO_2 capture and conversion to methane via photosynthesis and biomass digestion. More details can be found in Chapter 3 and Zvolinschi et al. (2006b);

[b] Electricity generated by a windmill (Neelis et al. 2000);

[c] Hydrogen (650 kg H_2 per day) is manufactured by means of water electrolysis, and then sold at car-refuelling stations (Neelis et al. 2000).

The study by Neelis et al. (2000) analysed hydrogen as a carrier in fuel-cell cars (see second row in Table 2.6). The first production method is by means of a large-scale natural gas steam reforming process; the other is by means of electrolysis of water using windpower to run the electrolysis process. The large-scale reforming route uses only non-renewable exergy, while the electrolysis route uses electricity from a windpower plant. This explains the different scores for α. The environmental compatibility, ζ_c, shows that a high exergy input is required for CO_2 abatement after the reforming step. There is discharge of exergy as low-temperature heat only, when hydrogen is produced by electrolysis. Clearly, the last approach is much more environmentally friendly and sustainable, with high scores for α and ζ_c. Its drawback is, however, the much lower exergy efficiency ($\epsilon = 0.068$ compared to 0.21).

2.8 Strengths and limitations of exergy analysis

We have seen above that exergy calculations can be used to assess how effective energy is converted in a single process, like in the aluminium production case (Example 2). The analysis then gives information about how to improve the

present state of operation with the same equipment. Exergy analysis can also be used to evaluate new ideas for equipment improvement, like in Example 3, where the concept of a heat-integrated distillation column was discussed. The savings in lost exergy during process operation in terms of reduced power costs may defend larger investment costs needed in the new design. Exergy analysis can also be used to approach a whole production chain (e.g., hydrogen in different propulsion systems). There are no scale, price, space or time limitations to exergy analysis. In addition, exergy can be used to give value to a natural resource (e.g., fossil fuel or mineral ore) in terms of how much exergy is needed to restore it.

The main advantage of exergy analysis is that it is possible not only to improve a single process, but also to compare and evaluate different processes. Exergy-based indicators are useful here. They give aggregated information to the layman, as far as one is able to aggregate *without introducing weighting factors*. The details behind the exergy efficiency, ϵ, are important for the industry. The renewability fraction, α, and the environmental compatibility, ζ and ζ_c, may be more important for the public sector.

Exergy cannot yet be used as a measure of potential environmental and biological harm for the material wastes and emissions disposed into the atmosphere, hydrosphere or lithosphere. This limitation is partly due to the methodology that is commonly used in exergy analysis literature to compute the chemical exergy of chemical compounds, see the arguments in Ayres and Masini (2004).

Economic consideration is not considered in exergy analysis. The economic value of materials and work varies over the course of time. The price of electricity depends on whether electricity is produced using solar cells, wind or natural gas. The fact that exergy analysis is not concerned with the price of electricity or commodities may in some contexts be regarded as an advantage. Technologies can be compared without regard to the present day's economy, but with the perspective of being good for the environment. Exergy analysis provides a time-dependent scale that measures how good a system is by means of its exergy renewability, exergy efficiency, and environmental compatibility.

Considerable work still remains to be done in the area of exergy analysis. The exergy requirements for abatement of material wastes from production and consumption processes in our society cannot be systematically compiled. This information should be an advantage for industrial ecology. Irreversible thermodynamics (Førland et al. 2001, Kjelstrup and Bedeaux 2001) teaches us more about the reasons for the exergy losses and the nature of the second

law optimal operation paths in industrial processes, and can bring time and area as variables into the analysis. This is elaborated upon Chapters 5 and 6 of this thesis. Such knowledge may also help improve the exergy analysis tool in future, and, as a consequence, it may help industrial ecology to better understand resource use and transformation in energy-intensive industry.

Chapter 3

Exergy sustainability indicators as a tool in industrial ecology. Application to two gas-fired combined cycle power plants

Anita Zvolinschi[a,b], Signe Kjestrup[b], Olav Bolland[c] and Hedzer J. van der Kooi[d]

[a]Industrial Ecology Programme, [b]Department of Chemistry and
[c]Department of Energy and Process Engineering
Norwegian University of Science and Technology
NO-7491 Trondheim, Norway

[d]Delft Department of Chemical Technology
Delft University of Technology, 2628 BL Delft, The Netherlands

This chapter is based on an article accepted to be published in
Journal of Industrial Ecology.

Abstract

Life-cycle analysis is an established tool for industrial ecology. An analysis of the energy use in the chemical and energy intensive industry is still under discussion in this field. We argue that the concept of exergy can play a role in industrial ecology, using a recent policy question as illustration. The question is whether to build a natural gas- or a hydrogen-fired gas-turbine combined-cycle power plant to meet increased needs for electricity in Norway. Several indicators are relevant for this discussion, and we calculate three based on exergy calculations, as proposed in the literature. The indicators are the exergy renewability, the exergy efficiency, and the environmental compatibility. We show how these indicators can be used to evaluate *paths for sustainable power production* in two gas-fired combined cycle power plants. We found that the two power plants in question were equivalent, as judged by their exergy renewability and their environmental compatibility, but not by their exergy efficiency. This indicator favoured the standard power plant, possibly in combination with CO_2 sequestration in a depleted gas reservoir. The analysis suggested that the present situation for power production from fossil fuels is such that one may have to choose in general between power production with a high exergy efficiency, but low exergy renewability, or the opposite; with low exergy efficiency and high exergy renewability. The general importance of exergy analysis was demonstrated by this example. It enables communication between different professional groups. The technological details, understood by the engineers, can be transposed to meaningful aggregated indicators for decision makers.

Keywords: Power plant; Combined cycle; Exergy analysis; Exergy-based indicators

3.1 Introduction

Industrial ecology is meant to be "an agent of change" for industry by providing principles and tools that can foster a change towards a more sustainable society. Principles like "industrial metabolism" (Ayres and Simonis 1994), "closed industrial ecosystem" (Frosch and Gallopoulos 1989), "technological food webs" (Graedel and Allenby 1995) and "industrial symbiosis" (Ehrenfeld and Gertler 1997) are now used as general principles in industrial ecology. Tools, such life-cycle analysis and net energy analysis, generate comparative studies of material and energy conversion processes. However, these tools are accounting

for energy needs in terms of lower heating values (LHVs). The second law of thermodynamics is not considered then. As a result, the various qualities of energy are not calculated, and cannot thus be compared or studied in energy converting processes.

Several papers have presented the importance of understanding the quality of energy needs in industrial systems, and furthermore, the need to discuss where and how the energy quality or exergy degrades in these systems, see for example Connelly and Koshland (1997), Cornelissen (1997), Lowenthal and Kastenberg (1998), de Swaan et al. (2004), Sciubba (2004). The benefits of exergy-based metrics over the metrics based on material and energy intensity were illustrated by Yi et al. (2004). This paper aims to continue this discussion.

We shall see that the results of exergy analysis can be aggregated in three exergy-based indicators in industrial ecology. We argue that these indicators will quantify different aspects of sustainable power production, namely its renewability, exergy efficiency, and the exergy requirements for abatement of CO_2 emission. We demonstrate the usefulness of these indicators by examining a recent Norwegian policy problem dealing with additional electricity generation in Norway. Norway has to comply with its Kyoto Protocol target. This means that CO_2 emissions must be reduced by about 3 million tonnes CO_2 equivalents compared with the 1996 level, and about 12 million tonnes CO_2 equivalents compared with the projected figure for 2010, see White Paper No. 29 (Ministry of the Environment 1998). The proposal to build two natural gas-fired power plants at Kårstø and Kollsnes will be evaluated on this background. The construction of power plants with some kind of CO_2 abatement option is necessary. Therefore, Bolland et al. (2001) and latter Ertesvåg (2005) have proposed a power plant that burns hydrogen instead of natural gas, hydrogen that is obtained by a natural gas reforming process (Bolland et al. 2001, Ertesvåg 2005). This plant is therefore taken as one of the options. As the other option we take the standard IEA power plant (Greenhouse R&D Programme 2000).

We aim to compare these plants using exergy analysis (i.e., mapping of energy quality use and degradation in all process steps), and three exergy-based indicators that reflect important aspects of the sustainability of a system (i.e., renewability, efficiency, and recycling of materials). The aim is to bring out arguments that favour one type of power plant over the other in a systematic manner, and in a way that will be also useful for other electricity generation systems. Before the systems are calculated in detail, we present the exergy-

based indicators and the methodology employed. Subsequently, we describe, analyse, and characterise the two options for electricity generation. Finally, we discuss issues that could help to understand the usefulness and the meaning of the present study.

3.2 Three exergy-based indicators

Exergy measures the energy quality of any material flow or stock. Unlike mass and energy, exergy is not conserved; in every successive process step exergy is degraded. Identifying exergy degradation during the processing of a material allows us to interpret its causes. Improvement options can then be evaluated and compared.

The three indicators intended to quantify the sustainability of the power production paths, are: (a) the exergy renewability (α), which considers the exergy input of renewable resources ($E_{in,renewable}$) compared to the total of all exergy inputs (E_{in}); (b) the exergy efficiency (ϵ), which shows how well the energy quality is preserved in the system; (c) the environmental compatibility (ζ), which considers the exergy needed to preferably abate all emissions and all products after the end of their life. These indicators were first introduced by Dewulf et al. (2000), who also provided illustrations of their use in the evaluation of the sustainability of electricity generation in a co-generation power plant and in a photovoltaic power plant (Dewulf et al. 2000).

The exergy of solar radiation and the solar exergy stored in biomass are considered as renewable resources for exergy, while the exergy of fossil fuels is non-renewable. After this classification is made, the exergy renewability indicator (α) is calculated as:

$$\alpha = \frac{E_{in,renewable}}{E_{in}} \tag{3.1}$$

In agreement with the second law of thermodynamics, during any real process there is an energy quality loss due to the necessary driving forces that drive the process in the direction wanted. This loss is also called the exergy loss. It follows directly that an important strategy for improving the sustainability of systems is to reduce the rate of exergy loss or entropy production, or, in other words, to increase the exergy efficiency. The exergy efficiency (ϵ) is defined as the ratio of the useful exergy output (E_{out}) and the exergy needed to obtain that, (E_{in}):

$$\epsilon = \frac{E_{out}}{E_{in}} \tag{3.2}$$

In the present case, the useful exergy output is the net electric power made available for society by the power plant, and the exergy input is the exergy content of the natural gas as it is in the gas reservoir, plus any possible solar exergy input or other inputs.

Given that we do not want to increase emission levels by industrial production, all used products and wastes must be abated at approximately the same rate as they are produced. Buffering of used products and wastes in the environment may be necessary, however. When natural gas is used as a feedstock for a power plant, the product is electric power, and as waste we have among the other gases, carbon dioxide. Closure of the carbon cycle requires that we return carbon to the state it had in the reservoir, i.e. to natural gas. Only in this manner we can speak of a power production without CO_2 emissions.

The environmental compatibility (ζ) was defined by (Dewulf et al. 2000) as follows:

$$\zeta = \frac{E_{in}}{E_{in} + E_{in,abatement}} \tag{3.3}$$

where E_{in} is the exergy input to the production processes, the same as in Eqs. (3.1) and (3.2), and $E_{in,abatement}$ is the total exergy input required to abate all emissions and wastes and eventually all used products. In the present study there is no abatement needed for the electricity, as its end product is heat in the natural environment. Exergy inputs are needed to abate all emissions, but we shall only consider the emission of CO_2. A complete return of CO_2 to natural gas is unfortunately not technically feasible, so we are limited to deal with two approximations to a closed carbon cycle.

In the ideal situation, one may say that man-made systems should have perfectly closed material cycles and should perform these cycles in a most efficient way (i.e. reversibly) according to the second law of thermodynamics. The only input to the system should be renewable exergy from the Sun, and the only output should be heat (entropy). In such a situation, all exergy-based indicators defined here are unity. This situation cannot be achieved in reality, however. It is still possible to use the indicators to examine the question posed

in the introduction; can one power plant be favoured over the other when CO_2 abatement processes are included in the analysis completely or partially. As we shall see, the indicators are able to point to a path of sustainable power production.

3.3 Power plants with CO_2 abatement options to be compared

Both power plants use natural gas from a North Sea natural gas reservoir. The plants are designed to have the same exhaust compositions to allow for a fair comparison between them. This is achieved by amine absorption processes, which are integrated with the power plants. The power production capacity of both plants is the same, 400 MW, so the technologies of the plants fit with this production capacity.

(a) Plant A is a standard power plant (Greenhouse R&D Programme 2000), which is a combined cycle that combusts natural gas in a gas turbine. Amine absorption processes are integrated with the gas-turbine combined cycle to capture CO_2 from the exhaust gases.

(b) Plant B is a hydrogen-fired power plant, which is an integrated system between a natural gas reforming plant for hydrogen production and a gas-turbine combined cycle where hydrogen is combusted (Bolland et al. 2001, Ertesvåg 2005). Before hydrogen is combusted, the gas mixture of hydrogen and CO_2 is separated in an amine chemical absorption plant.

The outlets of Plants A and B are the same by this choice.

We have chosen to analyse two options for CO_2 abatement. They are:

(c) Option C, consisting of three steps that convert the captured CO_2 from Plant A or B into synthetic gas, a pipeline-quality methane-rich gas. The steps are: 1) Photosynthetic conversion of CO_2 into biomass (Goldman 1979), 2) Anaerobic digestion of biomass (Legrand 1993), and 3) Biogas processing (Kapoor and Yang 1989).

(d) Option D, with only one step, namely sequestration of CO_2 from Plant A or B into a depleted natural gas reservoir. This option is motivated by the feasibility of CO_2 sequestration (White 2003) and the limited exergy efficiency of CO_2 conversion to biomass (Bisio and Bisio 1998).

The different plants and processes are illustrated in Fig. 3.1. Full details about

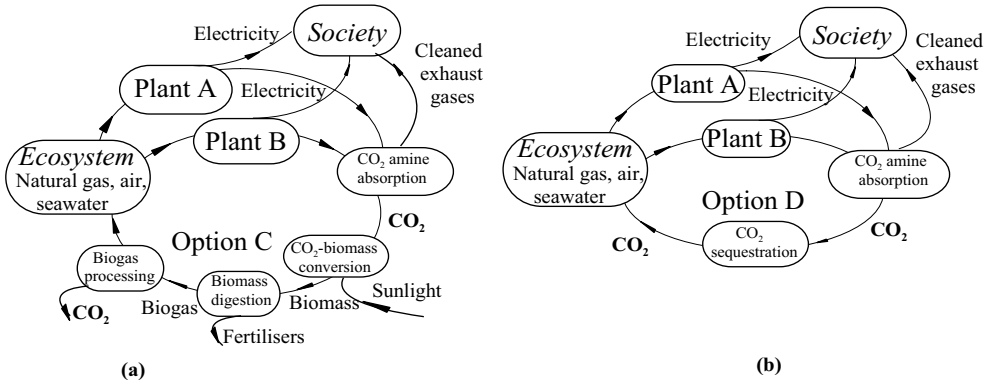

Figure 3.1. Partially closure of the carbon used in Plants A and B combined with Option C (a) or Option D (b).

the natural gas processing in the power plants and on the abatement options are given in Appendices A and B, respectively.

3.4 Methodology

The gas-turbine combined cycle power plants were modelled using GTPRO software from Thermoflow (Elmasri 1996), while the hydrogen production plant and the amine absorption plant were modelled using PRO/II software from PRO/II (Simulation Sciences SIMSCI 2001). Detailed process descriptions, process stream data and boundary conditions are given in Appendices A and B. The software provided material- and energy-flow sheets for the processes of interest. Exergy inputs and outputs of all individual streams were calculated from the data in these flow-sheets using standard methods (Kotas 1985, Szargut et al. 1988). The environmental reference temperature was 15^0C and the pressure was 1.01 bar. The chemical exergy of each stream was computed in an in-house program using the standard chemical exergy values of components as proposed by Szargut et al. (1988). Options C and D were likewise calculated using Microsoft Excel. Technical details of these options can be found in Appendix B. Making sure that mass and energy conservation principles were obeyed, the exergy loss in each process was determined by subtracting the exergy output from the input. Data for the modelling of the CO_2 amine absorption process were taken from Sander (1991). All these data provided the input needed for the calculation of exergy-based indicators.

Exergy analysis localises and quantifies the energy quality degradation or ex-

ergy loss due to mass and energy conversions. It is normal in exergy analysis to present the results in Grassmann diagrams (Grassmann 1984), which are exergy utilisation maps. This practice was followed here for presenting exergy utilisation in the power plants.

The construction and dismantling phases of any subsystem were not considered in neither the exergy analysis nor in calculation of exergy-based indicators (see Discussion). No economic assessment was performed.

3.5 Results

3.5.1 Power plants

The summary of the exergy calculation of the power plants is presented in the first two columns of Table 3.1, and in Grassmann diagrams in Figs. 3.2 and 3.3. The detailed data behind the table and the diagrams are given in Appendices A and B.

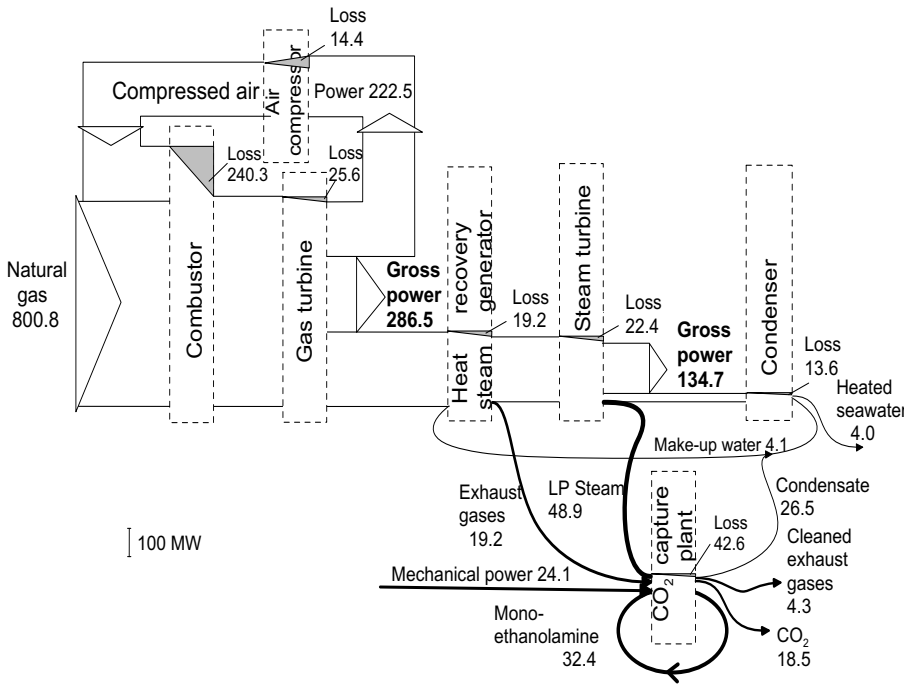

Figure 3.2. Grassmann diagram (in MW) for mapping the exergy losses in Plant A.

Table 3.1. Exergy inputs (renewable and non-renewable), losses (internal and external), and outputs (net electric power, CO_2, fertilisers and synthetic gas) for Plant A (A) and Plant B (B) with and without Option C (C) or Option D (D). All numbers are in MW. The uncertainty in the numbers is estimated to ± 3%. PP is power plant and FE is fuel expander.

Stream or process	A	B	A+C	B+C	A+D	B+D
Exergy input						
Non-renewable						
Natural gas	800.8	859.2	960.4	992.8	1035.2	1108.0
Mono-ethanolamine	32.4	57.6	38.8	63.2	42.0	74.0
NH_3, P_2O_5, K_2O	-	-	1.6	1.6	-	-
Carbon	-	-	0.8	0.8	-	-
Renewable						
Sunlight	-	-	761.6	808.4	-	-
Seawater	0.0	0.0	0.0	0.0	0.0	0.0
Make-up water	4.1	8.8	9.0	9.6	5.5	11.6
Algae	-	-	0.4	0.4	-	-
Total exergy input	837.3	925.6	1772.6	1876.8	1082.6	1193.6
Internal exergy losses						
Hydrogen plant	-	126.8	-	146.8	-	172.4
Power plant	335.5	291.6	402.4	338.0	464.8	377.6
CO_2 capture plant	42.6	9.3	66.0	12.0	71.2	16.0
Option C						
CO_2 conversion	-	-	351.3	367.3	-	-
Biomass digestion	-	-	6.5	7.2	-	-
Biogas processing	-	-	21.0	27.4	-	-
Option D						
CO_2 sequestration	-	-	-	-	70.9	107.8
External exergy losses:						
Exhaust gases	4.3	8.3	2.0	2.0	5.5	10.8
Warm seawater	4.0	7.6	0.0	0.0	5.2	10.0
Total exergy loss	386.4	443.6	849.2	900.7	617.6	694.6
Gross power output	421.2	437.6	495.2	508.8	519.2	586.8
Aux. power for PP	8.8	9.6	8.8	9.6	11.2	12.0
Aux. power from FE	11.7	4.0	7.6	8.0	9.6	8.4
Exergy to abate CO_2:						
in CO_2 capture plant	24.1	32.0	28.0	32.0	30.8	46.8
in Option C or D			66.0	75.2	86.8	132.8

Table 3.1 (continuation).

Stream or process	A	B	A+C	B+C	A+D	B+D
Exergy outputs:						
Net electric power	400.0	400.0	400.0	400.0	400.0	400.0
CO_2	18.5	24.4	4.4	5.2	23.0	25.0
Mono-ethanolamine	32.4	57.6	38.8	63.2	42.0	74.0
Carbon	-	-	0.8	0.8	-	-
Fertilisers	-	-	22.8	30.5	-	-
Synthetic gas	-	-	456.8	476.4	-	-
Total exergy output	450.9	482.0	923.4	976.1	465.0	499.0

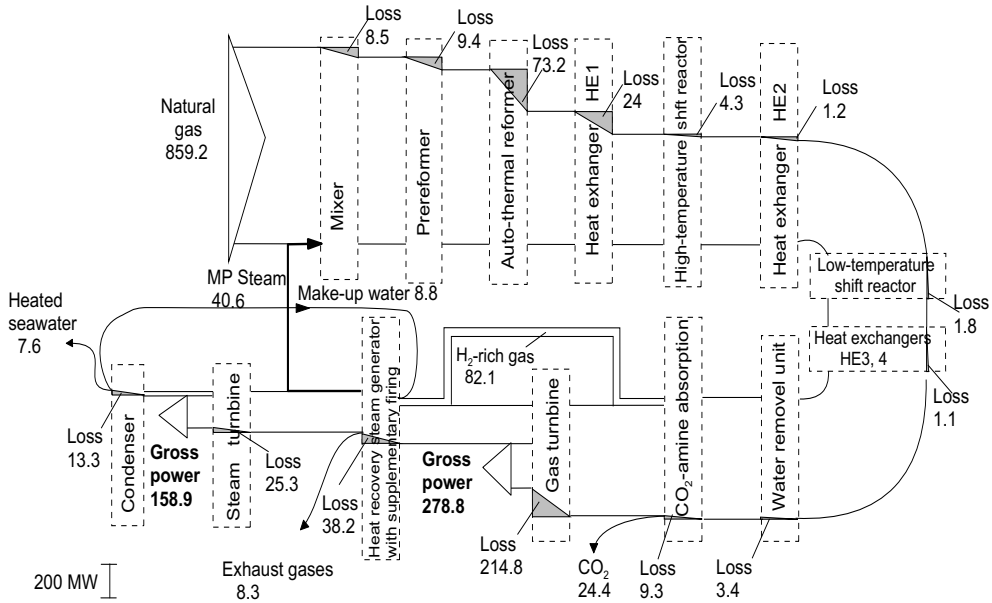

Figure 3.3. Grassmann diagram (in MW) for mapping the exergy losses in Plant B.

Table 3.1 gives normalised results using the standard IEA power plant as a reference. The power available for the society from this plant is 400 MW. The Grassmann diagrams give an overview of the actual numbers for the two plants. The thickness of the arrows in these diagrams (in MW) is proportional to the exergy content of a stream, while the grey space is the exergy loss in a certain process (in MW). The uncertainty in the exergy data is estimated to be $\pm$ 3%. The error is due to assumptions made in the calculations, like the assumptions of ideal gas and of equilibrium reactors. The accuracy in the ratios is similar.

Table 3.1 shows that the ratio of natural gas exergy input to net power output is 2.0 in Plant A, and it is 2.1 in Plant B. We can also see that the main reason for this difference are the exergy losses in the hydrogen production plant. As can be seen from the Grassmann diagrams (Figs. 3.2 and 3.3), the two technological options appear rather different, with Plant B being much more complex than Plant A. These diagrams show the distribution of the natural gas exergy input, and of the exergy losses in the power plants.

The major sources of lost exergy in Plant A, according to Fig. 3.2, are the gas turbine (4.3 kWh/kg natural gas), the amine absorption process (0.8 kWh/kg natural gas), and the steam turbine (0.3 kWh/kg natural gas). In Plant B, the losses are more spread out, see Fig. 3.3. Again the gas turbine has most of the losses (2.9 kWh/kg natural gas), with the reformer as number two loss source (1.0 kWh/kg natural gas).

We see that amine absorption needs a substantial exergy input. In Plant A this exergy comes from thermal and electric energy in combined cycle. In Plant B, the best option is to withdraw the thermal energy from the steam produced in the hydrogen plant. In doing so, the electric-power production in the combined cycle of the Plant B is less affected. For further technical details on Plants A and B, and on Options C and D see Appendix A and B, respectively. We found that CO_2 absorption in amine causes an exergy loss of 5.3% of the natural gas chemical exergy input to Plant A. In Plant B this loss was only 1.1%.

3.5.2 Carbon mass balance

The only chemical element cycle studied here, is the carbon cycle. The carbon mass flow rates (in kg-C/s) for each power plant with and without their combination with abatement Options C and D are given in Table 3.2. Here, the amount of carbon taken from the natural gas reservoir is given in the first

column for Plant A (upper half of the table) and Plant B (lower part of the table). Inflow contributions are given in the three first columns, while outflow values are given in the last three columns. The table shows, for instance, that

Table 3.2. Input (in) and output (out) of the carbon mass flow rate (M_C) for Plant A (A), Plant B (B), Plant A and B with Option C (A+C and B+C, respectively), and Plant A and B with Option D (A+D and B+D, respectively).

	A	A+C	A+D	A	A+C	A+D
Flow description	$M_{C,in}$			$M_{C,out}$		
Natural gas	10.79	13.30	13.95			
Air	0.06	0.07	0.09			
Exhaust gases				1.00	1.01	1.49
CO_2				9.85	2.06	12.55
Synthetic gas				-	7.00	-
Fertilisers				-	3.30	-
Total carbon	10.85	13.37	14.04	10.85	13.37	14.04
	System					
	B	B+C	B+D	B	B+C	B+D
Flow description	$M_{C,in}$			$M_{C,out}$		
Natural gas	11.83	14.60	15.25			
Air	0.08	0.09	0.10			
Exhaust gases				1.11	1.03	1.62
CO_2				10.80	3.26	13.73
Synthetic gas				-	7.16	-
Fertilisers				-	3.24	-
Total carbon	11.91	14.69	15.35	11.91	14.69	15.35

only 7 out of a total of 13.3 kg-C/s is recovered in the synthetic gas in Option C, while the same ratio for sequestrated gas is 12.5 out of 14.0 kg-C/s. In Option C, 77% of carbon inflow from natural gas was converted into synthetic gas (7 kg-C/s) and fertilisers (3.3 kg-C/s). The remaining part of carbon was found in the cleaned exhaust gases released to the atmosphere (1 kg-C/s), and in the CO_2-rich gas obtained from biogas processing (2 kg-C/s).

The mass flow rate of carbon that was extracted from the natural gas reservoir and used in Plant B (11.8 kg-C/s) was 1.0 kg-C/s higher than in Plant A (10.8 kg-C/s). The same difference in the input flow rates was found when the CO_2 captured in Plant A and B was abated by Option C or D.

We see that the recycling of carbon is not complete, and that Option D by far stores most of the carbon extracted from the natural gas reservoir.

3.5.3 Exergy inputs for CO_2 abatement in Option C

Option C consisted of three steps. The detailed of each step are given in Appendix B, but a summary is given in Figs. 3.4 (a) (Plant A combined with Option C) and (b) (Plant B combined with Option C). The exergy needed for

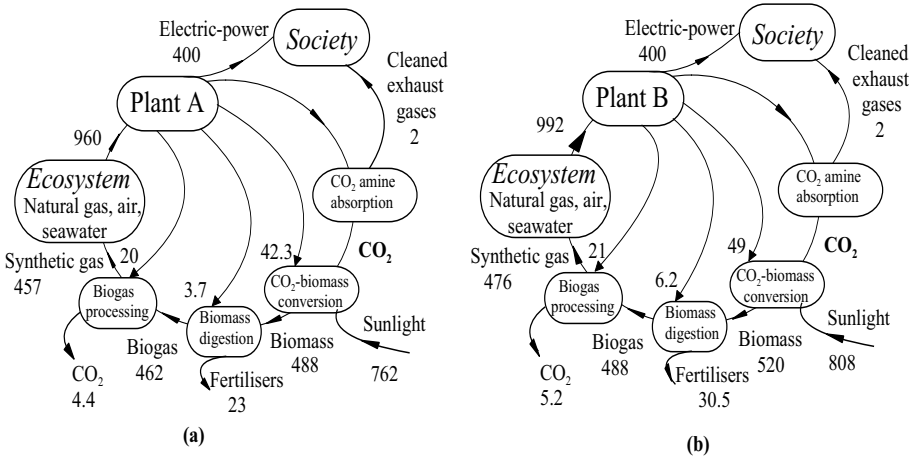

Figure 3.4. Exergy needs (in MW) for abatement of the CO_2 emissions from Plant A with Option C (a) and from Plant B with Option C (b).

the three steps in Option C were taken from the power plants themselves. The same type of exergy input in Option D was listed in Table 3.1, see the two last columns. The exergy losses in the processes are also shown in this table.

The exergy needed to convert CO_2 into synthesis gas by Option C was 66 MW for Plant A, and 75 MW for Plant B. The marine areas that are required to trap all CO_2 coming from Plant A and B into biomass, were 6100 ha and 6500 ha, respectively.

When the CO_2 emission is abated by sequestration (Option D), the total exergy needed for abatement was 87 MW for Plant A, and 133 MW for Plant B.

3.5.4 Exergy-based indicators

The exergy-based indicators were calculated from Table 3.1, using Eqs. (3.1) - (3.3). All terms in these equations are given in MW in the first three columns of Table 3.3, while the indicators for Plants A and B with and without Options C and D alternatively are shown in the last three columns of Table 3.3.

Table 3.3. Total exergy input (E_{in}), renewable exergy input ($E_{in,renewable}$), useful exergy output (E_{out}), exergy input for CO_2 abatement ($E_{in,abatement}$), and exergy-based indicators (α - exergy renewability, ϵ - exergy efficiency, and ζ - environmental compatibility). The uncertainty in the exergy indicators calculations is estimated to ± 3%.

System	E_{in} (MW)	E_{out} (MW)	$E_{in,renewable}$ (MW)	$E_{in,batement}$ (MW)	α (-)	ϵ (-)	ζ (-)
A	837	400	4	24	0.005	0.48	0.97
A+C	1772	400	771	94	0.435	0.22	0.95
A+D	1082	400	6	118	0.005	0.37	0.90
B	926	400	9	32	0.009	0.44	0.97
B+C	1877	400	818	107	0.435	0.21	0.94
B+D	1194	400	12	180	0.009	0.34	0.88

The exergy renewability indicators of both plants are near zero, $\alpha = 0.005$ (Plant A) and $\alpha = 0.009$ (Plant B). The numbers refer to the operational phase of the plants. The low values can be explained by almost no input of renewable resources with exergy content different from zero (the specific chemical exergy of seawater that is needed in a large quantity is almost zero). The exergy renewability increases when we attempt to close the carbon cycle by Option C. The value becomes 0.44 for both power plants when they are combined with Option C. The main reason for this gain in α compared with that for Plant A and B alone, is the exergy input from the Sun. When Plants A or B are combined with Option D the value of α does not change, as almost all exergy inputs are non-renewable sources.

The exergy efficiency, ϵ, is always higher for Plant A than for Plant B, see sixth column in Table 3.3. The difference in ϵ between Plant A and B is 0.04 points. This difference remains if Option D is included, see column six, rows three and six in Table 3.3. It becomes smaller (0.02) if Option C is used.

The environmental compatibility, ζ, was calculated for the varying degrees of CO_2 capture. Already Plants A and B contain an abatement process, the CO_2 capture by means of an amine absorption plant. The values of ζ were pairwise

the same within the accuracy given in numbers: for Plants A and B alone the values of ζ were 0.97, for the plants combined with Option C they were 0.95 and 0.94, and with Option D they were 0.90 and 0.88.

3.6 Discussion

The exergy indicators will first be discussed per se, before we use them in an overall evaluation of the particular problem posed, namely that of which power plant to build, Plant A or Plant B, alone, or with abatement Options C or D. We continue to give general perspectives related to the use of these indicators in industrial ecology.

3.6.1 The meaning of the exergy-based indicators

We have seen from the results in Table 3.3 that all options discussed here are far from being renewable. The exergy renewability indicators for Plants A and B, alone or combined with Option D are for all practical measures zero. The only way to raise the value of this indicator is to use Option C in combination with the power plants. Only these combinations point to a more sustainable power production from the point of view of α. In the ideal situation $\alpha = 1$, here we found values of near 0.4. The high value of the exergy renewability for the power plants in combination with Option C may be an argument for developing this option for CO_2 abatement.

The efforts to approximately close the carbon cycle, and thus to attain a higher exergy renewability indicator, do not come without drawbacks. The raise in α to 0.4 is accompanied by a drop in the exergy efficiency, from 0.48 to 0.23 in Plant A, and from 0.44 to 0.21 in Plant B, respectively. Also, it should be remembered that only a fraction of the total amount of carbon (77%) is taken care of in this option, cf. Table 3.2. Clearly the exergy efficiency is significantly reduced when the exergy renewability increases.

The exergy efficiencies give a clear message when it comes to comparing Plants A and B alone. There is reason to prefer Plant A to Plant B from an exergy efficiency point of view, because Plant A has a higher value of ϵ. So, it is not irrelevant whether we abate CO_2 by amine absorption before or after the power production, as judged from the indicator alone. A comment on our choice of alternatives to be compared is now in place. We have chosen as base cases, plants which already have a certain degree of CO_2 abatement, i.e. in terms of amine absorption processes. The exergy efficiency of Plant A and Plant B

without the amine absorption processes were 0.55 and 0.47, respectively (not shown in Table 3.3). Without the amine absorption processes, the end-states of Plants A and B are different, however, meaning that these systems cannot be compared in a fair way. We compared the plants on a fair basis, nevertheless, Plant A is still best, from an exergy efficiency point of view. This conclusion will not change if we combine the plants with Option D; the exergy efficiency will sink to 0.37 (Plant A with Option D) or 0.34 (Plant B with Option D). When the plants are combined with Option C, their exergy efficiency indicators become the same ($\epsilon = 0.22$), a very low value. A shift of the system boundaries to include ammonia and fertilisers production, will not improve the indicators for Plant B.

The environment compatibility indicator (ζ) does not give any argument to favour Plant A over Plant B, whether the plants are alone, or are combined with Options C or D.

The above analysis was carried out without considering the exergy needs and losses to build and dismantle the power plant. (Lombardi 2003) showed that these assumptions were good (within 1% point) for combined cycle power plants of the same size based on coal gasification. For the hydrogen-fired combined cycle power plant, with its extra equipment, the assumption may be less good, but of the same order of magnitude.

3.6.2 The political debate; which power plant to build

The indicators used here are obtained with relatively high accuracy. This is an advantage for a decision-making process. The environmental compatibility did not give a preference for any of the power plants, so a decision to build one of them should use arguments connected to the other indicators. The exergy efficiency indicators gave the message that Plant A without extra abatement processes beyond the amine absorption processes is preferable to Plant B with amine absorption of CO_2. If Option C is selected, this has the drawbacks that there is a very large reduction in the exergy efficiency, a rather large area is needed, and there is still incomplete abatement of emissions. The question that emerges from this discussion, is whether it then pays to abate by sequestration (Option D) or by an mono-ethanol amine absorption process alone. The difference in environmental compatibility between Plant A and Plant A with Option D is less than 10%. The reason for this difference is the extra electric power needed to store CO_2 in the depleted gas reservoir. The storage problem of CO_2 captured from the amine solution is on the other hand

not solved in the case given by what we have called Plant A.

From the above considerations we appear to be in a trade-off situation, a typical situation for politicians. The analysis tells that we are in a situation where we have to choose between power production with high exergy efficiency, but low exergy renewability (Plant A with Option D), or the opposite; with low exergy efficiency and high exergy renewability (Plant A with Option C). Plant B does not perform better than any of these options, and can be taken out from the trade-off. Such a trade-off situation may be common for situations when fossil fuels are the resources. We have shown above that exergy analysis and exergy indicators can offer a quantitative basis for analysis of gains and losses. This input may be useful for politicians in their weighted decision, but also for the governmental sector in their research funding priorities.

3.6.3 General perspectives

The Kyoto Protocol can be seen as a first effort by the international community to commit itself to reduce CO_2 emissions worldwide. The present example shows that it is possible to analyse in a systematic manner alternative routes for power production in gas-fired combine cycle power plants with varying degrees of CO_2 abatement. By taking into account the second law of thermodynamics, we can establish a scale for energy quality, namely the exergy scale. The quality of energy in its various forms is calculated as exergy. This then allows a comparison of any energy converting process, exemplified here by two power production systems. In the first place, the detailed exergy analysis given in Grassmann diagrams and Appendices A and B, is useful. In the second place, the exergy-based indicators are useful.

For the professional engineer, exergy analysis can be used to localise points where research efforts should be concentrated in order to increase exergy efficiency. The analysis allows a comparison and assessment of different material and energy conversion systems with the same function on the same scale. It helps industrial ecology to adhere to the first law as well as to the second law of thermodynamics. The engineering professionals can assess the potential for improvements of a system, and transmit this potential to the industrial ecologist, who will then be informed about the possible limits of the indicators.

The technological details are given in Appendices A and B. It is clear from these appendices that there are numerous technological details behind the indicators. Such a wealth of technical details is difficult to comprehend for non-engineering

professionals. It is in this context that exergy-based indicators, first proposed by Dewulf et al. (2000), can be useful, as we have illustrated by our example. These indicators can include all technical details on a meaningful aggregated level, and they are therefore much more accessible to decision makers than otherwise.

We saw in the definition of the indicators that they all have an ideal limit of unity. These are unrealistic limits of operation, because any natural or man-made system has an exergy efficiency below unity. The conversion of solar energy in plants is never without exergy losses. It is therefore beyond expectation that any man-made system can reach the ideal limit for exergy efficiency. As a consequence the environmental compatibility is always affected by exergy losses and the exergy inputs needed to abate emissions, wastes and used products. The construction of multilevel material cycles within industrial systems for all emissions, wastes, and used products, is a task for industrial ecology.

It is in this situation we need a practical route towards sustainability and a methodology to assess the route. This is why we would like to name the exergy indicators *sustainability indicators*, because they give such a direction. They do not become unity, but they should be as high as possible. A realisable target for the exergy efficiency in single-process units was discussed by Bejan and Tondeur (1998), Nummedal et al. (2003), Johannessen and Kjelstrup (2005). If production is carried out with such a practical limit on the exergy loss (namely with minimum entropy production), the exergy efficiency of many processes can be raised beyond the present day's level. It follows that the need for exergy for abatement processes in attempts to close material cycles, becomes smaller. If at the same time, fossil fuels are replaced by renewable energy sources, we will be on a path that will increase all exergy indicators. This is a path towards *sustainable power production*.

We have seen above how the laws of thermodynamics, as embraced by exergy analysis, can be used to give information that can help politicians in their choice between future options for power production. The three exergy-based sustainability indicators, recently proposed in the literature, were central in this context. Based on this framework, we argue that industrial ecology, with its concept of sustainability and its willingness to be an agent of change towards a more sustainable society, should adopt these indicators. The indicators can be used widely. In particular, they can be used to establish a scale to measure power production systems. Nevertheless, other indicators are needed as

sustainability is more than exergy renewability, exergy efficiency, and environmental compatibility (Mayer et al. 2004).

3.7 Conclusions

We found that some recently proposed exergy-based sustainability indicators can be used to assess the sustainability of options for power production, and we have proposed that the indicators become tools within the industrial ecology framework. We have shown this using the example of a natural gas- and a hydrogen-fired combined cycle power plant, an actual power production policy problem in Norway. Aggregated information for decision makers was obtained from three exergy-based indicators.

The particular problem was concluded as follows. The two power plants with abatement options were equivalent, as judged by their exergy renewability indicator and by their environmental compatibility alone, but the exergy efficiencies of all systems gave a clear message. The option to deal with CO_2 abatement beyond amine absorption, using solar energy halved the exergy efficiency of both power plants. Therefore, sequestration of CO_2 in a depleted gas reservoir seemed the most viable path. But also this system (Plant A with Option D) lowered the exergy efficiency significantly. The analysis suggested that the present situation for power production from gas-fired combined cycle power plants is such that we may have to choose between power production with high exergy efficiency, but with low exergy renewability, or the opposite; with low exergy efficiency and high exergy renewability.

The importance of exergy analysis is that it enables communication between different professionals. The technological details, understood and provided by the engineers, can be translated to a meaningful aggregated level, and on this level, they can be comprehended by decision makers.

We proposed to name the exergy indicators *sustainability indicators*, because they show which direction to take towards more and more *sustainable power production*. The first efforts have been made to set a realisable target for the exergy efficiency in different industrial processes (Wall 1988, de Swaan et al. 2004). More work is needed to continue this effort and promote the necessary changes in technology.

Acknowledgement

Anita Zvolinschi acknowledges the financial support from the Research Council of Norway.

Chapter 4

Exergy and life cycle inventory analysis of a paper production and recycling system in Norway

Anita Zvolinschi[a,c], Helge Brattebø[a,b] and Signe Kjelstrup[c]

[a]Industrial Ecology Programme
[b]Department of Hydraulic and Environmental Engineering
[c]Department of Chemistry
Norwegian University of Science and Technology
NO-7491 Trondheim, Norway

This chapter was submitted to

Energy - The International Journal

and is an extended version of the paper published in the

Proceedings of the 16th ECOS Conference, Copenhagen, July 2003.

Abstract

The objectives of this study are to present a set of indicators derived from exergy analysis (EA) and life cycle inventory (LCI) analysis, and to use these indicators to evaluate resource use and environmental performance of a system with three wastepaper management scenarios. The system consists of all activities required to produce the newsprint paper and to reuse the wastepaper by means of recycling and/or incineration with thermal energy recovery. The exergy-based indicators proposed for the evaluation are the exergy renewability, the exergy efficiency and the environmental compatibility. The indicators from LCI, given per air-dried tonne (adt) of newsprint produced, are the electricity, thermal energy, renewable and non-renewable resources demand, the cumulative loads of emissions to air (CO_2, NO_x, CO), to water (chemical oxygen demand matter, total phosphorus, total nitrogen), and to landfills (municipal solid waste). Two system boundaries were applied to the system: a narrow one, which is a gate-to-gate evaluation, and a wide one, which is a gate-to-grave evaluation. The results showed that the system has significantly different indicators in the three scenarios, both in the narrow and wide system boundary. The study showed that both sets of indicators are needed in a pursuit for the best wastepaper management scenario. The present analysis favours the system in the scenario with a high degree of paper recycling. The LCI of paper based on exergy values for emissions into air and water and for solid wastes are also presented and discussed.

Keywords: Pulp and paper mill; Wastepaper recycling; Life cycle inventory; Exergy analysis; Exergy-based indicators

4.1 Introduction

The availability of recovered wastepaper from society and environmental engagement of the paper production mills have led to changes inside the paper industry. New technologies like paper de-inking have been introduced, while less process-water and less non-renewable resources have been used (Axegard et al. 2002). New technical solutions for reducing energy demands in processes like paper drying have been discussed (de Beer et al. 1998). Many of these changes affect the way the exergy of resources is utilised and converted throughout the whole paper production chain or the whole paper cycle including wastepaper recycling. The effects may result in exergy savings or exergy

expenses. The environmental-related performance may also change. The trade-off between exergy savings or better environmental performance is an issue of central interest to industrial ecology.

The industrial ecology field is a promising research field that is looking at material and energy resources and flows and at environmental burdens from single industries to entire economies, as well as from individual processes to a cluster of interlinked industrial systems, including transport. This is the reason why this study partially covers the need of industrial ecology for new integrated approaches to find new insights into patterns of production and trade-offs between different technological options.

Exergy analysis (Wall 1988, Gong 2005) and life cycle analysis (Bergsdal et al. 2005) have been used to evaluate energy resources conversion and environmental performance for paper production processes and paper life cycles, respectively. The exergy analysis studies have shown that the pulp and paper industry has large opportunities for improvements in exergy efficiency in pulp and paper production processes, and indicated priorities for exergy savings (Wall 1988, Gong 2005). In particular, Wall (1988), Gong (2005) carried out the exergy analysis of a sulphate-pulping and paper mill, and Gemci and Ozturk (1998) carried out the exergy analysis of a sulphide-pulp and paper mill. Thus, a chemical pulping process has been studied in both studies. This study examines a thermo-mechanical pulping process integrated with a paper production process as well as with a de-inking process. This fact makes this study different from the above exergy analysis studies.

Beyond the domain of engineering, exergy analysis has been applied to strengthen the biophysical basis of life cycle analysis. Methods like the exergetic life cycle analysis (Cornelissen and Hirs 2002) and the life cycle exergy analysis (Wall and Gong 2001, Gong and Wall 2001) have been proposed as new approaches to evaluate the resource utilisation and conversion in industrial systems placed in a product life-cycle perspective. Others also have used exergy to examine the environmental impact (Rosen and Dincer 1999, Ayres et al. 1998, Daniel and Rosen 2002). Some recent studies have attempted to assess the impact of paper production and recycling by performing a life cycle assessment (Finnveden et al. 2000, Bergsdal et al. 2005). These studies have shown that recycling of paper is in general favourable with regard to overall emissions of greenhouse gases and the total municipal solid wastes (Finnveden et al. 2000, Bergsdal et al. 2005).

As a continuation of the above studies, this study evaluates the material and

energy resource utilisation and conversion and the environmental performance of a paper production and recycling system in Norway. The system is evaluated in three different wastepaper management scenarios. The first scenario, Scenario Z, has no wastepaper recycling; the wastepaper is here incinerated with thermal energy recovery. The second and third scenarios, Scenario L and Scenario H, have a low (20%) and a high (80%) degree of wastepaper recycling, respectively. The evaluation is based on three exergy indicators together with several indicators from the life cycle inventory. The objectives are to help identify what is the best option for paper production and wastepaper recycling from an exergy analysis and a life cycle inventory analysis point of view, and illustrate the benefits of exergy method in life cycle inventory analysis.

This study starts with a definition of industrial ecology and a description of the methods and the indicators used in our evaluation. The goal of the study, the system and its boundaries, the function unit and scenarios of the system are then described. The results of the life cycle inventory analysis and those of the exergy analysis and their related indicators are presented. Finally, the usefulness of these indicators is discussed in context of industrial ecology.

4.2 The industrial ecology approach

Industrial ecology is one of the most positive movements towards a more ecological paradigm in industry (Frosch and Gallopoulos 1989, Graedel and Allenby 1995, Ayres 1996). White (1994) has defined it as a "study of the flows of materials and energy in industrial and consumer activities, of the effects of these flows on the environment, and of the influences of economic, political, regulatory, and social factors on the flow, use and transformation of resources". All system-oriented approaches that address a life-cycle perspective may become tools of industrial ecology.

This study applies an industrial ecology approach to answer to the question: What is the best option for wastepaper management in relation to a specific paper production mill? Although this kind of approach is certainly not the first time the topic is dealt with, most of the previous studies have used only one method to deal with recycling of wastes. Our approach is carried out by means of two methods, each with its own scale of applicability. The first method is the exergy analysis, and the second is the life cycle inventory analysis. These methods were applied here because, in the authors' opinion, they allow a complete analysis and offer a comprehensive accounting and evaluation of material flows as well as of resources, emissions, and solid wastes in industrial processes.

4.2.1 The exergy analysis and its indicators

Exergy analysis is a method that offers the possibilities to account for all kinds of material and energy resources and flows on a same basis (i.e. the exergy basis), and to evaluate the resource utilisation and transformation by means of exergy requirements, internal and external exergy losses and exergy efficiencies of the individual processes as well as of the whole system.

In this study, the inputs and outputs of the system are accounted based on mass and exergy. The exergy calculation methods proposed by Kotas (1985) and Szargut et al. (1988) have been used to determine the exergy content of the material and energy resources and flows involved in the system. The exergy loss of the system and its components are determined using the following exergy balance:

$$E_{in} = E_{out} + E_{loss} = E_{products} + E_{wastes} + E_{loss} \tag{4.1}$$

where E_{in} is the sum of exergies of the material and energy inputs, E_{out} is the sum of exergies of the material and energy outputs, $E_{products}$ is the sum of exergies of the products and by-products, E_{wastes} is the sum of exergies embodied in emissions in air and water, and in solid wastes, and E_{loss} is the sum of exergy losses due to the irreversibility that occurs during the processes for material and energy resources and flows conversion.

Based on Eq. (4.1), the exergy efficiency (ϵ) can be calculated as:

$$\epsilon = \frac{E_{out}}{E_{in}} = \frac{E_{products} + E_{wastes}}{E_{in}} \tag{4.2}$$

In addition to the exergy efficiency, two other indicators are used in this study to evaluate the resource use of the whole system. These indicators were first proposed by Dewulf and Langenhove (2002). The first indicator is the exergy renewability (α), and is calculated as follows:

$$\alpha = \frac{E_{in,\ renewable}}{E_{in}} \tag{4.3}$$

where $E_{in,renewable}$ is the sum of exergies of renewable resources, and E_{in} is the sum of exergies of the material and energy inputs. In this study, we consider renewable resources as being those that can be obtained from solar energy conversion in a relatively short time, e.g. wood and wood-based fuels or bio-fuels. The latter indicator proposed by Dewulf and Langenhove (2002) is the environmental compatibility (ζ). This indicator is a quotient of all exergy

inputs for production processes ($E_{in,production}$) and the sum of all exergy inputs including those needed for abatement ($E_{in,abatement}$) of all unutilised streams (Dewulf and Langenhove 2002). It is calculated as follows:

$$\zeta = \frac{E_{in,\ production}}{E_{in,\ production} + E_{in,\ abatement\ products} + E_{in,\ abatement\ wastes}} \tag{4.4}$$

The environmental compatibility measures the efforts on an exergy basis to diminish the emissions to air and water, and the solid wastes discarded into the environment, and to reuse the products and by-products of the system. Buffering of emissions and wastes into the natural environment may be allowed within acceptable levels, which are usually prescribed by environmental regulations and laws. In this study, the exergy needs for abatement are the exergy required in the following processes: (1) reduction of the emissions into water; (2) transportation of newsprint paper and wastepaper; (3) incineration of the wastepaper; and (4) de-inking of recycled wastepaper.

4.2.2 The life cycle inventory and its indicators

A life cycle inventory is performed in this study following the SETAC code of practice (SETAC 1994), the Nordic guidelines Lindfors (1995), and the ISO standards (ISO-14040 1996, ISO-14041 1997). These sources ask for an inventory table, in which the material and energy inputs and outputs and the environmental interventions crossing the system boundary are identified and quantified, usually as cumulative mass demands and loads. The quantification of resources is usually done using their mass and energy content. The energy content of a resource is commonly understood as the lower heating value of that resource. In this study, the inventory tables are presented based on mass and exergy, and not based on the lower heating value.

The construction and dismantling of the components in the system, e.g. machinery and infrastructure, are usually considered in the inventory table. In this study, we assumed that the construction and dismantling of components in the system have a less significant contribution to the overall inventory. In agreement with other studies (McDaugall et al. 2001, Weitz et al. 1999), all upstream life cycle activities (raw materials extraction and machinery manufacturing) are assumed to be held constant. Moreover, the activities associated with the printing and use of the newsprint paper are not considered.

The indicators derived from the life cycle inventory are the total demand for electricity, thermal energy, non-renewable and renewable primary resources,

and the cumulative loads of emissions to air and water, and the total amount of solid waste. All these indicators are given for one tonne of paper produced at Norske Skogn's mill at Skogn, Norway.

4.2.3 The goal and scope definition of the study

The overall goal of the study is to provide information and develop tools to evaluate the resource use and environmental performance of three alternatives for wastepaper management in Trondheim city in its relation with the Norske Skog's mill at Skogn, Norway. The primary audience of this effort is the mill and the local government and solid waste planners in Trondheim. The main feature of the proposed industrial ecology approach takes into consideration the intended audience of the study using the results from both exergy analysis and life cycle inventory.

Considering that these results may be used to support a decision-making process, it was decided to make the knowledge of the technical processes and the quality of data as comprehensive as possible. First, all the processes of the selected scenarios were broken down with the aim of identifying and characterising each single process in the system by means of the material and exergy input/output inventories. This gives the possibility to detect where engineers could intervene in order to improve design and/or operating criteria. Then, with reference to data quality, the data required for the study has been derived from on-site investigations. For each process in the system, all the data have been collected during technical visits (from August 2002 to February 2003) to the Norske Skog mill in Skogn, or deduced from the official documents and environmental declarations of the mill, and of the waste-to-energy plant in Heimdal, near Trondheim.

4.2.4 The system and its boundaries

The study refers to a steady-state condition of a system which is posed in three scenarios for wastepaper management in Trondheim. Figure 4.1 shows an overview of the system and its boundaries applied in the study. Two system boundaries were applied in the study. The first boundary, representing a gate-to-gate study, is a narrow boundary. It consists of the plants for pulp and paper production and for generation of the electricity and thermal energy requirements at the Norske Skog's mill at Skogn. The latter boundary, representing a gate-to-grave study, is a wide boundary. In addition to the plants in the narrow boundary, the wide boundary consists of the plants for wastepaper

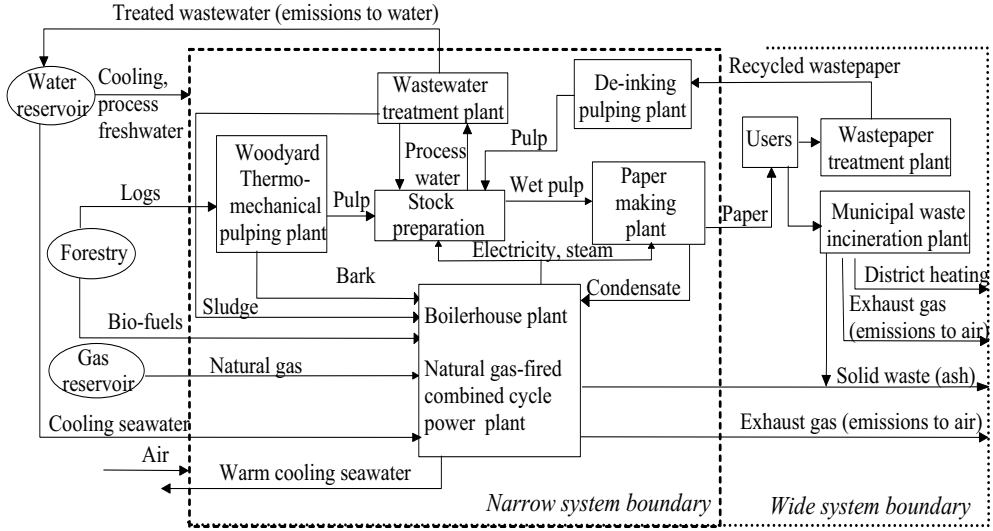

Figure 4.1. Overview of the system with its components in the narrow and wide system boundaries.

treatment and incineration, and a transportation network between the mill and Trondheim city, the city and the wastepaper treatment plant, and the city and the municipal waste incineration plant. The system is characterised as a closed-loop system, because it has only one product in each of the two boundaries considered. In the narrow system boundary, the final product of the system is the newsprint paper to be used by the users in Trondheim city. In the wide boundary, the final product of the system is the thermal energy to be used for district heating by the users in Trondheim city. The fact that only one single product is obtained in each system boundary applied in this study means that no allocation of resources or pollutants and solid wastes is necessary.

4.2.5 The functional unit

The function of the system under study is to produce one air-dried tonne (adt) of newsprint paper at the Norske Skog's mill (with a capacity of 500 000 tonnes of newsprint paper per year) and to manage the wastepaper obtained after the use of newsprint paper by means of wastepaper incineration and/or closed loop paper recycling. All processes required to produce the newsprint paper and manage the wastepaper are considered. Therefore, the stages of newsprint pa-

per production and transportation, and wastepaper collection, transportation, sorting, bale pressing, and thermal energy recovery are individually analysed and quantified in terms of the indicators derived from exergy analysis as well as in terms of the loads of emissions into air and water, and the solid wastes at local level.

4.3 The scenarios and their processes

Three scenarios for wastepaper management were selected in this study. In the first scenario, Scenario Z, primary fibres from wood logs are used for paper production in an integrated pulp and paper mill (Norske Skog's mill at Skogn), while the wastepaper collected from users in Trondheim is sent to a municipal waste incineration plant (MWIP). In the second and third scenarios (Scenario L and H, respectively), both primary fibres from wood and secondary fibres from de-inking wastepaper are used for paper production. Scenario L has a low degree of wastepaper conversion into newsprint paper (i.e. 20% of the total paper produced), while Scenario H has a high degree (80% of the total paper produced). These degrees of wastepaper are transported to a wastepaper treatment plant (WPTP) for sorting and bale pressing prior to transportation back to the mill for recycling. In these scenarios, the wastepaper that is not recycled into newsprint paper is transported to the MWIP where it is incinerated with thermal energy recovery.

On-site the Norske Skog's mill at Skogn has a system consisting of the following integrated plants, as they are part of the narrow system boundary (see Fig. 4.1).

1. A woodyard (W), where the softwood (Norwegian spruce, Picea abies) purchased from forestry is debarked. The bark obtained is sent to a boiler house plant for thermal energy recovery, while the wood logs and chips are sent to two different pulping facilities.

2. A thermo-mechanical pulping plant (TMP), consisting of two pulping facilities (TMP I and TMP II), where the primary pulp is obtained from pulping of wood logs and chips from wood yard. The main processing steps here are: debarking, chipping, two-step refining and bleaching. One of the refining steps in TMP II is carried out in a pressurised condition (4 bar) that makes it possible to recover a significant amount of thermal energy as steam (3.3 bar, 195^0C). The steam obtained here is first cleaned from solid impurities and then used to heat up the process water

for the paper drying machine.

3. A paper making plant (PMP), where the pulp suspensions of different solid consistencies is passed through three paper drying machines (PM 1, PM 2 and PM 3). Medium pressure steam from the boiler house plant and from the recovery facility at TMP II is supplied to the drying cylinders of each paper drying machine.

4. A de-inking plant (DIP), where the wastepaper is re-pulped into the secondary pulp by means of the following processing steps: a high consistency pulping, coarse and fine screening, two-stage chemical flotation, and bleaching. Intermediate steps of watering-dewatering facilitate removal of non-fibre items such as printing ink and fillers.

5. A wastewater treatment plant (WWTP), where the process wastewater from the TMP, PM, and DIP is bio-mechanically treated to diminish the content of the total phosphorus, nitrogen and suspended solids, and the oxygen demand of the biological and chemical materials in wastewater effluents. The treated water is discarded as into the local environment.

6. A boiler house plant (BHP), where a superheated steam (55 bar, 450^0C) is generated by means of a fluidised bed boiler (50 MW), burning bark, a moving grit boiler (35 MW), burning wood wastes and rejects, a oil boiler (25 MW), and an electric boiler (40 MW).

7. A natural gas-fired combined cycle power plant (NGPP) provides electricity to all above plants and to those located in the wide system boundary.

In the wide boundary, the system consists of the following facilities (see Fig. 4.1):

1. A wastepaper treatment plant (WPTP), where a partial degree of the collected wastepaper from the users in the region of Trondheim city is first sorted by quality and then pressed to form bales which are transported to the mill for paper recycling.

2. A municipal waste incineration plant (MWIP), where the whole (Scenario Z) or the partial degrees (Scenario L and H) of wastepaper collected from the users in Trondheim is incinerated with thermal energy recovery. The saturated steam (10 bar) obtained here is used in a heat district network in Trondheim.

3. A transportation network (T), where all requirements for transport of paper and wastepaper are included. This network comprises of the distances between the mill and Trondheim (80 km), between Trondheim and the wastepaper treatment plant (10 km), between Trondheim and the municipal waste incineration plant (8 km), and between the wastepaper treatment plant and the mill (90 km).

The processes in the forestry and in the gas and oil extraction industry, and those for production of chemicals (e.g. ink for paper printing) and other auxiliary materials, have not been considered in either exergy analysis or life cycle inventory analysis.

4.4 Data sources and assumptions

The annual environmental reports from the Norske Skog mill, Norske Skog - Internal Report (2000, 2003) released for the years 2000 and 2003 were used to make the inventory table of the material and energy inputs and outputs of the mill in Scenario Z and L, respectively. To this data the data for the electricity generation in a natural gas-fired combined cycle power plant (Keiseras 1991, Zvolinschi et al. 2002), and the data for the diesel fuel demand and the diesel combustion emissions in a 20-tonne capacity truck (Kuemmel et al. 1997), and the data for the wastepaper treatment plant (Arena et al. 2003) and for the municipal waste incineration plant (Heimdal Heating Plant 2000), were added to find the inventory tables for the scenarios in the wide system boundary. These data were used to estimate the inventory table for the system in Scenarios Z, L, and H, on the narrow and wide system boundaries.

The inventory tables obtained were used to calculate the life cycle inventory indicators. The exergy indicators were calculated from the exergy analysis that was performed based on the inventory table of the whole system as well as based on the inventory tables of for each plant, in both narrow and wide system boundary. Process description, assumptions and inventory tables of the components of the system are presented in Appendix C.

4.5 Results and discussion

4.5.1 The life cycle inventory analysis and its indicators

The life cycle inventory was aimed to identify and quantify the environmental interventions crossing the narrow and wide boundaries of the system for Scenarios Z, L and H. Inventory data were collected in two inventory tables, one for the inputs (Table 4.1) and one for the outputs (Table 4.2). These tables present the mass (M) and exergy (E) input and output data per one functional unit of the system (i.e., per one air-dried tonne of paper). The inputs were divided into non-renewable and renewable primary resources, while the outputs were divided into products, by-products, exhaust air and its components, discarded wastewater and its components, and solid wastes. The last row of Table 4.2 give the results of the mass and exergy balance of the system in every scenario and system boundary applied.

Similar inventory tables were obtained for every component of the system. These tables are given in Appendix C, see Tables C1-C13.

The following step in the life cycle inventory analysis was to evaluate the system by its demands for electricity, thermal energy, non-renewable and renewable primary resources (Fig. 4.2), and by its loads for emissions into air and water, and municipal solid waste (Figs. 4.3 - 4.7).

The demands for material and energy resources

Figure 4.2 gives the trends of the demands for electricity, thermal energy, non-renewable and renewable primary resource in the system.

The first observation is that the trends obtained for these demands favoured the system in the scenario with a high degree of wastepaper recycling (Scenario H). Both electricity and thermal energy demand are halved in Scenario H compared with Scenarios Z and L. The reason for this reduction is the partial substitution of thermo-mechanical pulping for production of primary pulp to de-inking pulping for production of secondary pulp.

The second observation is that the demand for electricity is not affected by the change of the system boundary, while the other demands are progressively influenced by this change, less in Scenario Z and more in Scenario H.

Table 4.1
Mass (M) and exergy (E) input inventory of the system in Scenarios Z, L and H, for the narrow and wide system boundaries (data are per air-dried tonne of paper), TS = total dry solids

	Scenario Z				Scenario L				Scenario H			
	Narrow scale		Wide scale		Narrow scale		Wide scale		Narrow scale		Wide scale	
Input flow description	M (t)	E (GJ)	M (t)	E (GJ)	M (t)	E (GJ)	M (t)	E (GJ)	M (t)	E (GJ)	M (t)	E (GJ)
Non-renewable resources												
Fossil fuel resources												
Natural gas for power plant	2.0	85.6	2.0	85.7	1.7	74.8	1.7	75.1	0.9	38.0	0.9	38.2
Diesel for transport	0.0	0.0	2.7	116.5	0.0	0.0	2.7	115.8	0.0	0.0	2.7	113.5
Oil for boiler house plant	0.0	0.1	0.0	0.1	0.0	0.1	0.0	0.1	0.1	4.1	0.1	4.1
Auxiliary material resources												
Chemicals for wastepaper treatment	0.0	0.0	0.0	0.1	0.0	0.0	0.0	0.1	0.0	0.0	0.0	0.1
Chemicals for wastewater treatment	0.0	0.0	0.0	0.0	0.0	0.0	0.0	0.0	0.0	0.0	0.0	0.0
Renewable resources												
Main material resources												
Softwood from forestry (47 %TS)	1.2	14.9	1.2	14.9	1.0	11.7	1.0	11.7	0.1	1.1	0.1	1.1
Bark from forestry (39.5 %TS)	0.2	1.1	0.2	1.1	0.1	0.7	0.1	0.7	0.0	0.2	0.0	0.2
Chips from forestry (47 %TS)	0.5	5.9	0.5	5.9	0.4	4.7	0.4	4.7	0.1	1.2	0.1	1.2
Sulphate cellulose (90 %TS)	0.0	0.0	0.0	0.0	0.0	0.0	0.0	0.0	0.0	0.0	0.0	0.0
Wastepaper from sorting site (90 %TS)	0.0	0.0	0.0	0.0	0.2	3.4	0.0	0.0	0.8	13.6	0.0	0.0
Biofuels												
Wood waste for boiler house plant (70 %TS)	0.0	0.2	0.0	0.2	0.1	0.3	0.1	0.3	0.1	0.3	0.1	0.3
Water resources												
Cooling water (10 grd C)	24.5	0.0	24.5	0.0	21.4	0.0	21.5	0.0	10.9	0.0	10.9	0.0
Fresh water for process (10 grd C)	23.0	0.0	36.9	0.0	26.0	0.0	37.0	0.0	12.1	0.0	12.9	0.0
Air resources												
Air for paper drying	13.5	0.0	13.5	0.0	14.2	0.0	14.2	0.0	12.0	0.0	12.0	0.0
Air for fuel burning	17.7	0.0	65.4	0.0	15.8	0.0	61.8	0.0	9.7	0.0	50.4	0.0
Total input	82.7	107.7	147.1	224.4	80.9	95.7	140.5	208.4	46.8	58.4	90.2	158.6

Table 4.2
Mass (M) and exergy (E) output inventory oo the system in Scenarios Z, L and H, for the narrow and wide system boundaries (data are per air-dried tonne of paper), BOD = biological oxygen demand, COD = chemical oxygen demand

	Scenario Z				Scenario L				Scenario H			
	Narrow scale		Wide scale		Narrow scale		Wide scale		Narrow scale		Wide scale	
Output flow description	M (t)	E (GJ)	M (t)	E (GJ)	M (t)	E (GJ)	M (t)	E (GJ)	M (t)	E (GJ)	M (t)	E (GJ)
Products												
Newsprint paper	1.0	17.0			1.0	17.0			1.0	17.0		
Thermal energy (sat. steam at 10 bar)			17.1	5.1			13.7	4.1			3.4	1.0
Internal combustion engine work		0.0		9.3		0.0		9.3		0.0		9.1
By-products												
Warm cooling water (18 grd C)	24.5	0.0	24.5	0.0	21.4	0.0	21.5	0.0	10.9	0.0	10.9	0.0
Exhaust air from hood (13 % water, 55 grd C)	15.4	0.3	15.4	0.3	16.2	0.2	16.2	0.2	13.5	0.0	13.5	0.0
Exhaust air and its components	19.7	0.6	68.1	2.4	17.5	0.5	64.1	2.3	10.7	0.3	51.5	1.9
Oxygen	3.9	0.5	7.0	0.9	3.5	0.4	6.8	0.8	2.2	0.3	5.0	0.6
Nitrogen	13.6	0.3	52.6	1.4	12.2	0.3	48.9	1.3	7.5	0.2	38.8	1.0
Carbon dioxide	5.6	2.5	16.0	7.3	4.9	2.2	15.0	6.8	2.5	1.1	11.6	5.2
Nitrogen monoxide, in kg and MJ	9.4	0.2	103.3	2.7	8.5	0.2	101.7	2.6	4.6	0.1	96.0	2.5
Carbon monoxide, in kg and MJ	158.7	1558.5	708.9	6961.6	147.5	1448.5	694.2	6816.8	3.8	37.1	539.8	4818.4
Hydrocarbons, in kg and MJ	6.8	110.1	103.9	1693.5	6.2	101.3	102.7	1674.5	0.7	10.9	95.3	1553.4
Particulates, in kg and MJ	30.0	1.8	2758.6	1.8	26.2	1.6	2737.3	1.6	13.4	0.8	2671.6	0.8
Discarded wastewater and its components	22.0	0.0	21.5	0.0	24.7	0.0	24.7	0.0	10.6	0.0	10.6	0.0
Biological material (BOD7), in kg and MJ	4.0	0.1	4.0	0.1	3.4	0.1	3.2	0.1	0.8	0.0	0.8	0.0
Organic material (COD), in kg and MJ	13.5	0.5	13.5	0.5	11.3	0.4	10.8	0.4	2.7	0.1	2.7	0.1
Total nitrogen, in g and kJ	159.0	30.1	159.0	30.1	133.6	25.3	127.2	24.0	31.8	6.0	31.8	6.0
Total phosphorus, in g and kJ	15.1	0.1	15.1	0.1	12.7	0.0	12.1	0.0	3.0	0.0	3.0	0.0
Suspended solids, in g and kJ	2630.0	5.3	2630.0	5.3	2209.2	4.4	2104.0	4.2	526.0	1.1	526.0	1.1
Solid wastes												
Ash,solid dust	0.1	0.0	0.4	0.1	0.1	0.0	0.3	0.1	0.2	0.0	0.2	0.0
Total output	82.7	17.9	147.1	17.2	80.9	17.8	140.5	15.9	46.8	17.3	90.1	12.1
Input (from Table 4.1) - Output	0.0	89.8	0.0	207.2	0.0	77.9	0.0	192.5	0.0	41.1	0.0	146.5

The third observation is that the demand for non-renewable primary resources is largely affected by the change of system boundary. Including the transport network in the system boundary has a large contribution to the demand of non-renewable primary resources of the whole system. However, this demand is decreasing for Scenario H compared with Scenarios Z and L, because of the decrease of the demand of natural gas that is used for electricity generation.

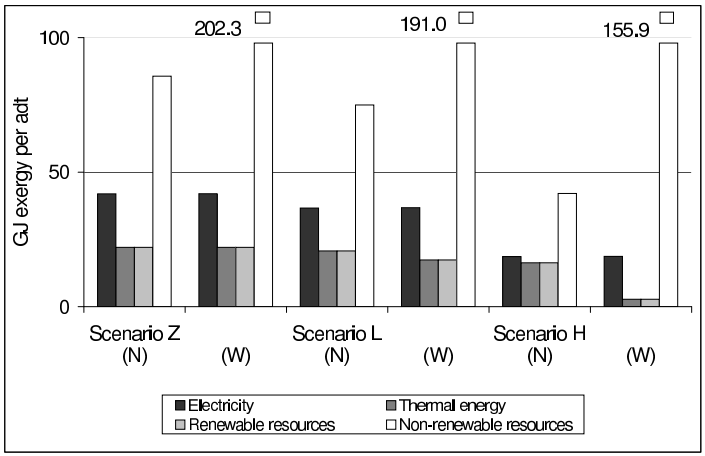

Figure 4.2. The demands for electricity, thermal energy, renewable and non-renewable primary resources of the system in Scenarios Z, L and H, for the narrow (N) and wide (S) boundaries.

The loads of emissions into air and water, and solid wastes
Figures 4.3 - 4.7 illustrate the trends of the emissions of carbon dioxide, nitrogen monoxide, and carbon monoxide into the atmosphere, the emissions of chemical oxygen demand matter, nitrogen and phosphorus into the water effluent, and the amount of municipal solid waste.

Figure 4.3 shows that the trends in CO_2 emissions favour the system with a high degree of paper recycling (Scenario H). The load of the CO_2 emissions from Scenario H is the lowest one compared with that from Scenarios Z and L. The CO_2 emissions are reduced from 5.6 (Scenario Z) to 2.5 tonnes CO_2/adt (Scenario H). The figure also shows that the load of CO_2 emission is highly depended on the system boundary. In the wide boundary, the load of CO_2 emissions from the system is decreased from 16 (Scenario Z) to 11.6 tonnes

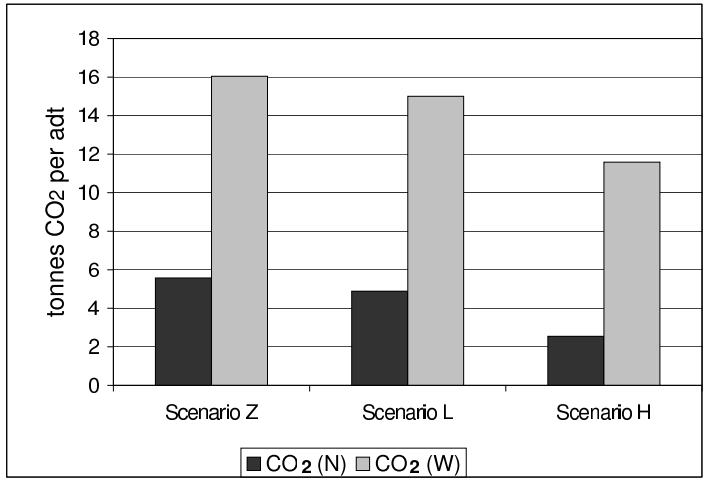

Figure 4.3. CO_2 emissions from the system in Scenarios Z, L and H, for the narrow (N) and wide (W) system boundaries.

CO_2/adt (Scenario H). The difference that occurs between the narrow and wide scenario is the contribution that the transportation network has on the cumulative load of CO_2 emission of the system.

Scenario H is also favoured by the trends given in Fig. 4.4 for the emissions of nitrogen monoxide and carbon monoxide into the atmosphere. The decrease in the transportation demand from Scenario Z to Scenario H reduces the load of both NO_x and CO emissions. The load of NO_x emission is reduced from 9.4 in Scenario Z to 4.6 kg NO_x/adt in Scenario H, when the system has a narrow boundary, while it is reduced from 103 in Scenario Z to 96 kg NO_x/adt in Scenario H when the system has a wide boundary.

Figures 4.5 and 4.6 give the loads of the emissions of chemical oxygen demand (COD) matter, nitrogen (N_t) and phosphorus (P_t) in the wastewater effluent that is discarded into the local fjord. These loads are reduced when a high degree of wastepaper is recycled and used for newsprint paper production. The change in system boundary does not affect the values of these loads due to the fact the processes beyond those for pulp and paper production do not have such kinds of emissions. Figure 4.7 shows that recycling a high degree of wastepaper has a slightly negative effect on the amount of municipal solid waste (MSW) for the system in Scenario H with narrow boundary, while it

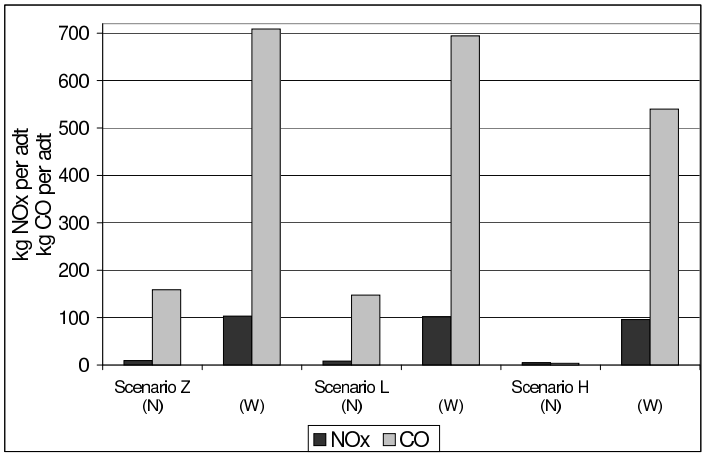

Figure 4.4. NO_x and CO emissions from the system in Scenarios Z, L, and H, for the narrow (N) and wide (W) system boundaries.

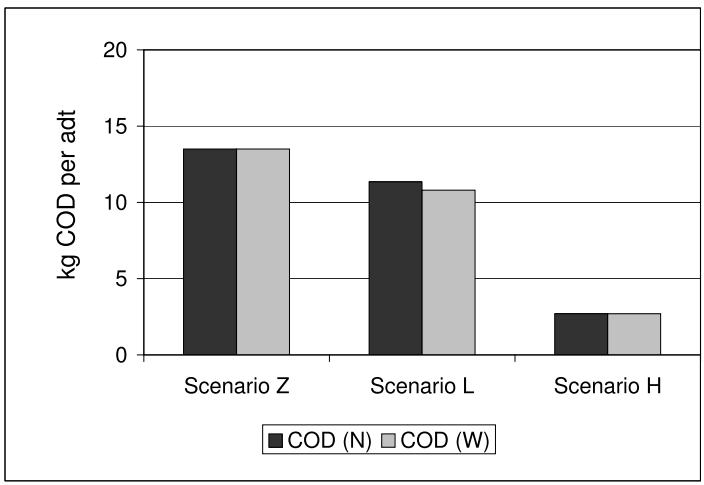

Figure 4.5. Chemical oxygen demand (COD) of the wastewater effluent from the system in Scenarios Z, L and H, for the narrow (N) and wide (W) system boundaries.

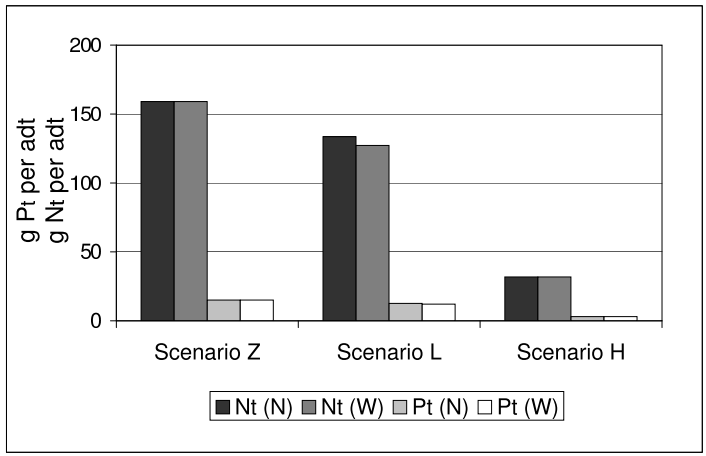

Figure 4.6. Total nitrogen (N_t) and phosphorus (P_t) emissions in the waste water effluent from the system in Scenarios Z, L and H, for the narrow (N) and wide (W) system boundaries.

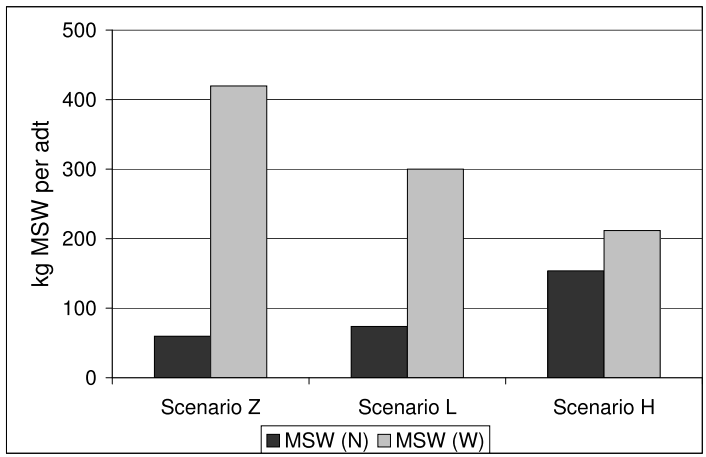

Figure 4.7. Municipal solid waste (MSW) of the system in Scenarios Z, L and H, for the narrow (N) and wide (W) system boundaries.

has a large positive effect for the system in Scenario H with wide boundary. The trends in the figure give the amount of the municipal solid waste is 70 kg MSW/adt for Scenario Z and 160 kg MSW/adt for Scenario H, when the system has a narrow boundary, while it is 410 kg for Scenario Z and 210 kg for Scenario H, when the system has a wide boundary.

4.5.2 The exergy analysis and exergy-based indicators

The exergy analysis was aimed to quantify based on exergy the inputs, outputs, and losses of the system in each scenario applied (Tables 4.1 and 4.2), as well as the inputs, outputs, and losses of the components in the system (Tables C1-C13). Based on these data, the exergy indicators (Table 4.4 and Fig. 4.8) were determined using Eqs. (4.2) - (4.4).

Exergy losses
The total exergy loss of the system in Scenarios Z, L and H is given in the last row of Tables 4.2 and 4.3, respectively. The values in Table 4.2 were obtained from the exergy balance (Eq. (4.1)) applied to the input/output exergy inventory data of the whole system (Tables 4.1 and 4.2), while the values in Table 4.3 were obtained from the sum of the exergy losses that occur in each component in the system (Tables C1-C13). It is important to observe that these values match with good accuracy. This kind of comparison may be used to reveal the accuracy of the inventory data collected at the boundary of the system and its relation with the processes that take place inside the system.

Table 4.2 shows that, for the narrow boundary, the system in Scenario Z has a total exergy loss of 90 GJ/adt, while in Scenarios L and H it has a total exergy loss of 78 and 41 GJ/adt, respectively. The total exergy loss became 207 GJ/adt for the system in Scenario Z with a wide boundary, and 150 GJ/adt for that in Scenario H with a wide boundary. The reason behind this increase is the contribution of the transportation network to the total exergy loss of the system (see Table 4.3, the row for transport, or Table C13).

Table 4.3 shows that the transportation network, the power plant and the boiler house plant are the components with the largest exergy losses, and thus, they are the largest contributors to the total exergy loss of the system with wide boundary. The exergy loss distribution (D in Table 4.3) gives that 52% of the total exergy loss of the system is due to the transportation network in Scenario Z, while 71% is in Scenario H. Although the exergy efficiency is high (ϵ = 49%), the power plant accounted for 21% of the total exergy loss in Scenario

Z, while it accounted for 20% and 13% in Scenario L and H, respectively.

For the narrow system boundary, the amount and the distribution of exergy losses in the system are different (not shown). The power plant (with $D = 53\%$) and the boiler house plant (with $D = 25\%$) remain the main contributors to the total exergy loss of the system. The next places are taken by the paper-making plant (with $D = 12\%$) and thermo-mechanical pulping plant ($D = 8\%$).

In addition to the exergy losses and their distribution in the system, the exergy efficiencies of the components of the system are important. We can see from Table 4.3 that the exergy efficiencies of the components of the system are not much effected by either the change of scenario or the change of system's boundary (not shown). There is one exception, however. It is the case for the paper-making plant (see Table 4.3, the row for paper-making plant and the columns for ϵs). The different exergy efficiencies obtained for the paper-making plant can be explained by the fact that this plant operated with different parameters for the paper machines and with different exergy inputs (see Tables C4 and C5).

It is possible to disaggregate the exergy losses further, and thus to determine the exergy efficiency at a more disaggregated level of the system. For example, the determination of the exergy losses among the components of the paper-making plant may facilitate us to find opportunities to improve this plant. In Appendix C, we have analysed the three paper machines in the paper-making plant in each scenario (see Tables C4 and C5). It is then important to address these opportunities by evaluating the whole system.

To summarise here, the exergy analysis revealed that the power plant and the boiler house plant ought to be more efficient. One solution would be to convert a part of the thermo-mechanical exergy of the steam generated in the boiler house plant into mechanical power by means of steam turbines. Another solution, which requires higher investment on-site the mill, is to replace the existing boiler house plant with a heat and power co-generation plant. Thus, both electricity and thermal energy demand can be supplied by the same source. It is obvious that the exergy efficiency of transportation ought to be improved as much as possible. The best choices of transportation equipment, fuel and logistics should be found in order to lower the influence of the transportation network to the system.

Exergy-based indicators

Table 4.4 presents the exergy indicators and the terms used to calculate these indicators. Equations (4.2) - (4.4) were applied to determine the values of these indicators for the system in Scenarios Z, L and H, with narrow (N) and wide (W) system boundary. The values obtained for the indicators are also presented in Fig. 4.8 to illustrate the trends of these indicators due to the change of wastepaper recycling scenario and due to the change of system boundary.

Table 4.3 Exergy loss (E_{loss}, in GJ/adt), exergy loss distribution (D, in %), and exergy efficiency (ϵ, in %) of the components of the system in Scenarios Z, L and H, for the wide system boundary.

System	Scenario Z			Scenario L			Scenario H		
	E_{loss}	D	ϵ	E_{loss}	D	ϵ	E_{loss}	D	ϵ
W	0.53	0.3	97.6	0.77	0.4	95.5	0.09	0.1	97.6
TMP	8.13	4.0	78.6	6.37	3.3	78.5	1.51	1.0	74.9
PMP	4.90	2.4	80.4	7.74	4.0	68.4	3.42	2.4	85.2
BHP	28.41	14.0	22.8	23.8	12.5	22.8	14.3	9.9	22.2
NGPP	43.0	21.3	49.7	37.7	19.7	49.7	19.2	13.3	49.7
DIP	0.0	0.0	-	0.12	0.1	97.5	0.4	0.3	97.7
WWTP	0.03	0.0	10.7	0.05	10.7	0.02	0.0	10.7	
T	105.6	52.1	9.4	104.9	54.9	9.4	102.9	71.3	0.4
WPTP	0.0	0.0	-	0.09	0.0	97.3	0.09	0.1	99.3
MWIP	11.9	5.9	31.1	9.5	5.0	31.1	2.4	1.6	31.1
Total	202.5	100.0		191.2	100.0		144.3	100.0	

Abbreviations: W = woodyard; TMP = thermo-mechanical pulping plant; PMP = paper mill plant; BHP = boiler house plant; NGPP = natural gas-fired power plant; DIP = de-inking plant; WWTP = wastewater treatment plant; T = transport; WPTP = wastepaper treatment plant; MWIP = municipal waste incineration plant.

As we can see from Table 4.4, the exergy data for the calculation of exergy indicators and the values of exergy indicators were affected by the change in the degree of wastepaper utilization for newsprint paper production. The higher the degree of wastepaper utilization as feedstock for the paper mill the lower was the total exergy input and output of the system, for both the narrow and wide boundaries. The opposite effect was found for the total renewable exergy input when the system boundary is wide. This can be explained by the fact that the exergy of the wastepaper is not accounted for here, because

Table 4.4 The exergy input (E_{in}), exergy output (E_{out}), renewable exergy input ($E_{in,\ renewable}$), exergy for abatement ($E_{in,\ abatement}$), and the exergy indicators (ϵ - exergy efficiency, α - exergy renewability, ζ - environmental compatibility) of the system in Scenarios Z, L and H, for the narrow (N) and wide (W) system boundaries.

	Scenario Z		Scenario L		Scenario H	
	N	W	N	W	N	W
Exergy input, E_{in} (GJ/adt)	107.7	224.4	95.7	208.4	58.4	158.6
Exergy output, E_{out} (GJ/adt)	17.9	17.1	17.8	15.8	17.3	12.1
Renewable exergy input, $E_{in,\ renewable}$ (GJ/adt)	22.1	22.1	20.7	17.3	16.3	2.8
Exergy for abatement, $E_{in,\ abatement}$ (GJ/adt)	0.0	116.6	1.0	116.9	2.7	116.3
ϵ (-)	0.17	0.08	0.19	0.08	0.30	0.08
α (-)	0.20	0.10	0.22	0.08	0.28	0.02
ζ (-)	0.00	0.34	0.01	0.36	0.04	0.42

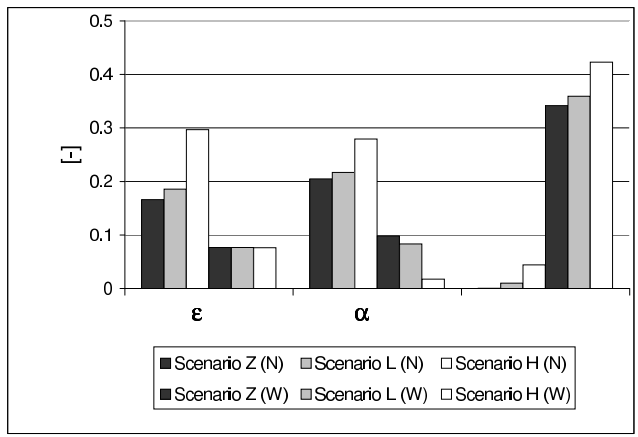

Figure 4.8. Exergy efficiency (ϵ), exergy renewability (α) and environmental compatibility (ζ) of the system in Scenarios Z, L and H, for the narrow (N) and wide (W) system boundaries.

it is a resource that was used inside the boundary of the system, and thus, it did not cross the boundary. The exergy input that was spent for abatement of wastes increased with the degree of wastepaper utilization in the mill as well as with the extension of the system boundary. The higher the degree of wastepaper utilization in the mill the higher the amount of emissions to wastewater effluent, which in effect required more exergy input to be spent in order to acquire the standard regulation regarding the level of water-borne emissions. The transportation and the wastepaper sorting and incineration facilities were regarded in this study as means to abate the wastepaper. The exergy inputs to these parts of the system were accounted as exergy needs for the abatement of the wastepaper. This is the reason for the large numbers obtained for the exergy required for abatement in Scenario Z, L and H with wide boundary (see row four, columns two, four and six, in Table 4.4).

When looking at Figure 4.8, one can see that the three exergy indicators favour Scenario H, when they addressed the system with a narrow boundary. This means that a high degree of wastepaper utilization in the mill is an advantage for the mill.

The exergy efficiency (ϵ) of the system in Scenario Z ($\epsilon = 0.17$) was the lower than that of the system in Scenario L ($\epsilon = 0.19$) and Scenario H ($\epsilon = 0.30$). This means that Scenario H is favoured by the exergy efficiency indicator when the system was in the narrow boundary. No preference for any scenario is given by the exergy efficiency indicator when the system was in the wide boundary. Here, the value of ϵ was 0.08 for all scenarios. It is important to remark the significant reduction of exergy efficiency due to the change of system boundary. This reduction can be explained by the fact that the wood-based exergy input of the system in the narrow boundary was converted into a product with high exergy content (i.e. newsprint paper), while it was converted into a product with low exergy content (i.e. low-pressure steam) in the system with a wide boundary.

The exergy renewability (α) of the system in Scenario Z was 0.20. It increased with the degree of paper recycling in the system; α was 0.22 and 0.28 for the system in Scenarios L and H, respectively. The opposite effect on α was found when the system boundary was wide. Here, the value of α was reduced from 0.1 in Scenario Z to 0.02 in Scenario H. This reduction can be explained by the additional non-renewable exergy input required for wastepaper transportation and treatment, while the amount of renewable exergy input is reduced.

The environmental compatibility (ζ) preferred the system in Scenario H over

Scenarios Z and L, for both system boundaries. The values of ζ were less than 0.1 for all scenarios with a narrow boundary, and were around 0.3 for Scenarios Z and L and about 0.4 for Scenario H, for the wide system boundary. The rise of ζ by a factor of three is due to the fact that the amount of exergy needed for the abatement of the wastewater and wastepaper was considerably higher in the system with a wide boundary compared to that with narrow boundary (see fourth row in Table 4.4), while the amount of exergy needed for the production of paper was only increased by a factor of two (see first row in Table 4.4).

4.6 Conclusions

We found that exergy analysis should be complementary used to the life cycle inventory analysis in order to determine the best option for wastepaper recycling. We have evaluated three different scenarios for wastepaper recycling. The scenarios concerned a zero, a low and a high degree of wastepaper utilization as feedstock for paper production. Several indicators based on the exergy and life cycle inventory analysis were used to find the best degree of wastepaper recycling.

The results of the study showed that the scenario with a high degree of paper recycling is the best alternative as confirmed by almost all exergy indicators and life cycle inventory indicators. The inventory tables (Tables 4.1 and 4.2), usually requested to be presented on mass basis in ISO-14040 (1996), ISO-14041 (1997), were here presented on both mass and exergy bases. This revealed the following additional characteristics of each scenario: the exergy demands of resources, the exergy loads of emissions and wastes, the exergy losses and indicators of the system.

The difficulty in accounting for different kinds of material and energy resources in the life cycle inventory analysis was alleviated using exergy. Thus, the same basis was applied to compare the demands for electricity, thermal energy, renewable and non-renewable primary resources. Although the exergy values of emissions and wastes cannot adequately measure the impact of waste streams on the environment, they can show the importance (from an exergetic efficiency point of view) of preventing pollution or collecting and recycling the waste in more aggregated levels of the system. Comparisons of exergy loss between paper production and recycling scenarios revealed the amount, distributions and locations for this loss. If the exergy losses associated with wastepaper transportation are excluded, the results showed that the power plant, the boiler house plant and the paper making plant were the greatest contributors to the

total exergy loss of the system, and thus, the components that should be first improved.

The work reported here should help waste planners in resolving the increasing concern about the growing amount of municipal solid waste in the future. This paper has demonstrated that the concept of exergy may provide quantitative insights into the resource use and environmental performance of paper production and recycling.

Acknowledgement

Norske Skog at Skogn, Norway, is thanked for making all the data available for the analysis.

Chapter 5

The second law optimal operation of a paper drying machine

Anita Zvolinschi[a,b], Eivind Johannessen[a] and Signe Kjelstrup[a]

[a]Department of Chemistry
[b]Industrial Ecology Programme Norwegian University of Science and Technology
NO-7491 Trondheim, Norway

This chapter is based on an article in

Chemical Engineering Science (2006), Vol. 61, pp. 3653-3662.

Abstract

Paper drying is an exergy costly operation, so also a few per cent savings may be of importance. The entropy production for the paper drying process was therefore optimised for a conventional multi-cylinder drying machine, the PM2 newsprint machine at Norske Skog ASA in Skogn, Norway. The machine has 51 cylinders grouped in three drying groups; the cylinders are either heated from the inside by steam, unheated or operated under vacuum conditions. The same inlet drying air is supplied in all upper air-pockets of the machine. Our drying model for the paper temperature profile was first compared with the measured data from the machine. The total entropy production of the drying process was next calculated, and then minimised subject to a fixed outlet paper moisture content. Inlet humidity and cylinder group conditions were varied. Optimum conditions were obtained for a range of inlet air humidities, and for different cylinder groupings. We found that it was very favourable to increase the inlet air humidity. Other changes had a negligible effect on the total entropy production. The results further pointed to the need for a revision of the current model, as the second law of thermodynamics was violated at high air humidities with this model.

Keywords: Mass transport; Heat transport; Evaporation; Entropy production; Paper drying; Optimisation

5.1 Introduction

To diminish energy resource utilisation is an important task for chemical engineers. This means that excess exergy losses should be avoided. Exergy analysis normally takes a black-box approach; it calculates the exergy loss from the input and output exergy streams of a definite system. A black-box approach can be used to minimise the exergy losses in a process or a process chain, but a local description of entropy production gives more details. Such an approach was used to minimise the entropy production in chemical reactors (Nummedal et al. 2005) and distillation columns (Røsjorde et al. 2005b). We study here the paper drying process, which has been reported as a process with high heat (Manninen et al. 2002) and high exergy requirements (de Beer et al. 1998). The exergy loss of a specific paper drying machine has already been presented (Zvolinschi et al. 2003).

No attempts to map and minimise the entropy production of a paper drying

process have been done until now. Therefore, we shall formulate, calculate and optimise the entropy production for a conventional paper drying machine. The machine consists of 51 internal steam-heated and unheated cylinders, or cylinders operated under vacuum.

The total entropy production is minimised by applying a constrained second-law optimisation method. The same method was used to minimise the entropy production in chemical reactors (de Koeijer et al. 2004a, Nummedal et al. 2005). In our study, the temperatures of the saturated steam supplied to the drying groups are the optimisation variables, and the paper dryness at the dry-end of the machine is the constraint. This product quality parameter is a logical constraint. The effects of varying the inlet air conditions and re-grouping the drying groups on the total entropy production are of interest. We shall discuss the meaning of the second-law optimal operation of the paper drying machine, and advise on a more energy efficient process.

The equations for the mass and heat fluxes, and the relations for the heat transfer coefficients used in our drying model, are common in paper drying modelling and simulation. Several models have been presented in the literature, the first was given by Nissan (1956). Recent work validated the simulation results with measured data in industrial machines (Wilhelmsson et al. 1993, Sidwall et al. 1999, Nilsson 2004). In all these models, the analogy between heat and mass transfer (Incropera and Witt 1985) was used to find the heat transfer coefficient. Although this analogy has predicted paper temperature and moisture content profiles that were in good agreement with the measurements, we shall see that it also gives a negative entropy production in several locations in the paper drying machine. This suggests that future work should make an effort to revise current models. We shall suggest directions for such work.

5.2 The paper drying machine

The machine that we studied, the PM2 Valmet paper drying machine at Norske Skog, Skogn, Norway, produces newsprint paper with a basis weight of 45 g dry paper/m^2. The production capacity is about 540 000 tonnes per year. The paper furnish contains 75% thermo-mechanical pulp processed from virgin wood and 25% de-inked pulp from recycled paper.

A schematic of the cross-section of the paper drying machine is shown in Fig. 5.1. In this high-speed machine the paper sheet travels with an aver-

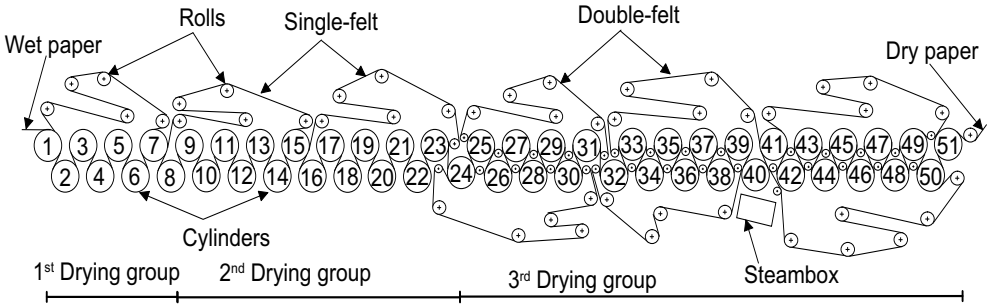

Figure 5.1. Cross-section of the paper drying machine.

age speed of 20.8 m/s. A closed and ventilated room, called the machine hood, surrounds the entire machine, which is operated under atmospheric pressure. The paper sheet has the following parameters: a width of 6.65 m, a total length of 198.8 m, a length between two cylinders of 1 m, and a wrap angle of 220°.

The inlet drying air is supplied with same parameters in all air-pockets, which are located between all upper cylinders of the machine. The cylinders have a diameter of 1.5 m, and they are grouped in three drying groups that conform with the specifications given in Table 5.1. The quality of steam supplied and its distribution into the drying groups can be changed as other paper grades are produced, or as the region between the two drying regimes (i.e. the constant and falling-rate drying regimes) is modified. In addition, the supply of steam in each individual cylinder can be maintained off or on, the exception is for those cylinders operated under vacuum.

There are two types of felt configurations in the machine; the single-felt configuration in the first and second drying group, and the double-felt one in the third group, see Fig. 5.1. The felt configuration in the paper drying machine can be also modified. For example, the second drying group can be operated with a double-felt configuration.

Table 5.1. Drying group specifications

Drying group	Cylinders	Heated cylinders	Unheated cylinders
First	1 – 8	3, 5, 7	1
Second	9 – 23	all odd numbers	16, 18, 20, 22
Third	24 – 51	24 – 30, 32 – 50	31, 51

Cylinders that are not mentioned are operated under vacuum conditions.

The drying process occurs through repeated modes, depending on where the paper sheet is located in the drying machine. We identified five types of modes that were defined by letters from A to E. In drying modes A, C and E, the paper sheet travels on a cylinder, heated, unheated or operated with vacuum, respectively. In drying modes B and D, the paper sheet travels between two cylinders, being in contact with the felt on one or two sides, respectively. The whole machine is a combination of 102 drying modes. As we shall see, the change of the mode type throughout the drying machine leads to a discontinuous variation in the paper temperature. Near heated cylinders the paper temperature is high, away from them, it is low.

The operating parameters of the drying machine that are considered are given in Table 5.2. These data and those given in Table 5.1 and in the text above, defined the reference system, and they were the starting point for the optimisation.

Table 5.2. Operating parameters of the PM2 Valmet paper drying machine

Parameter	Value
Inlet paper temperature, ^{0}C	40
Inlet paper moisture content, kg H_2O/kg dry paper	1.20
Outlet paper moisture content, kg H_2O/kg dry paper	0.07
Inlet air temperature, ^{0}C	45
Inlet air humidity, kg H_2O/kg dry air	0.026
Inlet steam temperature and pressure, ^{0}C / bar	
First drying group	89 / 1.06
Second drying group	111 / 1.48
Third drying group	121 / 2.04

5.3 Balance equations

The paper travels from the wet to the dry-end of the machine, see Fig. 5.1. We defined this travel direction as the z-direction. We consider the balance equations for mass and internal energy in a small element dz normal to the paper sheet. Gradients within the paper sheet, in the y- and x- directions of the paper sheet are neglected. The heat radiated from the paper to air is also neglected.

In stationary state, the conservation of mass gives

$$\frac{dw}{dz} = -\frac{n}{v\ B}\ J \tag{5.1}$$

while the conservation of internal energy gives

$$\frac{dh_p}{dz} = \frac{n}{v\ B}(J_{q,\mathrm{cyl}} + J_{q,\mathrm{air}} - J h_{\mathrm{H_2O}}^{\mathrm{in\ air}}(T_{\mathrm{air}})), \tag{5.2}$$

where h_p and $h_{\mathrm{H_2O}}^{\mathrm{in\ air}}$ are the specific enthalpy of paper and vapour water in air, respectively, J is the evaporation flux of water from the paper sheet, $J_{q,\mathrm{cyl}}$ and $J_{q,\mathrm{air}}$ are the heat fluxes from cylinder to paper, and from air to paper, respectively. The factor n equals 1 in case of the drying modes A, C and E, or it equals 2 in case of the drying modes B and D.

Using the assumption that the specific enthalpy of paper is

$$h_p = h_{\mathrm{dry}-p}(T_p) + w h_{\mathrm{H_2O}}^{\mathrm{in\ paper}}(T_p, w) \tag{5.3}$$

and the derivative of this equation with respect to dz is

$$\begin{aligned}
\frac{dh_p}{dz} &= \frac{\partial h_p}{\partial T_p}\frac{dT_p}{dz} + \frac{\partial h_p}{\partial w}\frac{dw}{dz} \\
&= C_{p,p}\frac{dT_p}{dz} + \frac{\partial\left(w h_{\mathrm{H_2O}}^{\mathrm{in\ paper}}(T_p, w)\right)}{\partial w}\frac{dw}{dz} \\
&= C_{p,p}\frac{dT_p}{dz} - \frac{J}{v\ B}h_{\mathrm{H_2O}}^{\mathrm{in\ air}}(T_{air}) + \frac{J}{v\ B}\frac{\partial(w\Delta H)}{\partial w}
\end{aligned} \tag{5.4}$$

where in the last equality Eq. (5.1) was used, one can obtain by introducing Eq. (5.4) in Eq. (5.2) and after some rearrangement

$$\frac{dT_p}{dz} = \frac{n}{v\ B\ C_{p,p}}\left(J_{q,\mathrm{cyl}} + J_{q,\mathrm{air}} - J\frac{\partial(w\Delta H)}{\partial w}\right). \tag{5.5}$$

Integration of Eqs. (5.1) and (5.5) gives the change in the paper moisture content (w) and paper temperature (T_p), respectively, as the paper sheet travels through the whole drying machine. The solution of Eq. (5.5) can be compared with the measured data.

5.4 The entropy production

The local entropy production (σ) is found from the entropy balance of a small element dz with unit cross-sectional area. The result is

$$\sigma = b\left(v\ B\frac{ds_p}{dz} - \frac{J_{q,\mathrm{cyl}}}{T_{\mathrm{cyl}}} - \frac{J_{q,\mathrm{air}}}{T_{\mathrm{air}}} - Js^{\text{in air}}_{\mathrm{H_2O}}(T_{\mathrm{air}})\right). \tag{5.6}$$

Using the assumption that the specific entropy of paper is

$$s_p = s_{\mathrm{dry}-p}(T_p) + ws^{\text{in paper}}_{\mathrm{H_2O}}(T_p, w) \tag{5.7}$$

and the derivative of this equation with respect to dz is

$$\begin{aligned}
\frac{ds_p}{dz} &= \frac{\partial s_p}{\partial T_p}\frac{dT_p}{dz} + \frac{\partial s_p}{\partial w}\frac{dw}{dz} \\
&= \frac{C_{p,p}}{T_p}\frac{dT_p}{dz} + \frac{\partial\left(ws^{\text{in paper}}_{\mathrm{H_2O}}(T_p, w)\right)}{dw}\frac{dw}{dz} \\
&= \frac{C_{p,p}}{T_p}\frac{dT_p}{dz} - \frac{J}{v\ B}s^{\text{in air}}_{\mathrm{H_2O}}(T_{\mathrm{air}}) + \frac{J}{v\ B}\frac{\partial(w\Delta S)}{\partial w}
\end{aligned} \tag{5.8}$$

(where in the last equality we have used again Eq. (5.1)), one can obtain after some rearrangement

$$\begin{aligned}
\sigma = \ nb\Big[&J_{q,\mathrm{cyl}}\left(\tfrac{1}{T_p} - \tfrac{1}{T_{\mathrm{cyl}}}\right) + J_{q,\mathrm{air}}\left(\tfrac{1}{T_p} - \tfrac{1}{T_{\mathrm{air}}}\right) \\
&+J\left(-\tfrac{1}{T_p}\tfrac{\partial(w\Delta H)}{\partial w} + \tfrac{\partial(w\Delta S)}{\partial w}\right)\Big].
\end{aligned} \tag{5.9}$$

Here, ΔH and ΔS are the enthalpy and entropy change, respectively, for water between the states in the paper sheet and the surrounding air. The thermodynamic relations of ΔH and ΔS are given in the Appendix D. The value of σ must be always positive according to the second law of thermodynamics. The first two terms on the right-hand side give the contributions to the entropy

production from the heat transport, while the last term gives the contribution from the mass transport. Thermodynamic forces and fluxes acting in the paper drying process can now be identified, referring to Eq. 5.9. The two driving forces for heat transport are $(1/T_p - 1/T_{\text{cyl}})$ and $(1/T_p - 1/T_{\text{air}})$, and the driving force for the mass transport is the expression that is multiplied with J in Eq. (5.9).

Integration of Eq. (5.9) over the total length of the paper sheet, from the wet to the dry-end of the drying machine, gives the total entropy production in the drying machine,

$$\left(\frac{dS}{dt}\right)_{\text{irr}} = \int_0^L \sigma \, dz \tag{5.10}$$

This is the objective function to be minimised subject to a fixed outlet paper moisture content (w_{out}= 0.07 kg H_2O/kg dry paper).

5.4.1 Flux equations for the paper drying process

The heat flux equations are normally written as

$$J_{q,\text{cyl}} = h_{\text{cyl}-p}(T_{\text{cyl}} - T_p) = h_{\text{cyl}-p} T_{\text{cyl}} T_p \left(\frac{1}{T_p} - \frac{1}{T_{\text{cyl}}}\right) \tag{5.11}$$

and

$$J_{q,\text{air}} = h_{p-\text{air}}(T_{\text{air}} - T_p) = h_{p-\text{air}} T_{\text{air}} T_p \left(\frac{1}{T_p} - \frac{1}{T_{\text{air}}}\right), \tag{5.12}$$

where $h_{\text{cyl}-p}$ and $h_{p-\text{air}}$ are the heat transfer coefficients from cylinder to paper and from paper to air, respectively. The relations of $h_{\text{cyl}-p}$ and $h_{p-\text{air}}$ are given in Appendix E.

Sherwood (1930) did pioneering work in the area of the drying of pulp and paper products. He showed that the resistance to mass transport is located in the air boundary layer surrounding the paper sheet, a layer which has a laminar flow. Starting from this, Incropera and Witt (Incropera and Witt 1985) derived the evaporation flux of water using the analogy of the heat and mass transfer. The analogy gave heat transfer coefficients instead of the mass transfer ones in the evaporation flux. Accordingly, several authors (Soininen

1995, Yeo et al. 2004, Nilsson 2004) calculated the evaporation flux of water from the paper sheet surface using

$$J = \frac{1}{C_{p,\mathrm{dry-air}} + X^* \, C_{p,\mathrm{H_2O}}} h_{p-\mathrm{air}}(X^* - X_{\mathrm{in,air}}). \tag{5.13}$$

Here, $C_{p,\mathrm{dry-air}}$ and $C_{p,\mathrm{H_2O}}$ are the heat capacities of dry air and water vapour, respectively, X^* is the saturation humidity above the paper sheet, and $X_{\mathrm{in,air}}$ is the inlet air humidity.

More sophisticated models are available for the paper-cylinder heat transfer coefficient. In the model used here, only the paper moisture content is important for the contact heat transfer coefficient (Rhodius and Gottsching 1979), while it is known from Wilhelmsson et al. (1994) that also the paper travelling speed and the felt tension and topography have influence on the contact heat transfer coefficient. An expression for this coefficient as function of the paper moisture content, paper speed, and felting type has been proposed by Yeo et al. (2004).

By comparing Eqs. (5.9) and (5.13), one can see that the driving forces for the mass transport are not the same. In the expression of J in Eq. (5.13), the driving force is $(X^* - X_{\mathrm{in,air}})$, while the expression of σ in Eq. (5.9), will give a different relation for the mass transport driving force. So far, the entropy production has not been used to define flux equations for paper drying. Because data available only for the fluxes given above, we shall proceed with these.

We shall see that the use of Eq. (5.13) can give a negative local entropy production, which means that Eq. (5.13) cannot correctly predict the evaporation flux for the entire range of operating conditions of the paper drying machine.

5.5 Calculations

We first analysed the PM2 paper drying machine as it is now operated, i.e. the reference system. The distribution of paper moisture content (w) and temperature (T_p) were found by numerical integration of Eqs. (5.1) and (5.5), over the total length of the paper sheet in the drying machine. The input data used for the calculation are given in Tables 5.1 and 5.2 and in the text in Section 5.2. Physical properties and heat capacities of the air and water vapour were taken from Pakowski et al. (1991).

The optimisation was performed numerically using the Matlab ® 6.1.0 (R12.1) optimisation toolbox function *fmincon*, which uses a sequential quadratic programming method to find a minimum of the objective function. The temperatures of the saturated steam supplied to the drying groups were the optimization variables, and the paper moisture content of 0.07 kg H_2O/kg dry paper was the constraint in the optimisation. The following lower and upper bounds were applied to the steam temperatures: 65 and 120^0C for that supplied in the first drying group, and 85 and 130^0C for that supplied in the second group. The temperature in the third group was chosen such that the specified outlet paper moisture content was fulfilled for a given choice of temperatures in the first two groups.

We studied the effects of varying the inlet air humidity and of re-grouping the drying groups, on the total entropy production.

5.6 Results

We first present the results that characterise the reference system, namely its profiles of paper temperature and moisture content (Fig. 5.2). The calculation is compared with several temperature measurements for the paper sheet (Fig. 5.3). We proceed with the results that show the entropy production along the machine (Fig. 5.4), and its distribution on drying modes in the reference and optimal systems (Fig. 5.5 and Fig. 5.6). Finally, we give the response of entropy production to changes in the inlet air and steam conditions (Fig. 5.7), and to re-grouping of the drying groups (not shown), for the optimal system.

5.6.1 Profiles of paper temperature and moisture content

Figure 5.2 shows the variation of T_p and w in the z-direction of the actual paper drying machine. The temperature profile shows clearly the increase and decrease of T_p as the paper sheet passes from one to another mode; it has a *zig-zag* pattern. The rise of T_p corresponds to the modes of type A. This rise is common to all drying groups. Immediately after the paper sheet leaves a mode of type A, and meets mode B or D between two cylinders, T_p drops because the paper sensible heat gained from the heated cylinder is largely used for surface water evaporation.

In the first drying group, the overall cooling of the paper sheet is about 7^0C, while it is about 16^0C in the second drying group. The presence of an unheated cylinder (cylinder 31) is the reason for the large shift in the T_p profile at $z=$

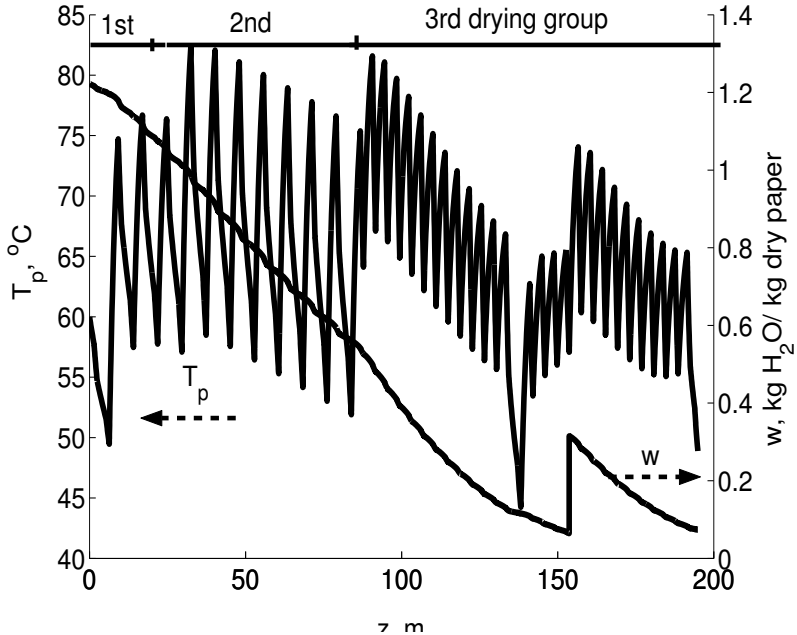

Figure 5.2. Paper temperature (T_p) and moisture content (w) in z-direction of the machine.

140 m. The gradual increase in the heat required for the evaporation of sorbed water, which starts to be important from the beginning of the third drying group, causes an overall decrease of paper temperature of about 13^0C until the paper sheet reaches cylinder 31. After this location, T_p increases with few degrees, and then it decreases until reaches the temperature of 50^0C at the dry-end of the machine.

The moisture content profile in Fig. 5.2 shows a constant decrease of w in the first and second drying groups, which corresponds to the constant drying rate regime. The falling drying rate regime starts at the beginning of the 3^{rd} drying group. The presence of the moisture control device under cylinder 40 at $z = 160$ m, i.e., the steam box that showers the paper sheet surface with steam (see Fig. 5.1), explains the jump in the profile of w at this location. This device is used for correcting the smoothness and moisture content of the paper sheet in the width direction of the drying machine.

5.6.2 Comparison with measured data

The paper temperature profile was compared to the paper temperature measurements, which were taken by means of an infrared pyrometer. Local moisture content data of the paper sheet were not available. Figure 5.3 compares the paper temperature profile (line) with the readings of paper temperature (square symbols). The measurements were taken at all locations where the paper sheet leaves a heated cylinder, and they were proceeded on 14 June 2001, at the PM2 Valmet paper drying machine (Norske Skog's mill 2001).

Figure 5.3 shows that the simulated paper sheet temperatures are higher by about 10^0C than those measured in the first two drying groups, while it is lower than those measured in the last group. A *zig-zag* pattern is not found because the number of measurements was not enough to show this pattern. The discrepancy between the calculated and measured temperatures indicates the deficiency of the flux equations that are used in the model and the inaccuracy in the measurements.

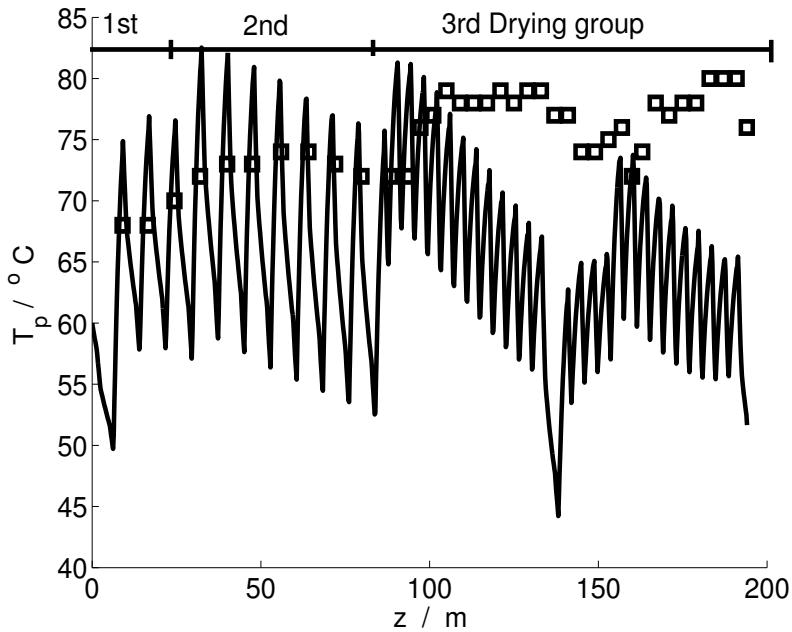

Figure 5.3. Paper temperature validation; measured (□) and simulated (−) data.

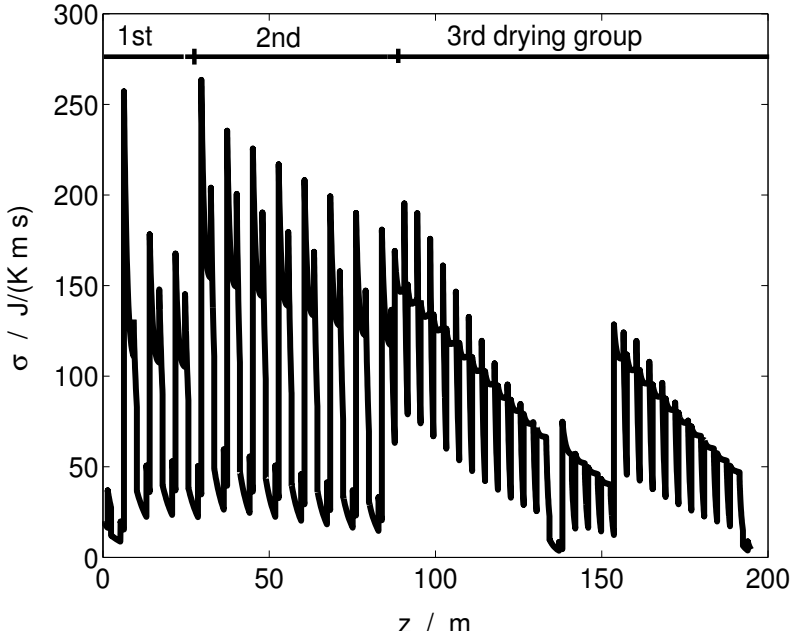

Figure 5.4. Local entropy production in z-direction of the machine.

5.6.3 Entropy production profile

The profile of entropy production (σ) in z-direction of the machine is shown in Fig. 5.4. The integral under the curve is the total entropy production in the machine. The integral is also the objective for our minimisation.

Similar to the paper temperature profile, the profile of σ has a *zig-zag* pattern, which reaches the peak values at the beginning of each drying group. At these locations, the heating conditions are changed. In the third drying group, when the falling drying rate regime starts, the value of σ is falling steadily to the end of the machine. The same *zig-zag* pattern, but with different locations of peak values, was obtained when the separate contributions from mass and heat transport to σ were studied (not shown).

5.6.4 Entropy production per drying mode

The entropy production rate per drying mode in the reference system is shown in Fig. 5.5. As expected, the highest values of entropy production are found at the heated cylinders (i.e. the drying modes A, square symbols). Unheated

cylinders (i.e. the drying modes C with diamond symbols) and cylinders operated under vacuum (i.e. the drying modes E, star symbols) have a smaller entropy production. When the paper travels between two cylinders, i.e. in drying modes B (circle symbols) or D (point symbols), the contributions are among the lowest ones. It is due to the mass transport that takes place at these locations.

The entropy production rate per drying mode in the optimal system is shown in Fig. 5.6. As response to the condition of minimum entropy production, all drying modes in the first drying group show lower entropy production in the optimal system compared with the reference. The most significant modification occurs at the heated cylinders located in the first drying group. These modes almost halved their entropy production, compare the square symbols in Fig. 5.6 with those in Fig. 5.5. The entropy production rate of drying modes C-E, which are located in the first two drying groups, approached the same value of 60 W/K per drying mode. By contrast, the corresponding drying modes in the reference system showed a larger variation in entropy production rate, between 30 and 150 W/K per mode.

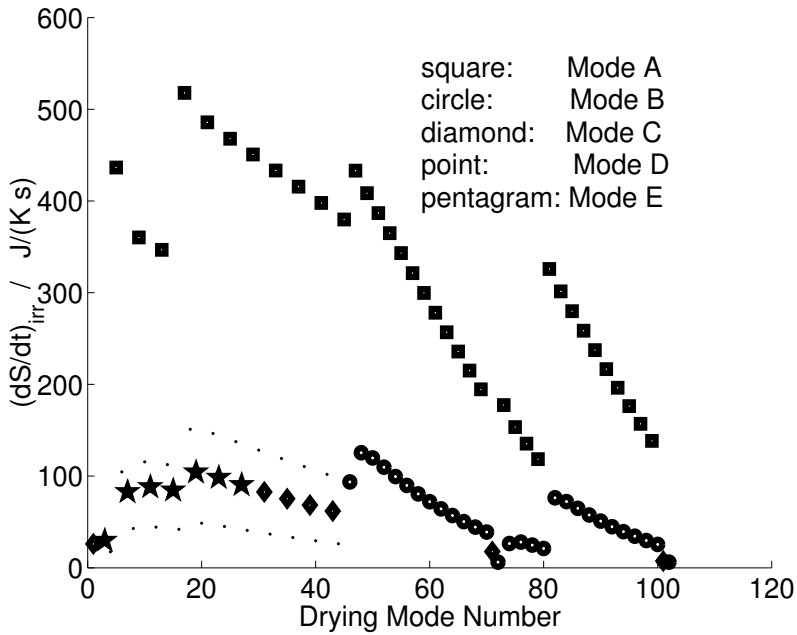

Figure 5.5. Entropy production rate per mode A (□), B (◯), C (◇), D (•), *and* E (★) *in the reference system.*

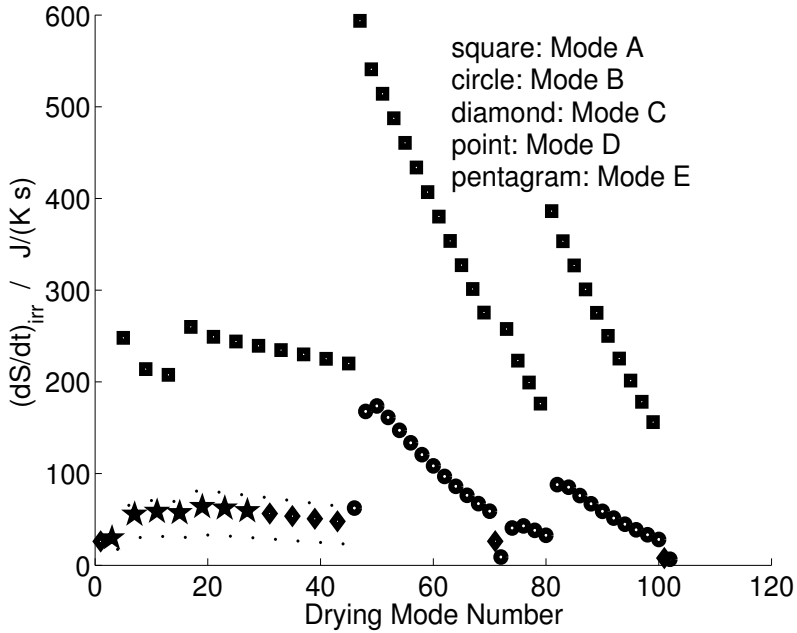

Figure 5.6. Entropy production rate per mode A (□), B (◯), C (◇), D (•), *and* E (★) *in the optimal system.*

5.6.5 Operating conditions and entropy production

Table 5.3 gives the total entropy production, and the contributions from the heat and mass transport, in the reference (ref) and optimal (opt) systems. The outlet paper moisture content was the same for all optimisations ($w_{\text{out}} = 0.07$ kg H_2O per kg dry paper).

In the first optimization, we changed the inlet steam temperatures. The inlet air conditions were then not allowed to vary, they were the same as in the reference system. A reduction of 3% in total entropy production was achieved from the reference system to the optimal system. This improvement can be accomplished if the saturated steam temperature is reduced by 5^0 and 22^0C in the first and second drying group, respectively, while it is increased by only 5^0C in the third drying group, see the third column in Table 5.3. The same response was also found by the entropy produced by the heated cylinders, see Fig. 5.6.

The second optimisation was performed to see the effect of changing the inlet

Table 5.3. The total entropy production and its contributions to the reference and optimal states, four air inlet humidities.

Inlet air humidity, kg H_2O/kg dry air	0.026	0.026	0.065	0.13
System	ref	opt	opt	opt
Total entropy production, kW/K	15.5	15.0	12.5	10.0
Contributions from				
Heat transport, kW/K	7.9	7.5	7.7	6.8
Mass transport, kW/K	7.6	7.5	4.8	3.2
Inlet steam temperature, ^{0}C				
First drying group	89	84	88	94
Second drying group	111	89	94	99
Third drying group	121	126	131	133

The corresponding steam inlet temperatures are also shown.

air conditions on the total entropy production. Figure 5.7 shows the minimum entropy production as a function of inlet air humidity, while the last two columns in Table 5.3 gives the optimal temperatures of the steam supplied to each drying group. The curve (Fig. 5.7) gives clear message: it is possible to reduce the total entropy production up to 35% by a five-fold increase in the inlet air humidity, and by changing the inlet steam temperature according to the values given in Table 5.3. As the inlet air humidity was set higher and higher, the values for the inlet steam temperatures in the first and second drying groups become closer and closer to the corresponding values in the reference system. The origin of the reduction is the large reduction in the driving force for mass transport, while the heat transport contribution remains on the same level.

The curve in Fig. 5.7 was not drawn beyond the point given by $X_{in,air} = 0.13$ kg H_2O/kg dry air. A minimum point on the curve was expected and found in Fig. 5.7, but this is not shown because in that area the local entropy production was negative at some locations in the paper drying machine.

The negative entropy production observed in Fig. 5.7 is of course a non-physical situation. The following locations in the machine gave negative local entropy production: at the heated cylinders 3, 21, 23, 41-44, and 48-51, and their adjacent drying modes, when the inlet air humidity was 0.26 kg H_2O/kg dry air. The reason was that the last term on the right-hand side of Eq. (5.9) was negative. We know that J and its corresponding force in Eq. (5.13) have the

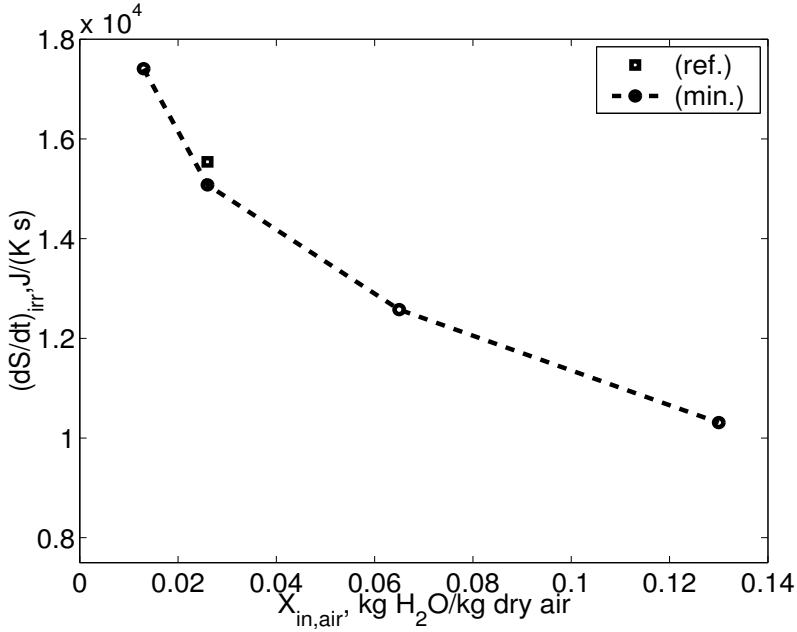

Figure 5.7. Total entropy production as a function of inlet air humidity in optimal systems (◯). The reference system is also given (□).

same positive sign, so it means that the thermodynamic driving force for mass transport given in Eq. (5.9) has a negative sign.

Re-grouping of the drying groups may be an industrial alternative to vary the heating conditions in the paper drying machine. The last optimisation was therefore done to see the effect of re-grouping on the total entropy production. When the second drying group was extended from 15 to 17 cylinders, or contacted from 15 to 13 cylinders, the total entropy production was reduced less than 0.1% compared to the reference system. The same small reduction was obtained when first drying group was contracted from 8 to 6 cylinders, while the second drying group was extended from 15 to 17 cylinders.

5.7 Discussions

We discuss the results for the entropy production and its reduction, before we discuss the practical and theoretical considerations that emerge.

5.7.1 The entropy production of paper production and the state of minimum entropy production

The goal of the present investigation was (1) to map the entropy production in a real paper machine and (2) to find the state of minimum entropy production for the machine and see how it depends on changes in operating conditions.

A mapping of the entropy production of paper drying has not been carried out from information of fluxes and forces before. Unlike in exergy analysis, detailed information about the cause and location of entropy production can be obtained, see Fig. 5.4. The integral of the function in this figure gives, at steady state, the entropy flow into the surroundings or the dissipation of exergy as heat in the surroundings. In the stationary state, entropy does not accumulate in the paper. We can see this loss of useful energy arises from Fig. 5.4, and its major contributions from Figs. 5.5 to 5.7. In the case of Figs. 5.4 - 5.6, with low inlet air humidity, the major causes of loss are almost equally distributed between heat and mass transfer (Table 5.3) while in Fig. 5.7, the loss due to heat transfer remains, and the loss due to mass transfer is reduced (Table 5.3 last two columns). Drying mode A is, not surprisingly, by far the most dissipative one (Fig. 5.5).

The steam temperature is a variable in these studies, and is the outcome of the calculation. These temperatures should be changed to achieve the effects presented. The inlet air humidity and a re-grouping the drying groups are realistic targets for variation. The optimisation rendered the entropy production from heat transfer relatively unaltered. A significant reduction possible was obtained by increasing the inlet air humidity. This can be understood as follows; energy is supplied to the steam as thermal energy, and a certain supply must be there to keep the desired product quality. Thus only a small variation in the supply parts is seen, also in a re-grouping of cylinders. With the set of variables chosen here, the possibility for a large reduction in entropy production lies in operating the evaporation process nearer to equilibrium.

To summarise, we have observed the following feature: if the inlet air humidity approached the saturation limit, the total entropy production of the drying machine can be reduced by 35% compared to the reference system. In terms of percentage, the state of minimum entropy production is little affected (3%) by the variations in steam temperatures or by re-grouping the drying groups.

5.7.2 Practical considerations

The absolute value of the entropy production of paper drying is very large. Per kg newsprint, we find from Table 5.3 that 2400 J/(K kg newsprint) entropy is produced. With a typical yearly production capacity of 5 x 10^8 kg newsprint, it is then easy to see that even a small reduction in percentage of the losses, may be worthwhile pursuing. From this perspective, the 3% reduction, obtained by changing the temperature of the inlet steam can be interesting (compare Tables 5.2 and 5.3). A change in the inlet temperature is possible to implement and also to control.

The value of inlet air humidity at minimum entropy production, 0.13 kg H_2O per kg dry air, is near the saturation point for the air located in some air-pockets in the machine. To operate the machine under such a high inlet humidity may be difficult in practice, because the likelihood for condensation increases, and condensation must be avoided everywhere in the machine hood. The results should be seen in this context: the thermodynamic limit that we find gives a clear message of which direction to move to save on the quality of energy. Operating practice and economy limit how far it is possible to go in this direction. We did not include economic considerations in the above analysis. Such are needed for the implementation of the results. It is nevertheless interesting to know the pure thermodynamic limits of operation, given that a particular production must be maintained. This limit exists, independent of the price of the power supply.

The drying rate depicted in Fig. 5.2, has a turning point about 0.55 kg H_2O/kg dry paper. The point is located to the boundary between the two last drying groups. This point has been associated with the critical moisture content point for the paper (Wilhelmsson et al. 1993, Sidwall et al. 1999). In most newsprint drying machines, the critical moisture content has been found to be higher (i.e. 0.7 kg H_2O/kg dry paper), but it is usually located within the second drying group (Wilhelmsson et al. 1993, Sidwall et al. 1999). At this point, the evaporation of sorbed water becomes the limiting factor for mass transport. The most intensive heating conditions are therefore often used at the start of the last drying group. This is also the case here, as evidence by the paper moisture profile in the same figure.

A key to good performance in modern paper drying, is to avoid over-drying before the critical moisture content point. Over-drying was clearly avoided in the state of minimum entropy production. This can be seen from the tem-

peratures of the saturated steam supplied in the first two drying groups: they dropped in the optimisation.

5.7.3 The model

In oder to model the paper drying process, we have used balance equations and common flux equations for the heat and mass transfer, see Eqs. (5.1), (5.5) and (5.11) - (5.13). The model captures the major temperature trends in the real machine only with relatively large uncertainty (Fig. 5.3). The results obtained in connection with Fig. 5.7 show that the model needs further attention. By increasing the inlet air humidity far enough, negative values were obtained for the local entropy production. This situation is of course non-physical. The entropy production was formulated using an entropy balance over the system, with given values for the heat and mass fluxes into and out of the system.

The theory of non-equilibrium thermodynamics gives a systematic way to put the fluxes in the system (Førland et al. 2001, Bedeaux and Kjelstrup 2005). For our case, they are

$$J_{q,\mathrm{air}} = -l_{qq}\left(\frac{1}{T_p} - \frac{1}{T_{\mathrm{air}}}\right) - l_{q\mu}\left(-\frac{1}{T_p}\frac{\partial(w\Delta H)}{\partial w} + \frac{\partial(w\Delta S)}{\partial w}\right) \tag{5.14}$$

and

$$J = -l_{\mu q}\left(\frac{1}{T_p} - \frac{1}{T_{\mathrm{air}}}\right) - l_{\mu\mu}\left(-\frac{1}{T_p}\frac{\partial(w\Delta H)}{\partial w} + \frac{\partial(w\Delta S)}{\partial w}\right). \tag{5.15}$$

Here l_{qq}, $l_{q\mu}$, $l_{\mu q}$, and $l_{\mu\mu}$ are transport coefficients for the interface. They have been evaluated by Bedeaux et al. (1999) in the absence of a flow parallel to the evaporation surface. The coefficients depend on the flow conditions at the surface, and therefore on the paper speed. etc.

By comparing these equations to the flux, Eqs. (5.12) and (5.13) we see first that the coupling terms are lacking in Eqs.(5.12) and (5.13) and that the driving force for mass transfer is different; it is the ideal approximation of the chemical potential difference. We have recently shown that it is not in agreement with the second law, to neglect coupling coefficients for transport across phase boundaries (Bedeaux and Kjelstrup 2005). The present model can thus be made to agree with the second law by developing Eqs. (5.14) and (5.15) further.

This investigation has been done as a first step in the direction of obtaining more correct equations for phase transformations. It is important to first see predictions from state-of-art equations actually used in the literature, and find the entropy production in a large-scale drying machine. The drying model used here uses the well-established heat and mass transfer analogy (Incropera and Witt 1985). This work shows that these equations may not be sufficient. The presence of coupling (Bedeaux and Kjelstrup 2005) means that mass transport can have a different direction than its main driving force, provided that a thermal driving force exists and is large enough. The coupling coefficients can thus affect the magnitude of the fluxes. By including the proper thermodynamic driving force, and coupling coefficients, we expect that the local entropy production always be positive for all conditions. We argue that there is a need to improve the model at this pint. Such work is in progress.

5.8 Conclusions

We have used a standard model for a paper drying machine, which produces newsprint, and characterised the paper drying process of a real machine, through its profiles of paper temperature and moisture content. The model was validated by some measurements. We argue that the local entropy production is needed in a validation of the model.

In several studies of optimal second-law performance, we kept the paper moisture content at the dry-end of the machine constraint, while the inlet saturated steam temperatures to the drying groups were optimisation variables. We found a large effect on the total entropy production by changing the inlet air humidity. The total entropy production was reduced by 35% compared to the reference system, if the inlet air humidity was five-fold increased. Smaller changes (i.e., 3%) were obtained when lower temperature was maintained for the steam supplied in the first drying groups. Both variations may be technically interesting because the entropy production from paper drying is so large.

Acknowledgements

The Research Council of Norway funded this research. Norske Skog ASA, Skogn in Norway made their data available.

Chapter 6

A process maturity indicator for industrial ecology

Anita Zvolinschi[a,b] and Signe Kjelstrup[b]

[a]Industrial Ecology Programme
[b]Department of Chemistry
Norwegian University of Science and Technology
NO-7491 Trondheim, Norway

This chapter is based on an article submitted to

Journal of Industrial Ecology

and is adapted from a work presented at the

International Society of Industrial Ecology Conference, Stockholm, June 2005.

Abstract

We present an indicator as a measure of one process, the distance between the actual state of operation for the process, and its most energy-efficient state of operation meaning the state having minimum entropy production. This state can be characterised as being mature; it has nearly constant entropy production in space or time. The indicator, called the process maturity indicator, π, is defined as the ratio between the minimum entropy production rate and the actual entropy production rate in the unit. We calculate π on the basis of literature data for some examples of process units in the chemical industry (i.e. heat exchanger, chemical reactor, distillation column, and paper drying machine). Our indicator, π, may be used to evaluate the design and is proposed as a realistic measure of the thermodynamic improvement potential in a process.

Keywords: Minimum entropy production; Industrial ecology; Optimisation; Process maturity

6.1 Introduction

Industrial ecology focuses on understanding the relationship between an industrial system and its surroundings, with the aim to create more sustainable industrial production. A system can be an individual process, a process chain, an entire industrial sector or a national economy. The relationship is mostly addressed using material balance tools, e.g. the material flow analysis (MFA) and substance flow analysis (SFA). Life-cycle analysis (LCA) treats both material and energy issues. The energy issue is treated in LCA by an aggregated indicator that measures the total energy requirement in terms of the heating value of all (combustible) energy inputs per unit of product or service. The present standard LCA does not address the energy quality of material and energy inputs, how fast this quality is degraded or destroyed, and how the rate of degradation can be reduced. Entropy balance-based tools, such as exergy analysis and irreversible thermodynamics, were developed for such purposes, see (Ayres 2002, Dewulf and Langenhove 2002) for exergy and (Kjelstrup and Bedeaux 2001) for irreversible thermodynamics.

The total entropy production rate can be found from the entropy balance or directly from irreversible thermodynamics. A state of minimum entropy production can then be determined by optimization, using the constraint that the production capacity of the system must be constant. The processes that

are performed with minimum entropy production, have the highest exergy efficiency. This state should be of interest for engineers, designers and industrial ecologists, because it defines a realistic limit for improving the exergy efficiency in a particular process unit.

This paper aims to bring knowledge from irreversible thermodynamics into industrial ecology. Irreversible thermodynamics offers a systematic way to find the driving forces and fluxes of a process. It is used on the scale of a single process unit or smaller. We shall address such single processes here and use results obtained earlier for the state of minimum entropy production.

We shall introduce a measure of the distance between the actual state and that with a constrained minimum entropy production. We have called this measure the *process maturity indicator*. It will be defined below as the ratio between the minimum and actual rate of total entropy production in a given process with a constraint in terms of product output. The indicator can be seen as a measure of the thermodynamic improvement potential of the process, having the state of minimum entropy production as the ideal state. The motivation for developing such an indicator arises from the need to understand why and how far our process units perform from the state of minimum entropy production, *a state in which the rate of energy quality degradation is reduced to a minimum.*

Process units such as heat exchangers, chemical rectors, distillation columns, and a paper drying machine will be used to illustrate and determine the process maturity indicator using the literature data available on these units (Røsjorde et al. 2004, Koeijer et al. 2004, Johannessen and Kjelstrup 2004, Zvolinschi et al. 2006a). These units are also central in the chemical process industry. The chemical industry is an important industrial sector that has a large contribution to the global economy, but also large implications for environmental change, see for example (Standigl 2004). The sector comprises a large range of process units, i.e. chemical reactors and separation units, almost all rely on heat exchange. As enormous losses of high quality energy take place in heat exchange and separation processes, much effort has been devoted to avoid such losses, see for example (Linnhoff and Smith 1979).

We present first the basis of irreversible thermodynamics. The definition and illustration of the process maturity indicator follow for the cases mentioned above. We can then address the meaning of the indicator.

6.2 Background

A process unit in its stationary state can be characterised by its total entropy production rate, $(dS/dt)_{irr}$. This quantity can be calculated by either an entropy balance applied to the incoming ($J_{s,in}$) and outgoing ($J_{s,out}$) entropy flows of the system with a cross section A, or by integrating the local entropy production rate (σ) over the volume (V) of the system, see Eq. (6.1).

$$\left(\frac{dS}{dt}\right)_{\text{irr}} = A(J_s^{out} - J_s^{in}) = \int_V \sigma \, dV > 0 \tag{6.1}$$

The entropy balance (the first equality) gives a black box description of the system, while the local entropy production rate gives more information. The entropy balance and the integral over σ give the same result, however, so both can be the object of minimisations. According to the second law of thermodynamics, entropy production must always be positive. Therefore, we can check for consistency of flux equations that are used in the model of the process using Eq. (6.1). Irreversible thermodynamics gives flux equations in agreement with the second law of thermodynamics.

The local entropy production rate contains information on all transport phenomena that take place within a system. One can gain information on fluxes and forces along the unit in the actual state of operation and in the state of minimum entropy production. The disadvantage is that more information is needed about the system. We shall here assume that such information is available.

Irreversible thermodynamics (de Groot and Mazur 1984, Førland et al. 2001), defines the local entropy production by Eq. (6.2).

$$\sigma = \sum_{i=1}^{n} J_i X_i \tag{6.2}$$

Here, J_i is the local flux of any entity i considered and X_i is the conjugate driving force. Each flux (J_i) is a local linear combination of all driving forces by means of the phenomenological coefficients (L_{ij}):

$$J_i = \sum_{i,j=1}^{n} L_{ij} X_j \tag{6.3}$$

For example, for a system with two fluxes and two driving forces, the following relations can be written to characterise it:

$$J_1 = L_{11}X_1 + L_{12}X_2 \text{ and } J_2 = L_{21}X_1 + L_{22}X_2 \tag{6.4}$$

The total entropy production rate, $(dS/dt)_{irr}$, times the temperature of the environment, T_0, is equal to the degradation rate of energy quality of resources in a system. It is also called the exergy loss, E_{loss}, and is given by Eq. (6.5). This relation represents the Gouy-Stodola's theorem, which was independently stated by Gouy (1889) and Stodola (1898).

$$E_{loss} = T_0 \left(\frac{dS}{dt} \right)_{irr} \tag{6.5}$$

Thus, a high rate of total entropy production implies a high rate of energy quality degradation of resources. This was already stated by Tolman and Fine (1948). Their work supplemented the earlier work of Onsager (1931a,b), and that of Prigogine (1955) on the entropy production in stationary state systems. Onsager proved that between phenomenological coefficients in Eq. (6.3) there is a relationship ($L_{ij} = L_{ji}$), the so-called Onsager's reciprocal relation, Onsager (1931a,b).

To give an example of the local entropy production rate, we give the expression for a plug flow reactor (Nummedal et al. 2005). Normally in a reactor, there are three phenomena that produce entropy: the reactions that take place, the heat transfer between the reaction mixture and the cooling/heating agent, and the pressure drop due to the material flows throughout the reactor. The local entropy production rate per unit area, (σ in W/K m^2), becomes (Nummedal et al. 2005):

$$\sigma = \Omega \, \rho_{\mathrm{B}} \sum_j \left[r_j \left(-\frac{\Delta_{\mathrm{r}} G_j}{T} \right) \right] + \pi \, D \, J_{\mathrm{q}} \, \Delta \left(\frac{1}{T} \right) + \Omega \, v \left(-\frac{1}{T} \frac{dP}{dz} \right) \tag{6.6}$$

where Ω is the cross-sectional area of the reactor (m^2), ρ is the catalyst density (kg catalysts/m^3 reactor), D is the reactor diameter (m^2), $\Delta_{\mathrm{r}} G_j$ is the Gibbs energy of reaction j (J/mol), and T is the temperature of reaction mixture (K).

Equation (6.6) was used to study the total entropy production rate in a tubular steam reformer (Nummedal et al. 2005). It contains products of fluxes and their conjugate forces. The first term is due to all reactions; the flux is the reaction rate of reaction j, r_j, and the chemical force is $-\Delta_{\mathrm{r}}G_j/T$. The second term is due to heat transfer; the flux is the measurable heat flux, J_{q}, and the thermal force is $\Delta(1/T)$. The last term is due to the pressure drop; the flux is the fluid velocity, v, and the force is $(-1/T)(dP/dz)$, where P is the total pressure of reaction mixture, and z is the length of the reactor tubes.

Defining the total entropy production rate from Eq. (6.6) rather than from the entropy balance, gives us more information about the local dissipation of energy quality of resources. Therefore, it gives more insight into the state of entropy production of the system.

In this paper we are seeking a measure that is able to evaluate the performance of a process unit, when we demand that a certain amount of product is produced.

It is already common to use the exergy efficiency to evaluate processes. This efficiency is give by

$$\epsilon = \frac{E_{\mathrm{out}}}{E_{\mathrm{in}}} = 1 - \frac{T_0 \left(\frac{dS}{dt}\right)_{irr}}{E_{\mathrm{in}}} \tag{6.7}$$

where E_{in} is the exergy input of the system, and E_{out} is the exergy output of the system. The exergy balance, $E_{\mathrm{in}} = E_{\mathrm{out}} + T_0\ (dS/dt)_{\mathrm{irr}}$, and Eq. (6.5) have been used in last equality of Eq. (6.7). The exergy efficiency is unity when the entropy production is zero. This is then the theoretical limit of a fully reversible process, with large transfer areas or infinite time at disposal, or with very little product produced.

Our proposal for a new indicator aims to introduce a new and more realistic limit. A given sizable production J must occur in a finite time and with a finite sized apparatus to be of practical interest. The limiting value to compare with then has a finite entropy production. We will select this to be the minimum entropy production for the constraint in question. The new indicator will use the result from the following constrained optimization:

$$\text{Find } \ min\left(\frac{dS}{dt}\right)_{irr} \quad \text{for a given } \ J \tag{6.8}$$

6.2.1 Equipartition as a feature of minimum entropy production

Work over the last twenty years has shown that the most important feature of the state of minimum entropy production is its *equipartition* (Tondeur and Kvaalen 1987, Tondeur 1990, Andresen and Gordon 1992, 1994, Bedeaux et al. 1999, Sauar et al. 1996, 1997, Kjelstrup et al. 1999, 2000, Sauar et al. 2001, Nummedal and Kjelstrup 2001, Johannessen et al. 2002, Koeijer et al. 2004, Johannessen and Kjelstrup 2004, 2005, Zvolinschi et al. 2006a).

Tondeur and Kvaalen (1987) proposed that the total entropy produced in a contacting or separating device (e.g. heat exchanger, distillation column) is minimal when the local rate of entropy production is uniformly distributed along the state space and/or time variables. This theorem was called *Equipartition of entropy production* (EoEP), and it was demonstrated for globally linear flux-force relations obeying Onsager's reciprocal relations (Tondeur and Kvaalen 1987). In a further study of applications of the EoEP theorem, Tondeur (1990) said that "minimal dissipation for a specified duty corresponds to equipartition of flux, driving force and entropy production along the time and space variables of the process". This statement was linked to the flow configuration in heat exchangers, sorption and distillation columns, and other types of separation equipment. With a certain number of assumptions, he also made a link between the equipartition of entropy production and economic optimisation. The optimal size distribution in an economic sense is that in which the cost of energy quality degradation in any element is equal to the amortised proportional investment cost in that element. In more popular terms EoEP means that "heat transfer area should be concentrated in the region where heat transfer is most intense" (Bejan 1982). Other authors have found related theorems in different ways and for different conditions, see for example Andresen and Gordon (1992, 1994).

The work by Sauar et al. (1996) gave the theorem of *Equipartition of forces* (EoF), which states that a production system in the state of minimum entropy production can be characterised by constant thermodynamic driving forces. The theorem was proved using irreversible thermodynamics for processes where all transfer paths were parallel. No conservation equations were considered in the proof. The EoF theorem was proposed as design criterion for heat exchangers (Nummedal and Kjelstrup 2001), chemical reactors (Sauar et al. 1997, Bedeaux et al. 1999, Kjelstrup et al. 1999, 2000), and distillation columns (Sauar et al. 2001). The vulnerability of the EoF theorem appeared when difficulties were met in obtaining minimum entropy production in a reactor

system (Kjelstrup et al. 2000), and in obeying conservation equations in a diabatic distillation (Sauar et al. 1997).

The most convincing formulation of the optimization problem, to find minimum entropy production for a process unit with constant production was given by Johannessen and Kjelstrup (2005) using optimal control theory (Bryson and Ho 1975). This theory emphasises the number of control variables that can be used to change the system, vs. the number of state variables in the system itself. Conservation equations and other constraints were properly taken into account.

Johannessen and Kjelstrup (2005) revealed the nature of the state of minimum entropy production when there are less control variables than state variables in the system. Taking the plug flow reactor as an example, they found that the path of minimum entropy production followed a *highway* in state space, to a larger or smaller degree, depending on the boundary conditions of the system. The following chemical reactors were investigated: sulphur dioxide oxidation, ammonia synthesis, steam reforming, methanol synthesis and propane dehydrogenation. The results obtained were formulated as an hypothesis:

"EoEP, but also EoF, is a good approximation to the state of minimum entropy production in the parts of an optimally controlled system that have sufficient freedom" (Johannessen and Kjelstrup 2005).

Knowledge of the nature of the state of minimum entropy production is thus accumulating and industrial ecology might take advantage of this. It seems that an energy efficient system should possess certain characteristics; i.e. follows a highway for energy efficient operation in state space, operates with EoEP, or has relatively constant driving forces. Technologies that incorporate systems that pose minimum entropy production states can be called *mature*. Following Tondeur (1990) this may also, under favourable conditions, lead to economic advantages.

We therefore propose as a measure for process maturity, the state in which the process operates with a minimum of entropy production with the aim to produce the product J. This state of minimum entropy production has the highest exergy efficiency that is possible to obtain for this particular product (J). The limit value of unity cannot be achieved for a finite production, however.

The goal of the process engineer is to expend the available energy (exergy) wisely while achieving the technological goals of the process. Our claim is that

the reversible limit with zero entropy production is not useful in this context, as it does not tell how far the process operates from what is possible in practice.

6.3 Defining the process maturity indicator

We have seen above that a measure to evaluate an industrial system is its exergy loss or the entropy production of its processes. The larger the entropy production is, the larger are the emissions to the surroundings. The measure is therefore particularly important in the energy-intensive industry. From an ecological perspective, sustainability means that the industrial system must not release an intolerable load on the neighbourhood ecosystems, so that conditions for life are altered. Information on the state of minimum entropy production in industrial operation can be useful in industrial ecology, because it can help efforts to reduce emissions.

It is with this background that we propose a measure that indicates how far a process is operated from its state of minimum entropy production. We name this measure the *process maturity indicator*, π. The π is defined as the ratio of the minimum entropy production rate to the actual entropy production rate in a process taking place in a single process unit, see Eq. (6.9).

$$\pi = \frac{\left(\frac{dS}{dt}\right)_{irr}^{minim}}{\left(\frac{dS}{dt}\right)_{irr}^{actual}} \tag{6.9}$$

The indicator shows how far a particular process is from its maturity level. A process with a given production capacity is mature if it is operated with minimum entropy production. This state of operation has the lowest possible resource degradation or depletion, and therefore, it contributes to a longer preservation of natural reservoirs (e.g. the fossil fuel reservoirs). The ideal path of operation is, if applicable, the highway of the system in state space. If the process intensity is not too high, the highway will be characterised by constant entropy production (or constant driving forces). The degrees of freedom and the number of control variables have an impact on the path, and they must be specified (Johannessen and Kjelstrup 2005). Thus, the maturity level is not uniquely defined, it is also a matter of choosing proper variable sets. In spite of this uncertainty, we think that the idea may be fruitful. When π is low it means that the process is wasting exergy unnecessarily. This conclusion cannot be reached based on information on exergy efficiency (ϵ) alone. A low π means that there is a real space for technological improvements. The indicator

approaches unity when the process is operated at the state of minimum entropy production. The process is then mature, and nothing can be done to improve this particular process, apart from changing the number of system variables. Different processes routes to the same product, can be compared by their process maturity indicators, as well as with their exergy efficiency.

6.4 Calculations

We now calculate π for several process units, where data can be found in the literature. These are the processes of heat exchange in two heat exchangers, catalytic oxidation of SO_2 in two reactors, two-component separation in an adiabatic distillation column, and a paper drying process in a steam-heated multi-cylinder machine. The data for the calculations were obtained from Nummedal and Kjelstrup (2001), Koeijer et al. (2004), Johannessen and Kjelstrup (2004), and Zvolinschi et al. (2006a), respectively.

The results of the calculations are given in Table 6.1. The table lists the actual entropy production rate, $(dS/dt)_{irr}^{actual}$, and the minimum entropy production rate, $(dS/dt)_{irr}^{minim}$, for the selected processes, as well as their process maturity indicators.

The heat exchange processes were calculated because they are the simplest to understand. The results are given in the two first lines of the table. Both exchangers were geometrically identical, and had the same heat duty (60 kW). The following conditions were also the same: the mass flow of hot and cold streams (1 and 0.28 kg/s, respectively), the inlet and outlet temperatures of the hot stream (400 and 370 K, respectively), and the heat transfer coefficient (340 W/m^2K). The process maturity indicator π was 0.8 and 0.98 in the co- and counter-current heat exchangers, respectively. The first case had a low maturity indicator, indicating that an improvement potential is possible. In the second case, the EoF theorem was approximately fulfilled in the outset, and the maturity indicator was high, almost unity. We conclude that there is not much to do to improve the counter-current heat exchanger in the way it is operated now. The heat exchange process in a counter-current heat exchanger is a mature process, and is already well known by engineers.

The process maturity indicators for two chemical reactors for SO_2 oxidation are shown in the third and fourth lines of Table 6.1. One process has been established in the industry since the 1950s, while the other is newer.

Table 6.1. The actual entropy production rate, $(dS/dt)_{irr}^{actual}$, the minimum entropy production rate, $(dS/dt)_{irr}^{minim}$, in J/K per FU [a] (see notes b-f for the other specifications), and the process maturity indicator (π).

Process	$(dS/dt)_{irr}^{actual}$	$(dS/dt)_{irr}^{minim}$	π
Heat exchange[b] in:			
Co-current HE	0.48	0.38	0.80
Counter-current HE	0.48	0.47	0.98
SO_2 oxidation in:			
Four-bed reactor[c]	122.4	106.7	0.87
Tubular reactor[d]	60.3	53.8	0.89
Separation in:			
Adiabatic DC[e]	8.1	7.7	0.95
HIDiC[f]	37.5	24.6	0.65
Paper drying in:			
Conventional PM[g]	2400	2300	0.96

[a] FU is functional unit;

[b] FU is kJ heat duty in heat exchanger (HE) (Nummedal and Kjelstrup 2001);

[c] FU is one mole of sulphur trioxide produced in reactor (Koeijer et al. 2004);

[d] FU is one mole of sulphur trioxide produced in reactor (Johannessen and Kjelstrup 2004);

[e] FU is one mole of a propylene-propane mixture (50:50 vol.%), separated in distillation column (DC) (Røsjorde et al. 2005a);

[f] FU is one mole of benzene-toluene mixture (50:50 vol.%), separated in heat-integrated distillation column (HIDiC) (Røsjorde et al. 2005b);

[g] FU is one kg of dry-paper produced in paper machine (PM) (Zvolinschi et al. 2006a).

Koeijer et al. (2004) calculated the total entropy production rate for the first reactor from the entropy balance over the system that comprised a four-bed reactor and five intermediate heat exchangers (Fig. 6.1). The system was an industrial-scale reactor, and the entropy production was minimised by constraining the inlet and outlet parameters of the reaction mixture, with exception of the outlet reaction mixture pressure. A saving of 16.7% in the total entropy production rate was reported (Koeijer et al. 2004); the reduction of total entropy production was from 4.7 kW/K in the reference system to 4.1 kW/K in the optimal one, for a total heat transfer area of 4000 m^2 and an input molar

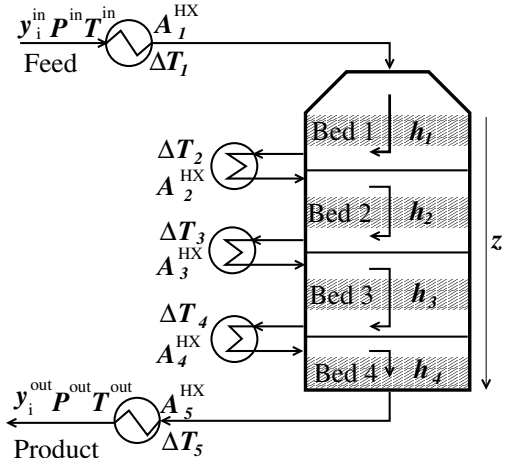

Figure 6.1. The four-bed SO_2 oxidation reactor system with five intermediate heat exchangers, according to Koeijer et al. (2004).

flow rate of 480 mol/s. This saving was possible without changing the reactor design, or the total area available for heat exchange. The maturity indicator was 0.87 for the reactor, a relatively low number, considering that the reactor has been in use since the 1950s. However, the absolute value of the minimum entropy production rate of this reactor was high ($(dS/dt)_{\mathrm{irr}}$ =4.7 kW/K).

Johannessen and Kjelstrup (2004) gave the minimum total entropy production rate for the plug flow reactor model (Fig. 6.2). The results for this reactor are given in the fourth line of Table 6.1. Johannessen and Kjelstrup (2005) found that the optimal tubular reactor was characterised by a reaction mode and a heat transfer mode. Only some parts of the reactor had constant entropy production. This may explain its low maturity indicator, 0.89. The number depends on the state of operation. This is illustrated in Fig. 6.3, which shows the state of minimum entropy production in terms of the temperature of reaction mixture and of cooling agent in two cases. The two actual systems are labelled "reference" in the figure. For the first case a saving of 10.4% in the total entropy production was obtained, while in the latter case a saving of 24.7% was obtained (with a corresponding reduction of the length of the reactor from 6.1 m to 5.2 m). It is the first case that is listed in Table 6.1. The temperature of cooling agent on the shell side of the reactor tubes was the control variable in the minimisation. A *hot spot* typical to an exothermic reactor is observed at the inlet (see Fig. 6.3). We see from Fig. 6.3 that a change in the premise for the optimisation, for instance a change in the number of variables,

gives different results for the total entropy production rate, and thus, for the π values.

The process maturity indicator ($\pi = 0.89$) of the tubular reactor was only slightly higher that than of the four bed reactor ($\pi = 0.87$). From the maturity indicators alone, it is thus not clear that one reactor is significantly better than the other. However, this becomes clear when we consider the entropy production rate. It is much smaller for the tubular reactor than for the fixed bed reactor. This shows that the maturity indicator alone should not be used to compare different processes. The first reactor is clearly less good than the second, with respect to use of exergy resources, but this is seen from the absolute numbers, not π.

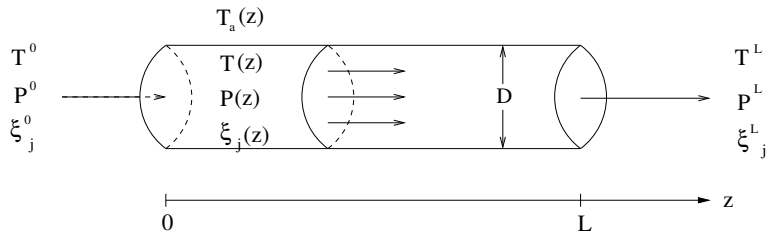

Figure 6.2. The single-bed tubular SO_2 oxidation reactor system considered by Johannessen and Kjelstrup (2004).

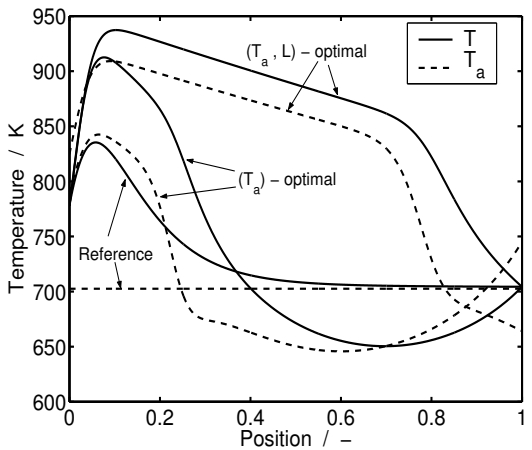

Figure 6.3. The temperatures of the reaction mixture (solid line) and the cooling agent (dashed line) as function of scaled reactor length, according to Johannessen and Kjelstrup (2004).

For an adiabatic distillation column separating propylene-propane, Røsjorde et al. (2005b) found a total entropy production rate of 8.1 J/K per mol of mixture separated. The optimal system gave an entropy production rate of 7.7 J/K per mol. A value of 0.95 was calculated for the process maturity indicator, see line five, Table 6.1. The separation of a propylene-propane mixture by means of adiabatic distillation is thus close to being mature. Industrial-scale distillation columns are mostly adiabatic columns. A conventional column has only two heat exchangers: the reboiler and the condenser. The optimal column on the other hand allows for heat exchange on all trays (Fonyo 1974), as it was approximately adopted in the diabatic column (de Koeijer et al. 2002), in the heat pump assisted distillation (Null 1976) and in the heat integrated distillation column (de Koeijer et al. 2002, Røsjorde et al. 2004).

The distillation column separating propylene-propane has a high process maturity indicator ($\pi = 0.95$), while the process separating benzene-toluene has a low indicator ($\pi = 0.65$), see Table 6.1. Both mixtures were considered as ideal mixtures, but the number of stages involved in the operation differs. The column with lowest number of stages has the lowest indicator, as expected. Figure 6.4 shows that a large number of stages brings the operating line closer to the equilibrium line, and to a smaller entropy production.

The standard way to characterise a distillation column is by means of a McCabe-Thiele diagram. Figure 6.4 shows the McCabe-Thiele diagrams for adiabatic and diabatic distillation columns for a binary mixture.

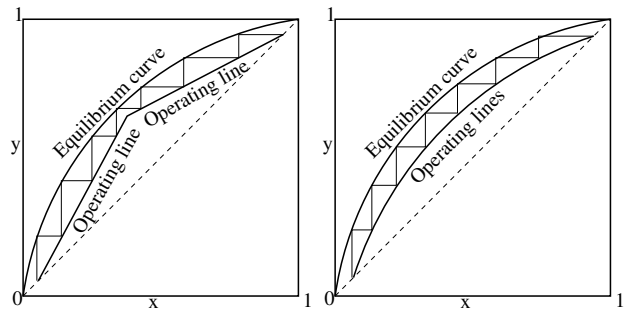

(a) Adiabatic (b) Diabatic

Figure 6.4. Operating lines in McCabe-Thiele diagrams of adiabatic (a) and diabatic (b) distillation columns.

The operating lines in the adiabatic columns are straight because the vapour and liquid flows are constant from tray to tray. The heat exchangers integrated on each tray of the diabatic distillation columns enable the operating lines to be curved and turn to approach the equilibrium line of operation. As a consequence, the total entropy production decreases, and the entropy production along the column becomes more constant.

Finally, the process maturity indicator was calculated for a paper drying machine, see the bottom line in Table 6.1. The entropy production was calculated and minimised for a constant production of paper in a conventional paper drying machine (Zvolinschi et al. 2006a). A saving of 3% (from 15.5 to 15 kW/K) in the total entropy production was reported for a fixed inlet air composition (0.026 kg H_2O/kg dry-air). The value of π in Table 6.1 refers to this case. The high value (0.96) shows that there is not much potential to improve the process by changing the inlet steam temperatures in heaters, while keeping the inlet air composition.

If we allow the inlet air moisture content to increase five-fold, the total entropy production can be drastically reduced, by as much as 35% (from 15.5 to 10 kW/K). Clearly a second law optimal paper drying machine should preferentially be operated with inlet air conditions as close as possible to the saturation point of the drying air at every location near the paper surface. This may not be technically feasible in practice, however.

From Table 6.1, we see that the absolute value of total entropy production per kg paper produced is several orders of magnitude larger than that found in the other processes. Thus, a very small technical improvement in the paper drying machine may have an important impact on the depletion rate of exergy resources. The process maturity indicator for the given inlet condition is high ($\pi = 0.96$), but a small improvement may still give large exergy savings. By allowing the inlet air composition to change, even larger improvements can be achieved. Again, we see that the absolute value of the total entropy production is important, not only π.

6.5 Discussion

The examples above have shown the strengths and the limitations of the process maturity indicator, as it was defined in this paper. The indicator is able to assess the operation of a given process in a realistic way. For instance, a direct message was given on how to operate a heat exchanger; counter-current, not

co-current. The first operates closer to the equipartition of entropy production. The indicator is a realistic measure, because it compares the actual process to an ideal version of itself (its state of minimum entropy production), and not to an unrealistic state (i.e. the reversible state of operation). By knowing the maturity indicator of a process both an engineer and a non-professional are informed about the improvement potential of that particular process.

The rate of depletion or degradation of resources is also a form of environmental damage. Diminishing the resource depletion by operating at the state of minimum entropy production, reduces the environmental impact of that operation. As a consequence, the exergy emissions per unit of time, if not in total, can be reduced. We thus advocate a slower use of exergy resources, with a rate of consumption that is real. The reversible limit for production cannot be used in this manner.

We cannot conclude from the maturity indicator, however, that we should prefer one process to another. For instance; almost the same maturity indicator was obtained for the two chemical reactors in Table 6.1. We saw that information about the absolute values of the losses was needed, to know which reactor to prefer, from an exergy efficiency point of view. A high process maturity indicator does also not necessarily tell that it is meaningless to improve a process. The case of paper machine drying showed that. This process is very exergy intensive, but even a small improvement may make large exergy savings.

In spite of its limitations, the indicator has some interesting properties. Researchers like Ayres et al. (1998), Kuemmel (1989), von Spakowski et al. (1991) and others have suggested that a system can best be related to its environment using exergy. The exergy directly measures the departure of the state of a system from that of the environment. The departure is zero only when the system is in equilibrium with its environment. Such an equilibrium is, however, never available in a real process. A state of minimum entropy production is, as we have already discussed, obtainable and directly connected to the actual process. The process maturity indicator has a reference state that is independent of the local environment. There is no need to define an environmental state with this reference, and an absolute comparison can be made of technological performance between different localities. The indicator can be used by the public sector to set criteria for production. It can also be used by the industrial sector to defend chosen designs and technologies. We can use the process maturity indicator to argue about improving industrial systems with respect to their effects on the environment. The process maturity indicator

only applies so far to single processes only. More work is needed to bring it to an aggregated level.

6.6 Conclusions

We have proposed the use of a process maturity indicator to evaluate the performance of single process units. The indicator brings knowledge from irreversible thermodynamics and second law optimisation to a level of interest for industrial ecology. It introduces as reference state, the state of (constrained) minimum entropy production in a system. This state is realizable and it does not depend on the environment. The indicator is a pure thermodynamic indicator, and is therefore only one of several indicators for the evaluation of optimal operation and/or design. It indicates a way in which we must proceed to set up industrial processes, possibly by paying more attention to equipartition theorems for process units. The process maturity indicator may give an argument for industrial ecology to implement into industrial practice, operation and design, the state of minimum entropy production as a possibility to reducing the exergy resource depletion in energy-intensive systems.

The process maturity indicator cannot be used to argue that one process should be replaced by another on thermodynamic grounds. For this, we need to compare the total entropy production rate of the competing technologies among other things.

Acknowledgements

The authors thank the Research Council of Norway for funding this research.

Chapter 7

Conclusions and recommendations for further work

The majority of the environmental problems we are confronted by today are a direct consequence of the way resources are used in economic activities. How to evaluate the use and transformation of resources in industrial systems has been the subject of intense research efforts during the last few years also in industrial ecology. The mass- and energy-based methods that are now used in industrial ecology do not take into account the fact that the energy quality of material and energy resources is degraded during their conversion in industrial processes. Therefore, this thesis has aimed to reinforce industrial ecology by theoretical input from engineering thermodynamics and irreversible thermodynamics in order to improve the basis for the evaluation of resource use and transformation in industrial systems. Exergy analysis and entropy production minimisation were applied to obtain four indicators on two different scales. The first scale was for integrated process units (i.e. industrial plants), while the latter was for single process units (i.e. industrial equipment). The main conclusions in this thesis are outlined below.

Chapter 1 explained why and how the second law of thermodynamics should be a part of industrial ecology. The various approaches to materials and energy flows analysis in industrial ecology literature were reviewed, the focus being on the evaluation tools for the resource use performance of industrial systems.

Chapter 2 explained the theoretical background of the thesis, and presented several applications of the exergy analysis and the entropy production minimisation of industrial processes.

Chapter 3 proposed three exergy indicators that may become tools in the industrial ecology framework. An actual energy policy question in Norway was answered using the following indicators: the exergy renewability (α), the exergy efficiency (ϵ), and the environmental compatibility (ζ). The question was whether to build a natural gas-fired or a hydrogen-fired combined cycle power plant to meet increased future demands for electricity in Norway. The study found that the two power plants with different degrees of CO_2 emission abatement were equivalent when judged by their α and ζ values, but not when judged by their ϵ values. The ϵ favoured the construction of the natural gas-fired combined cycle power plant in combination with CO_2 sequestration in a depleted natural gas reservoir. The ability of the exergy indicators to aggregate numerous technological details for decision makers and to indicate which are the paths for a sustainable power production in gas-fired combined cycle power plants was demonstrated. It was concluded that industrial ecology should adopt these indicators as tools to aggregate technological details of the power plants and to facilitate communication between engineers and politicians in the debate about which power plant should be constructed.

Chapter 4 addressed the same exergy indicators as in Chapter 3 to evaluate a paper production and recycling system in relation with an integrated pulp and paper mill in Norway. The system was set in three different scenarios for wastepaper management with two different system boundaries. The study showed that the scenario with a high degree of paper recycling (Scenario H) was favoured by the exergy and life cycle inventory indicators of the system in both narrow and wide system boundaries. It was found that the values of the exergy indicators are considerably affected by the change of system boundaries, while the values of the life cycle inventory indicators are only moderately affected by this change. In addition, the study showed that the exergy-enhanced life cycle inventory provides measure of resources, products and wastes at different aggregation levels, from single processes and paper production steps to a pulp and paper plant and different wastepaper management routes. Exergy values of emissions to air and water and that of solid wastes were presented and discussed. It was concluded that the exergy concept provides additional information at more aggregated levels by measuring resources and wastes on a common basis. In particular, it was found that exergy analysis of each step in the paper life cycle can address some trade-offs emerging from diverse tech-

nological options for paper production and the high or complete wastepaper recycling option. The findings of this chapter suggest that the life cycle inventory data basis for the paper mill should be enhanced with exergy data, and also that both sets of indicators were needed to determine the best degree of wastepaper utilisation in the mill.

Chapter 5 addressed the internal exergy losses due to entropy production in a paper drying machine which was identified in Chapter 4 as one of the most exergy-intensive process units in the mill. The total entropy production rate in the machine was calculated and minimised subject to a fixed outlet paper humidity content, while the inlet steam temperatures to the drying groups were optimisation variables. Several findings emerged from this chapter. First, it was found that the local entropy production was a useful tool to validate the model used to describe the paper drying process. Second, it was found that the second law optimal operation path of the machine is very near to the actual operating path when the steam temperatures were varied in the drying groups of the machine at constant inlet air humidity. When the inlet air humidity was five-fold increased, it was found that the total entropy production rate could be reduced up to 35% as compared to the reference system. The chapter gave a clear message of which direction to take in order to achieve exergy savings in the paper drying machine. Technical or economic constraints were not taken into consideration, however.

Chapter 6 presented information obtained in the literature for the calculation and minimisation of entropy production in various single process units. A thermodynamic criterion for optimal process operation and/or design was proposed as an indicator, which was termed the process maturity indicator (π). This indicator was suggested to be used in industrial ecology as a realistic limit for the improvement potential of resource use in any individual process unit. It was remarked that π can be used to compare different design choices and/or different operation conditions *for the same kind of process unit*, and not as an argument to replace one technology by another. A comparison of the total entropy production rate in the competing technologies must then to be conducted.

Taken together, the above findings suggest that by adopting α, ϵ, ζ, and π industrial ecology can address the second law of thermodynamics and thus obtain a thermodynamic basis for its need to evaluate the resource use and transformation in industrial systems at different aggregation levels, from single process units and production processes to integrated plants and production

and recycling routes. All these indicators are based on sound theoretical foundations, both in scientific and technical terms. They are all relevant to the need stated above. However, the full range of their merits was not tested in this thesis due to the fact that the scales of the applications used in this thesis were limited to the scale of integrated and individual process units.

Every indicator contributes to fulfil one or several objectives. For example, α measures the renewability level of a system in exergy terms, while ζ measures the compatibility of a system in terms of the exergy needs to abate the environmental negative effects of the emissions and wastes of the system. As demonstrated, the α and ζ were not very sensitive to the kind of fuel combusted in a combined cycle power plant (Chapter 3) or to the degree of wastepaper recycling in an integrated pulp and paper mill (Chapter 4). This may be understood as their responses to the fact that similar technologies were involved in the systems. However, when the system boundaries were changed these indicators also changed. Using α and ζ, industrial ecology acquires two indicators which reflect the relationship between an industrial system and its environment, through input exergy flows but not through output exergy flows.

The ϵ is the indicator that reflects this relationship through both input and output exergy flows. In all cases studied in this thesis, ϵ seems to be the most sensitive indicator to the technology change as well as to the change of system boundary. In addition, it can be determined at very local scales and thus can be associated with the π indicator. Due to this characteristic, one can monitor the evolution of the ϵ of a given system (process unit, plant, company, sector, economy) over time, giving a basis for comparing systems that have the same kind of function: plants in a given company that perform the same kind of production, companies in a given industrial sector, sectors among themselves, and so on. Finding patterns of the exergy efficiency on all of these scales enables industrial ecology to find the causes of good or poor resource use and transformation in a particular system. In addition, finding the processes with high exergy losses and with low exergy efficiencies targets the candidates for application of the entropy production minimization method. With raising fossil fuel prices, finding the targets is crucial for applying more research and development to these points. This is also an advantage that should be taken into consideration by industrial ecology.

Recommendations for further work

The thesis opens up several possibilities for further work. As noted, there is not yet much experience with entropy production calculation and minimisation in industrial ecology. Chapters 5 and 6 contain first proposals about how to use this experience in a limited number of single process units. The interpretation and characterisation of the resource use by means of π allows industrial ecology to reach the scale of single process units, a scale that has not been approached before. At this scale, the realistic potential for improvement in resource use performance is characterised by means of π. It is thus possible to build an understanding of resource depletion phenomena from the very first point where a phenomenum starts. Further work should be done to consider other kinds of process units. This depends on the possibility to model such processes and thus to obtain their thermodynamic fluxes and driving forces. The black-box approach of exergy analysis can to some degree overcome this limitation, however. The limitation of the black-box approach of the exergy analysis is that it cannot point where and what are the avoidable and unavoidable exergy losses due to different transport phenomena that occur in irreversible processes.

The potential of minimum entropy production in single process units has not yet been systematically adopted into the exergy savings in process integration. Future work should be directed to link the minimum entropy production to the exergo-economic optimum. Many efforts have been already made in the direction of finding the exergo-economic optimum of industrial processes using thermo-economic optimisation methods. Presently, these methods have addressed the industrial processes where exergy constitutes a very high proportion of the total cost or value of the product or service. Electric power generation in power plants is such an example. Given the interest in industrial ecology in more complex industrial processes, research should be directed to analyse and optimise processes where material recycling can occur. The exergy analysis might be useful here by associating the effects of material recycling with the exergo-economic optimum.

It still seems difficult to perform exergy analysis of industrial processes with complete or partial life cycles. Chapter 4 took a step in this direction by studying a partial life cycle of paper with three wastepaper recycling scenarios. The difficulty is that the data are often incomplete and unverifiable, and usually collected from different sources and in different units. Therefore, life cycle inventories tend then to be unrealistic and physically inconsistent, i.e. they may violate the mass and energy conservation laws as well as the second law

of thermodynamics (Ayres and Martinas 1995). Techniques for data reconciliation have been used in Process Systems Engineering since the 1980s. Such techniques proved to be successful in improving the quality of inconsistent data by enforcing models and other process information. Using these techniques for reconciling life cycle inventory is non-trivial. In addition, these inventories typically present industrial processes as black boxes, and do not provide information about the composition of resources and relevant reactions. Despite these limitations, use of inventory data combined with engineering knowledge about industrial processes can improve life cycle inventories. This may be taken as one direction for research in industrial ecology.

In the future the exergy-based indicators presented in this thesis should be made more comprehensive by also including ecosystem products and services, and thus approach the biosphere processes that accumulate exergy and therefore counterbalance the depletion of exergy in industrial systems. The following biosphere processes may be of interest: solar exergy conversion into biomass through autotrophic photosynthesis, biosphere circulation of substances and energy, formation of bituminous coal, limestones and other deposits of organic nature, to mention only some of them.

Another direction for future research may be to verify the conjecture between the chemical exergy of released waste materials (i.e. the waste exergy) from an industrial system and the potential environmental harm that these materials have on the environment. For this, the methodology used today to define the standard exergy reference states should be replaced by the sink-dependent definition of the exergy reference states, proposed by Ayres and Masini (2004). The chemical exergy of wastes, as calculated in terms of the sink-specific chemical compositions, may thus become a valid indicator of potential environmental harm.

Bibliography

Adriaanse, A., Bringezu, S., Hammond, A., Moriguchi, Y., Rodenburg, E., Rogich, D. and Schutz, H.: 1997. *Resource flows: The material basis of industrial economies*. World Resource Institute. Washington D.C.

Ahern, J.: 1980. *The exergy method of energy systems analysis*. Wiley. New York.

Ahrendts, J. 1980. Reference states. *Energy* **5**, 667–677.

Andresen, B. and Gordon, J. 1992. Optimal paths for minimizing entropy generation in a common class of finite-time heating and cooling processes. *International Journal of Heat and Fluid Flow* **13**, 294–299.

Andresen, B. and Gordon, J. 1994. Constant thermodynamic speed for minimizing entropy production in thermodynamic processes and simulated annealing. *Physical Review E* **50**, 4346–4351.

Arena, U., Mastellone, M. and Perugini, F. 2003. The environmental performance of alternative solid waste management options: a life cycle assessment study. *Chemical Engineering Journal* **96**, 207–222.

Aspen Plus: 2003. Website. http://www.aspentech.com (accessed January 2003).

Atkins, P. W.: 1998. *Physical Chemistry*. 6th edn. Oxford University Press.

Axegard, P., Backlund, B. and Warnqvist, B. 2002. The eco-cyclic pulp mill: Focus on closure, energy-efficiency and chemical recovery development. *Pulp and Paper Canada* **103**, 26–29.

Aylward, G. H. and Findlay, T. J. V.: 1994. *SI Chemical Data*. 3rd edn. Wiley, New York.

Ayres, R. U.: 1989. Industrial Metabolism. *in* J. H. Ausubel and H. E. Sladovich (eds), *Technology and the Environment*. National Academy Press, Washington DC.

Ayres, R. U.: 1996. *Industrial ecology: Towards closing the material cycles*. Edward Elgar Publishing Co. Vermont.

Ayres, R. U.: 2002. *A Handbook of Industrial Ecology*. Edward Elgar. Cheltenham.

Ayres, R. U. and Martinas, K. 1995. Waste potential entropy: The ultimate eco-toxic?. *Economie Appliqué* **XLVIII**, 95–120.

Ayres, R. U. and Masini, A.: 2004. Exergy: Reference States and Balance Conditions. *in* C. J. Cleveland (ed.), *Encyclopedia of Energy*. Vol. 2. Elsevier Academic Press. pp. 633–640.

Ayres, R. U. and Simonis, U.: 1994. *Industrial metabolism: Restructuring for sustainable development*. The United Nations University Press. Tokyo, Japan.

Ayres, R. U., Ayres, L. W. and Martinas, K. 1998. Exergy, waste accounting, and life-cycle analysis. *Energy* **23**, 355–363.

Ayres, R. U., Ayres, L. W. and Warr, B.: 2002. *Exergy, power and work in the US Economy*. INSEAD's Centre for the Management of Environmental Resources. Fontainebleau, France.

Bedeaux, D. and Kjelstrup, S. 2005. Heat, mass and charge transport, and chemical reactions at interfaces. *International Journal of Thermodynamics* **8**, 25–41.

Bedeaux, D., Standaert, F., Hemmes, K. and Kjelstrup, S. 1999. Optimization of processes by equipartition. *Journal of Non-Equilibrium Thermodynamics* **24**, 242–259.

Beer, T.: 2000. *CSIRO Atmospheric Research Report C/0411/1.1/F2: Life-cycle Emissions Analysis of Alternative Fuels for Heavy Vehicles*. Australian Greenhouse Office. Aspendale, Victoria, Australia.

Bejan, A.: 1982. *Entropy generation through heat and fluid flow*. Wiley. New York.

Bejan, A. and Tondeur, D. 1998. Equipartition, optimal allocation, and the constructal approach to predicting organization in nature. *Reveu Générale de Thermique* **37**, 165–180.

Beker, E. W.: 1994. *Microalgae: biotechnology and microbiology.* Cambridge University Press. Cambridge.

Bergsdal, H., Strømman, A. H. and Hertwich, E. G. 2005. Environmental assessment of two waste incineration strategies for Central Norway. *International Journal of LCA* **10**, 263–272.

Bisio, G. and Bisio, A. 1998. Some thermodynamics remarks on photosynthetic energy conversion. *Energy Conversion and Management* **39**, 741–748.

Bolland, O., Ertesvåg, I. S. and Speich, D.: 2001. Exergy analysis of gas turbine combined cycle with CO_2 capture using auto-thermal reforming of natural gas. *Proceedings of The Power Generation and Sustainable Development Conference.* Liege, Belgium.

Bosnjakovic, F.: 1965. *Technical Thermodynamics (in German).* Verlag Theodor Steinkopff. Dresden.

Bringezu, S., Hinterberger, F. and Schütz, H.: 1994. Integrating sustainability into the system of national accounts: The case of interregional material flows. *International Symposium Models of Sustainable Development - Exclusive or Complementary Approaches to Sustainability.* Paris, France. pp. 669–680.

Brodyansky: 1973. *Exergy method of thermodynamic analysis (in Russian).* Energiya. Moscow, Russia.

Brodyansky, V. M., Sorin, M. V. and Le Goff, P.: 1994. *The efficiency of industrial processes: Exergy analysis and optimization.* Elsevier. New York.

Brundtland, G. H.: 1990. *Our Common Future, World Commission on Environment and Development.* Oxford University Press. Oxford.

Bryson, A. and Ho, Y.: 1975. *Applied Optimal Control. Optimisation, estimation and control.* Wiley. New York.

Connelly, L. and Koshland, C. P. 1997. Two aspects of consumption using an exergy-based measure of degradation to advance the theory and implementation of industrial ecology. *Resource Conservation and Recycling* **19**, 199–217.

Constanza, R. and Herendeen, R. 1984. Embodied energy and economic value in the United States economy - 1963, 1967 and 1972. *Resources and Energy* **6**, 129–163.

Cornelissen, C.: 1997. *Thermodynamics and sustainable development: The use of exergy analysis and the reduction of irreversibility.* PhD thesis. University of Twente, the Netherlands.

Cornelissen, R. L. and Hirs, G. 2002. The value of the exergetic life cycle assessment besides the LCA. *Energy Conservation and Management* **43**, 1417–1424.

Daniel, J. J. and Rosen, M. A. 2002. Exergetic environmental assessment of life cycle emissions for various automobiles and fuels. *Exergy, An International Journal* **2**, 283–94.

de Beer, J., Worrell, E. and Block, K. 1998. Long-term energy-efficiency improvements in the paper and board industry. *Energy* **29**, 2403–2423.

de Groot, S. R. and Mazur, P.: 1984. *Non-Equilibrium Thermodynamics.* Dover. London.

de Koeijer, G., Johannessen, E. and Kjelstrup, S. 2004a. The second law optimal path of a four-bed SO_2 converter with five heat exchangers. *Energy* **29**, 525–546.

de Koeijer, G., Kjelstrup, S., van der Kooi, H. J., Gross, B., Knoche, K. F. and Andersen, T. 2002. Positioning heat exchangers in binary tray distillation using isoforce operation. *Energy Conversion and Management* **43**, 1571–1581.

de Koeijer, G., Røsjorde, A. and Kjelstrup, S. 2004b. Distribution of heat exchange in optimum diabatic distillation columns. *Energy* **29**, 2425–2440.

de Swaan, J. A., van der Kooi, H. and Sankaranarayanan, K.: 2004. *Efficiency and sustainability in the energy and chemical industries.* Marcel Dekker, Inc.. New York.

Denbigh, K. G. 1956. The second-law efficiency of chemical processes. *Chemmical Engineering Science* **6**, 1–9.

Dewulf, J. and Langenhove, H. 2002. Quantitative assessment of solid waste treatment systems in the industrial ecology perspective by exergy analysis. *Environmental Science and Technology* **36**, 1130–1135.

Dewulf, J. and Langenhove, H. V. 2003. Exergetic material input per unit service (EMIPS) for the assessment of resource productivity of transport commodities. *Resource, Conservation and Recycling* **38**, 161–174.

Dewulf, J. and Langenhove, H. V. 2005. Integrating industrial ecology principles into a set of environmental sustainability indicators for technology assessment. *Resource Conservation and Recycling* **43**, 419–432.

Dewulf, J., Langenhove, H., Mulder, J., van den Berg, M. and van der Kooi, H. 2000. Illustration towards quantifying the sustainability of technology. *Green Chemistry* **2**, 108–114.

Ehrenfeld, J. and Gertler, N. 1997. Industrial ecology in practice: The evolution of interdependence at Kalundborg. *Journal of Industrial Ecology* **1**, 67–79.

El-Sayed, Y. 1993. A second-law based optimisation (parts 1 and 2). *Journal of Energy and Gas Turbine Power* **118**, 693–703.

El-Sayed, Y. and Aplec, A. 1970. Application of thermoeconomic approach to the analysis and optimisation of vapor compression desalting system. *Journal of Energy Power* pp. 17–26.

El-Sayed, Y. and Evans, R. 1970. Thermoeconomics and the design of heat systems. *ASME Transactions Journal of Energy Power* **92**, 17–26.

Elmasri, M.: 1996. *GTPRO Users Manual*. Thermoflow Inc.. New York.

Ertesvåg, I. 2000. Exergy analysis of the Norwegian society. *Energy* **25**, 957–973.

Ertesvåg, I. 2001. Society exergy analysis: a comparison of different societies. *Energy* **26**, 253–270.

Ertesvåg, I. 2005. Energy, exergy and extended-exergy analysis of the Norwegian society 2000. *Energy* **30**, 649–675.

Evans, R.: 1969. *A proof that essergy is the only consistent measure of potential work for chemical systems*. PhD thesis. Dartmouth College, Ann Arbor MI.

Faber, M., Niemes, N. and Stephan, G.: 1995. *Entropy, environment, and resources*. Springer-Verlag. Berlin, Germany.

Finnveden, G.: 1994. Characterisation methods for depletion of energy and material resources. *in* H. U. de Haes, A. Jensen, W. Klöpffer and L. G. Lindfors (eds), *Integrating Impact Assessment into LCA*. SETAC Europe, Brussels, Belgium. pp. 61–65.

Finnveden, G. and Östlund, P. 1997. Exergies of natural resources in life cycle assessment and other applications. *Energy* **22**, 923–931.

Finnveden, G., Johansson, J., Lind, P. and Moberg, A.: 2000. *Life cycle assessments of energy from solid waste. Working Paper FMS 137.* University of Stockholm. Stockholm, Sweden.

Fitzmorris, R. E. and Mah, R. S. H. 1980. Improving distillation column design using thermodyanmic availability analysis. *AICE Journal* **126**, 265–274.

Fonyo, Z. 1974. Thermodynamic analysis of rectification. I. Reversible model of rectification. *International Journal of Chemical Engineering* **14**, 18–27.

Førland, K. S., Førland, T. and Kjelstrup, S.: 2001. *Irreversible Thermodynamics. Theory and Application.* 3rd. edn. Tapir. Trondheim, Norway.

Fratzcher, W.: 1962. *Der Anhang zu M. P. Wukalowitsch technische Thermodynamik. Einfürung des Exergiebegriffes in die technische Thermodynamik.* Dunod. Paris.

Fratzscher, W. 1961. Exergetical efficiency. *Brenstoff-Wärme-Kraft* **13**, 483–493.

Frischknech, R. 1997. The seductive effect of identical physical units. *International Journal of LCA* **2**, 125–126.

Frischknech, R., Heijungs, R. and Hofstetter, P. 1998. Einstein's lessons of energy accounting in LCA. *International Journal of LCA* **3**, 266–272.

Frosch, R. and Gallopoulos, N. 1989. Strategies for manufacturing. *Scientific American* **261**, 142–155.

Gaggioli, R. A.: 1980. *Thermodynamics: Second-law analysis.* ACS symposium series, No. 122, Charles C. Thomas.

Gaggioli, R. A.: 1983. *Efficiency and costing.* ACS symposium series, No. 235, Charles C. Thomas.

Gemci, T. and Ozturk, A. 1998. Exergy analysis of a sulphide-pulp preparation process in the pulp and paper industry. *Energy Conservation & Management* **39**, 1811–1820.

Georgescu-Roegen, N.: 1971. *The entropy law and the economic process.* Harvard University Press. Cambridge, MA.

Georgescu-Roegen, N.: 1976. *Energy and economic myths. Institutional and analytical essays.* Pergamon. Oxford.

Gibbs, J. W.: 1961. *The Scientific Papers of J.W. Gibbs.* Dover. New York.

Glasby, G. 1988. Entropy, pollution and environmental degradation. *Ambio* **17**, 330–335.

Goldman, J. 1979. Outdoor algal mass cultures. I. Applications. *Water Research* **13**, 1–19.

Gong, M. 2005. Exergy analysis of a pulp and paper mill. *International Journal of Energy Research* **29**, 79–93.

Gong, M. and Wall, G. 2001. On exergy and sustainable development II. Indicators and methods. *Exergy - An International Journal* **1**, 217–233.

Gouy, M. 1889. Sur l'énergie utilisable. *Journal de Physique* **8**, 501–518.

Graedel, T. and Allenby, B.: 2003. *Industrial Ecology.* 2nd edn. Prentice Hall, Engelwood Cliffs. New York.

Graedel, T. and Allenby, B. R.: 1995. *Industrial Ecology.* Prentice Hall, Engelwood Cliffs. New Jersey.

Grassmann, P. 1984. Engineering-thermodynamics and thermodynamics of life, the exergy. *Naturwissenschaften* **71**, 335–341.

Greenhouse R&D Programme, I.: 2000. *Leading options for the capture of CO_2 emissions at power stations. Report No. PH3/14.* Storck Engineering Consultancy. Amsterdam, the Netherlands.

Guinee, J. B., Gorre, M., Heijungs, R., Huppes, G., Kleijn, R., de Koning, A., van Oers, L., Sleeswijk, A. W., Duh, S., de Haes, H. U., de Bruijn, H., van Duin, R. and Huijbregts, M. A. J.: 2002. *Handbook on life cycle assessment: Operational guide to the ISO standards.* Kluver Academic Publisher. Dordrecht, the Netherlans.

Hafskjold, B. and Ratkje, S. 1995. Criteria for local equilibrium in a system with transport of heat and mass. *Journal of Statistical Physics* **78**, 463–494.

Hannon, B. 1973. The structure of ecosystems. *Journal of Theoretical Biology* **41**, 535–546.

Hau, J. L. and Bakshi, B. R. 2004. Expanding exergy analysis to account for ecosystem products and services. *Environmental Science and Technology* **38**, 3768–3777.

Heimdal Heating Plant: 2000. Heat from waste in Trondheim - for a good environment (in Norwegian). www.tev.no/fjernvarme-bedremilio.pdf (accessed January 2003).

Hellström, D. 1997. An exergy analsis for a wastewater treatment plant - an estimation of the consumption of physical resources. *Water Environment Research* **69**, 44–51.

Hertwich, E. G., Pease, W. S. and Koshland, C. P. 1997. Evaluating the environmental impact of products and production processes: a comparison of six methods. *The Science of the Total Environment* **196**, 13–29.

Hinterberger, F., Kranendonk, S., Welfens, M. and Schmidt-Bleek, F.: 1994. *Increasing Resource Productivity through Eco-efficient Services - Wuppertal Papers No. 13.* Wuppertal Institute. Wuppertal.

Incropera, F. P. and Witt, D. P. D.: 1985. *Fundamentals of Heat and Mass Transfer.* John Wiley & Sons. New York.

ISO-14040: 1996. *ISO Draft International Standard ISO 14040: Environmental Management - Life Cycle Assessment - Principles and Framework.* International Organization of Standardization (ISO). Geneva, Switzerland.

ISO-14041: 1997. *ISO Draft International Standard ISO 14041: Environmental Management - Goal and Scope Definition and Inventory Analysis.* International Organization of Standardization (ISO). Geneva, Switzerland.

Johannessen, E. and Kjelstrup, S. 2004. Minimum entropy production in plug flow reactors: An optimal control problem solved for SO_2 oxidation. *Energy* **29**, 2403–2423.

Johannessen, E. and Kjelstrup, S. 2005. Numerical evidence for a "highway in state space" for reactors with minimum entropy production. *Chemical Engineering Science* **60**, 1491–1495.

Johannessen, E., Nummedal, L. and Kjelstrup, S. 2002. Minimising the entropy production in heat exchange. *Internatinal Journal of Heat and Mass Transfer* **45**, 2649–2654.

Jorgensen, S. E.: 1997. *Integration of ecosystem theories: A pattern.* Kluwer Academic Publishers. Boston, MA.

Kapoor, A. and Yang, R. 1989. Kinetic separation of methane-carbon dioxide mixture by adsorption on molecular sieve carbon. *Chemical Engineering Science* **44**, 1723–1733.

Karlsson, M. and Soininen, M.: 1982. The influence of the hygroscopic properties of paper on the transient phenomena during contact drying of the paper webs. *in* J. Ashworth (ed.), *Third International Drying Symposium.* Vol. 1. Wolverhampton, UK. pp. 494–503.

Keiseras, B. K.: 1991. *Life-cycle Data for Norwegian Oil and Gas.* Tapir. Trondheim, Norway.

Kenney, W. F.: 1984. *Energy conversion in the process industries.* Academic Press. New York.

Kjelstrup, S. and Bedeaux, D.: 2001. *Elements of Irreversible Thermodynamics for Engineers.* International Centre of Applied Thermodynamics, Istanbul. ISBN 975-97568-1-1.

Kjelstrup, S. and Island, T. V. 1999. The driving force distribution for minimum lost work in a chemical reactor close to and far from equilibrium. II. Oxidation of SO_2. *Industrial Engineering Chemistry Research* **38**, 3051–3055.

Kjelstrup, S. and Møller-Holst, S. 1993. Exergy efficiency and local heat production in solid oxide fuel cells. *Electrochemical Acta* **38**, 447–453.

Kjelstrup, S., Bedeaux, D. and Sauar, E. 2000. Minimum entropy production by equipartition of forces in irreversible thermodynamics. *Industrial Engineering Chemistry Research* **39**, 4434–4436.

Kjelstrup, S., Sauar, E., Bedeaux, D. and van der Kooi, H. 1999. The driving force distribution for minimum lost work in a chemical reactor close to and far from equilibrium. I. Theory. *Industrial Engineering Chemistry Research* **38**, 3046–3050.

Klöpffer, W. 1997. In defense of the cumulative energy demand. *International Journal of LCA* **2**, 61.

Klüppel, H., Krüger, J., Mauch, W., Reinhardt, G., Saykowski, F., Schaefer, H., Schulze, T. and Wagner, H.: 1997. *Kumulatierter Energieauwand - Begriffe, Definitionen, Berechnungsmethode.* VDI Verlag GmbH. Düsseldorf.

Koeijer, G. D., Johannessen, E. and Kjelstrup, S. 2004. The second law optimal path of a four-bed SO_2 converter with five heat exchangers. *Energy* **29**, 525–546.

Kotas, T. J. 1980. Exergy criteria of performance for thermal plant. *International Journal of Heat and Fluid Flow* **2**, 147–163.

Kotas, T. J.: 1985. *The exergy method of thermal plant analysis.* Butterworths. London.

Kuemmel, B., Nielsen, S. K. and Srensen, B.: 1997. *Life-cycle Analysis of Energy Systems.* Roskilde University Press. Roskilde, Denmark.

Kuemmel, R. 1989. Energy as a factor of production and entropy as a pollution indicator in macro-economic modelling. *Ecological Economics* **2**, 162–180.

Legrand, R. 1993. Methane from biomass systems analysis and CO_2 abatement potential. *Biomass and Bioenergy* **5**, 301–316.

Lindfors, L. G.: 1995. *Nordic Guidelines on Life Cycle Assessment, Nordic Report.* Nordic Council of Ministers. Copenhagen, Denmark.

Linnhoff, B. and Smith, R. 1979. The thermodynamic efficiency of distillation. *Institution of Chemical Engineers Symposium Series* **56**, 47–73.

Lombardi, L. 2003. Life cycle assessment comparison of technical solutions for CO_2 emissions reduction in power generation. *Energy Conversion and Management* **44**, 93–108.

Lowenthal, M. D. and Kastenberg, W. E. 1998. Industrial ecology and energy systems: a first step. *Resources, Conservation and Recycling* **24**, 51–63.

Manninen, J., Puumalainen, T., Talja, R. and Pettersson, H. 2002. Energy aspects in paper mills utilizing future technology. *Applied Thermal Engineering* **22**, 929–937.

Marchal, R.: 1956. *La Thermodynamique et le théorème de l'énergie utilisable.* Dunod. Paris.

Matthews, E., Amann, C., Bringezu, S., Fisher-Kowalski, M., Huttler, M., Kleijn, R., Moriguchi, Y., Ottke, C., Rodenburg, E., Rogich, D., Schandl, H., Schutz, H., van der Voet, E. and Weisz, H.: 2000. *The weight of nations: Material outflows from industrial economies.* World Resource Institute. Washington DC.

Mayer, A. L., Thurston, H. W. and Powlowski, C. W. 2004. The multidiscilinary influence of common sustainability indices. *Frontiers of Ecological Environment* **2**, 419–26.

McDaugall, F. R., White, P., Franke, M. and Hindle, P.: 2001. *Integrated solid waste management: A life cycle inventory.* Blackweel Science (2nd edition).

Metso Corporation: 2000. Metso corporation. Website: http://www.metso.com/ (accessed in March 2003).

Ministry of the Environment: 1998. *Norwegian Climate Change Policy – Overview.* Ministry of the Environment, Report to the Storting (Norwegian Parliament), Report No. 29.

Moran, M. J.: 1982. *Availability Analysis: A Guide to Efficient Energy Use.* Prentice-Hall, Englewood Cliffs. New Jersey, USA.

Neelis, M., van der Kooi, H. J. and Geerlings, J. J. C. 2000. Exergetic life cycle analysis of hydrogen production and storage systems for automotive applications. *International Journal of Hydrogen Energy* **29**, 537–545.

Nilsson, L. 2004. Heat and mass transfer in multicylinder drying. I. Analysis of machine data. *Chemical Engineering and Processing* **43**, 1547–1553.

Nissan, A. 1956. A theory of drying using steam heated drums. *Chemistry and Industry* **2**, 198–211.

Norske Skog - Internal Report: 2000. *Environmental Report - 2000.* Norske Skog ASA, Skogn, Norway.

Norske Skog - Internal Report: 2003. *Environmental Report - 2003.* Norske Skog ASA, Skogn, Norway.

Norske Skog's mill: 2001. *Internal Report.* Norske Skog ASA, Skogn, Norway.

Null, H. 1976. Heat pumps and distillation. *Chemical Engineering Progress* **78**, 58–64.

Nummedal, L. and Kjelstrup, S. 2001. Equipartition of forces as a lower bound on the entropy production in heat exchange. *International Journal of Heat and Mass Transfer* **44**, 2827–2833.

Nummedal, L., Kjelstrup and Costea, M. 2003. Minimizing the entropy production rate of an exothermic reactor with a constant heat-transfer coefficient:

The ammonia reaction. *Industrial Engineering Chemistry Research* **42**, 1044–1056.

Nummedal, L., Røsjorde, A., Johannessen, E. and Kjelstrup, S. 2005. Second law optimization of a tubular steam reformer. *Chemical Engineering and Processing* **44**, 429–440.

OECD: 1996. *Pollution prevention and control: Environmental criteria for sustainable transport. Report: OECD/GD (96) 136.* Organization for Economic Co-operation and Development (OECD). Paris.

Onsager, L. 1931a. Reciprocal relations in irreversible thermodynamics. *Physical Review* **37**, 405–426.

Onsager, L. 1931b. Reciprocal relations in irreversible thermodynamics. *Physical Review* **38**, 2265–2279.

Pakowski, Z., Bartczak, Z., Strumillo, C. and Stenström, S. 1991. Evaluation of equations approximating thermodynamic and transport-properties of water, steam and air for use in CAD of drying processes. *Drying Technology* **9**, 753–773.

Petela, R. 1964. Exergy of heat radiation. *Journal of Heat Transfer* **86**, 187–192.

Prahl, J.: 1968. *Thermodynamics of paper fiber and water mixtures.* PhD thesis. Harvard University.

Prigogine, I.: 1955. *Thermodynamics of Irreversible Processes.* Charles C. Thomas. Springfield.

Rant, Z. 1956. Exergie, ein neues wort für "technische arbeitsfähigkeit" (Exergy, a new word for technical available work). *Forschungen im Ingenieurwesen* **22**, 36–37.

Reguera, D. and Rubi, J. 2001. Kinetic equations for diffusion in the presence of entropic barriers. *Physical Review E* **64**, 61–106.

Rhodius, D. and Gottsching, L. 1979. Paper and board drying process and its independence upon drying and paper technological parameters. IV. Drying in the multi-cylinder dryer section. *Papier* **33**, 1–9.

Rosen, M. A. and Dincer, I. 1999. Exergy analysis of waste emissions. *International Journal of Energy Research* **23**, 1153–1163.

Røsjorde, A., Fossomo, D. W., Kjelstrup, S., Bedeaux, D. and Hafskjold, B. 2000. Nonequilibrium molecular dynamics simulations of steady-state heat and mass transport in condensation. I. Local equilibrium. *Journal of Colloid and Interface Science* **232**, 178–185.

Røsjorde, A., Kjelstrup, S., Bedeaux, D. and Hafskjold, B. 2001. Nonequilibrium molecular dynamics simulations of steady-state heat and mass transport in condensation. II. Transfer coefficients. *Journal of Colloid and Interface Science* **240**, 355–364.

Røsjorde, A., Kjelstrup, S., Johannessen, E. and Hansen, R.: 2005a. Minimizing the entropy production in a chemical process for dehydrogenation of propane. *in* S. Kjelstrup, J. E. Hustad, T. Gundersen, A. Røsjorde and G. Tsatsaronis (eds), *Proceedings of The 18$^{\text{th}}$ ECOS Conference, Vol. II.* Tapir Academic Press: Trondheim, Norway. pp. 593–600.

Røsjorde, A., Nakaiwa, M., Huang, K., Iwakabe, K. and Kjelstrup, S.: 2004. Second law analysis of an internal heat-integrated distillation column. *in* R. Rivero, L. Monray, R. Pulido and G. Tsatsaronis (eds), *Proceedings of ECOS Conference, 2004, ISBN 968-489-027-3.*. Guanajuato, Mexico. pp. 107–115.

Røsjorde, A., Nakaiwa, M., Huang, K., Iwakabe, K. and Kjelstrup, S. 2005b. Second law analysis of an internal heat-integrated distillation column. *Chemical Engineering Science* **60**, 1199–1210.

Sander, M. T.: 1991. *Ecoamine FG feasibility study. Contract No. T-122.013. Prepared for Statoil by Fluor Daniel.* Flour Daniel.

Sauar, E., Kjelstrup, S. and Lien, K. M. 1996. Equipartition of forces. A new principle for process design and operation. *Industrial Engineering Chemistry Research* **35**, 4147–4153.

Sauar, E., Nummedal, L. and Kjelstrup, S. 1997. Equipartition of forces – Extention to chemical reactors. *Computers and Chemical Engineering* **21**, S29–S34.

Sauar, E., Siragusa, G. and Andresen, B. 2001. Equal thermodynamic distance and equipartition of forces principles applied to binary distillation. *Journal of Physical Chemistry A* **105**, 2312–2320.

Schimdt, E.: 1953. *Thermodynamik.* Springer-Verlag. Berlin.

Schmidt-Bleek, F.: 1994. *Wieviel Umwelt braucht der Mensch? mips - Das Maß für ökologisches Wirtschaften.* Birkhäuser Verlag GmbH. Berlin.

Sciubba, E. 2004. From engineering economics to extended exergy accounting: A possible path from monetary to resource based costing. *Journal of Industrial Ecology* **8**, 19–40.

Seager, T. P. and Theis, T. L. 2002a. Exergetic pollution potential: Estimating the revocability of chemical pollution. *Exergy –An International Journal* **2**, 273–282.

Seager, T. P. and Theis, T. L. 2002b. A uniform definition and quantitative basis for industrial ecology. *Journal of Cleaner Production* **10**, 225–235.

SETAC: 1994. *SETAC Guidelines for Life Cycle Assessment: A Code of Practice.* Society of Environmental Toxicology and Chemistry (SETAC). Washington DC.

Sherwood, T. K. 1930. The drying of solids. III. Mechanism of the drying paper. *Industrial and Engineering Chemistry* **22**, 132–136.

Sidwall, S., Bond, J. and Douglas, W.: 1999. Industrial validation of a multiple technique paper drying simulator. *TAPPI Proceedings of the Engineering/Process and Product Quality Conference.* Anaheim, CA. pp. 271–301.

Simulation Sciences SIMSCI: 2001. Simulation sciences 2001, Brea, CA, pro/ii version 6. CD-ROM. Software description at: http://www.simsci-esscor.com/us/eng/simsciProducts/productlist/proII/default.htm (accessed in September 2004).

Soininen, M. 1995. Modeling of web drying. *Drying Technology* **13**, 823–866.

Sorin, M. V. and Brodyansky, V. M. 1992. A method for thermodynamic optimization: I. Theory and application to an ammonia-synthesis plant. *Energy* **11**, 1019–31.

Spreng, D. T.: 1988. *Net energy analysis and the energy requirements of energy systems.* Praeger Publishers. New York.

Standigl, R. 2004. The chemical industry: Challenges and answers. *Chimie Ingenieur Technick* **76**, 21–29.

Statistics Norway: 2003. Website: http://www.ssb.no/english/subjects/ (accessed in March 2006).

Statistics Norway: 2004. Website: http://www.ssb.no/english/subjects/ (accessed in March 2006).

Stodola, A. 1898. The cycle processes of the gas engine (in German). *Z. VDI* **32**, 1086–1091.

Szargut, J. and Petela, R.: 1965. *Exergy (in Polish).* Wydawnictwa Naukowo-Techniczne. Warsaw, Poland.

Szargut, J., Morris, D. R. and Steward, F. R.: 1988. *Exergy analysis of thermal, chemical and metallurgical processes.* Hemisphere. New York, USA.

Tai, S. and anf T. Goda, K. M. 1986. Chemical exergy of organic matter in wastewater. *International Journal of Environmenal Studies* **27**, 301–314.

Tober, E.: 1997. *Chemical process optimisation with the aid of exergy, economics and life cycle assessment.* PhD thesis. Delft University of Technology, Delft, the Netherlands.

Tolman, R. C. and Fine, P. C. 1948. On the irreversible production of entropy. *Reviews of Modern Physics* **20**, 51–77.

Tondeur, D.: 1990. Equipartition of entropy production: A design and optimisation criterion in chemical engineering. *in* S. Sieniutycz and P. Salamon (eds), *Advances in Thermodynamics: Finite-time Thermodynamics and Thermoeconomics.* Taylor and Francis, New York. pp. 175–208.

Tondeur, D. and Kvaalen, E. 1987. Equipartition of entropy production. An optimality criterion for transfer and separation processes. *Industrial Engineering and Chemistry Research* **26**, 50–56.

Tribus, M.: 1961. *Thermostatics and Thermodynamics.* Van Nostrand. New York.

Tsatsaronis, G.: 2005. Definitions and nomenclature in exergy analysis and exergoeconomics. *in* S. Kjelstrup, J. E. Hustad, T. Gundersen, A. Røsjorde and G. Tsatsaronis (eds), *Proceedings of The 18$^{\text{th}}$ ECOS Conference, Vol. I.* Tapir Academic Press: Trondheim, Norway. pp. 321–325.

Ukidwe, N. U. and Bakshi, B. R. 2004. Thermodynamic accounting of ecosystem contribution to economic sectors with application to 1992 US economy. *Environmental Science and Technology* **38**, 4810–4827.

Valero, A., Tsatsaronis, G., von Spakowski, M., Fragopoulos, C., Lazano, M., Serra, L. and Piza, J. 1994. CGAM problem: definition and conventional solution. *Energy* **19**, 365–381.

Vilar, J. and Rubi, J. 2001. Thermodynamics beyond local equilibrium. *Proc. National Academy Science USA* **98**, 11–81.

von Spakowski, M. R., Fravat, D. and Batato, M. 1991. A global second law approach to the evaluation of energy-conservation systems taking into account economic and environmental factors. *Entropie* **164/165**, 139–156.

Wagman, D., Evans, H., Harlow, I., Bailey, S. and Shumm, R.: 1968. *Selected Values of Chemical Thermodynamic Properties.* US Government Printing Office. Washington DC.

Wagner, W. 2000. The IAPWS industrial formulation of 1997 for the thermodynamic properties of water and steam. *Journal of Engineering for Gas Turbines and Power - Transactions of the ASME* **122**, 150–182.

Wall, G.: 1977. *Exergy - A Useful Concept within Resource Accounting.* Institute of Theoretical Physics. Götegorg, Report No. 77-42.

Wall, G.: 1986. *Exergy - A Useful Concept.* PhD thesis. Chalmers University of Technology, Göteborg, Sweden.

Wall, G. 1988. Exergy flows in industrial processes. *Energy* **13**, 197–208.

Wall, G. and Gong, M. 2001. On exergy and sustainable development. *Exergy - An International Journal* **1**, 128–145.

Weitz, K., Barlaz, M., Ranjithan, R., Brill, D., Thorneloe, S. and Ham, R. 1999. Life cycle management of municipal solid waste. *International Journal of LCA* **4**, 195–201.

White, C. M. 2003. Separation and capture of CO_2 from large stationary sources and sequestration in geological formations - coal beds and deep saline aquifers. *Air and Waste Management Association* **53**, 645–715.

White, R.: 1994. Preface. *in* B. Allenby and D. Richards (eds), *The Greening of Industrial Ecosystems.* National Academy Press: Washington DC. pp. V–VI.

Wild, M., Ohmura, A. and Gilgen, H. 1998. The distribution of solar energy at the Earth's surface. *Geophysical Research Letter* **25**, 4373–4376.

Wilhelmsson, B., Fagerholm, L., Nilsson, L. and Stenström, S. 1994. An experimental study of contact coefficients in paper drying. *Tappi Journal* **77**, 159–68.

Wilhelmsson, B., Nilsson, L., Stenström, S. and Winmerstedt, R. 1993. Simulation models of multi-cylinders paper drying. *Drying Technology* **11**, 1177–1205.

Wright, S. 2004. Comparison of the theoretical performance potential of fuel cells and heat engines. *Renewable Energy* **29**, 179–195.

Yeo, Y., Hwang, K., Yi, S. and Kang, H. 2004. Modeling of the drying process in paper plants. *Korean J. Chemical Engineering* **21**, 761–766.

Yi, H., Hau, J., Ukidwe, N. and Bakshi, B. 2004. Hierarchical thermodynamic metrics for evaluating the environmental sustainability of industrial processes. *Environmental Progress* **23**, 302–314.

Zvolinschi, A., Johannessen, E. and Kjelstrup, S. 2006a. The second law optimal operation of a paper drying machine. *Chemical Engineering Science* **61**, 3653–3662.

Zvolinschi, A., Kjelstrup, S. and Holmberg, A.: 2003. Exergy analysis and life-cycle analysis of a paper mill. *in* N. Houbak, B. Elmegaard, B. Qvale and M. Moran (eds), *Proceedings of The 16th ECOS Conference, Vol. III.* Copenhagen, Denmark. pp. 1547–1554.

Zvolinschi, A., Kjelstrup, S., Bolland, O. and van der Kooi, H. 2006b. Exergy sustainability indicators as a tool in industrial ecology. Application to two gas-fired combined cycle power plants. *Journal of Industrial Ecology (accepted).*

Zvolinschi, A., Kjelstrup, S., Bolland, O. and vand der Kooi, H.: 2002. Including exergy analysis in industrial ecology: The case of combined cycle power plants. *in* G. Tsatsaronis, M. Moran, F. Cziesla and T. Brucknen (eds), *Proceedings of The 15th ECOS Conference, Vol. I.* Berlin, Germany. pp. 373–380.

Appendix A: Process descriptions, stream data, and boundary conditions for Plants A and B

A1. Process description and stream data for Plant A

Plant A is an integration between a standard power plant (Greenhouse R&D Programme 2000), which is a natural gas-fired gas-turbine combined cycle, and a CO_2 amine absorption (ABS) plant. Figure A1 shows the process flow diagram for this plant, while Tables A1 and A3 give the process stream data.

The combined cycle consists of a gas-turbine (GT) where natural gas (1) is combusted with air (2) previously compressed in an air compressor (AC). After the combustor, the high-temperature and high-pressure exhaust gases (4) enter a turbine (T) where they expand producing shaft work. This work is used to drive the air-compressor (AC) and the generator (G). The heat content of the exhaust gases (5) is transferred to the steam cycle in an unfired heat recovery steam generator (HRSG). The steam generated here expands successively in a steam turbine (ST) with three pressure levels: a high-pressure (HP-ST), a medium-pressure (MP-ST), and a low-pressure steam turbine (LP-ST), respectively. The steam cycle ends with a condenser (COND) that uses seawater as cooling agent. The off-stream cooling seawater is released in a large surface seawater body, body that can be a heat source for microalgae growing.

The exhaust gas (21) is not vented to the natural environment, but it is first cleaned from CO_2 in a monoethanolamine (MEA) chemical absorption process in the ABS plant. The plant consists of the following units: a feed cooler C1 (where stream 21 is cooled at 25^0C), a blower (where the pressure is slightly increased at 1.2 bar), a CO_2 absorption tower (where CO_2 is chemically absorbed by means of MEA), a regeneration column (where MEA is regenerated by means of a medium-pressure steam; a mixture of CO_2 and water vapour is released), a flasher (where water from the mixture is separated), a cross-heat exchanger (CHE), two pumps, and two air coolers C2 and C3. As basis for the exergy calculation of the CO_2 ABS plant, the Ecoamine FG process by Flour Daniel was used (Sander 1991). The characteristics of this process are: a MEA solvent flow of 2800 m^3/ h (1012 kg/m^3, 30 wt.% of MEA in liquid water), a medium-pressure steam flow of 27.9 m^3/h (with a pressure of 4.2 bar and with a temperature of 145^0C), and a 90% recovery of CO_2 (99 wt.% CO_2 purity). The detailed process flow diagram of the CO_2 ABS plant is given also in Fig. A1, downstream from the standard power plant.

Figure A1. Process flow digram for Plant A.

Table A1. Process stream data (stream number, mass flow rate (m), molecular weight (MW), molar composition (x_i)) for Plant A. For stream number, readers are referred to Fig. A1.

No	m	MW	x_i (mole %)					
	(kg/s)		CO_2	C_1	C_{2+}	H_2O	O_2	N_2
1	18.22	19.64	5.34	83.94	8.06	0.01		2.65
2,3	697.83	28.90	0.03			0.64	20.74	78.59
4, 5, 21	716.05	28.49	4.09			7.87	12.51	75.53
31, 32	129.27	18.02				100.00		
33	138.27	18.02				100.00		
34	83.97	18.02				100.00		
34 bis	54.30	18.02				100.00		
35	19.93	18.02				100.00		
36, 39	103.90	18.02				100.00		
37, 38	4419.35	18.02				100.00		
41	0.20	18.02				100.00		
43	675.35	27.82	0.42			9.56	12.54	77.48
44, 47[a]	790.16	23.10	1.30			87.63		
45, 46[b]	749.46	22.85	0.14			88.64		
48, 49	41.75	43.95	99.79			0.21		
50	40.70	43.97	99.94			0.06		

[a]The streams contain also MEA with a molar concentration of 11.07%.

[b]The streams contain also MEA with a molar concentration of 11.22%.

A2. Process description and stream data for Plant B

Plant B is an integration between a hydrogen production plant and a hydrogen-fired combined cycle power plant. A traditional steam reforming process produces a fuel with high-hydrogen content. Modern gas turbines with low NO_x combustors are restricted with regard to the nitrogen concentration in the fuel. Therefore, an air-blown auto-thermal reactor (ATR) was chosen to produce hydrogen from natural gas (Bolland et al. 2001, Ertesvåg 2005). Figure A2 shows the process flow diagram for Plant B, while Tables A2 and A3 give the process stream data.

Figure A2. Process flow diagram for Plant B.

In the hydrogen production plant, natural gas (1) is converted to a gas mixture of carbon dioxide, hydrogen, and water in the following steps. First, in a pre-reformer (PRE), most of the heavier hydrocarbons are reformed with steam into a synthesis gas mixture of hydrogen and carbon monoxide. The methane from natural gas stream is converted to a gas mixture (12) by means of an auto-thermal reforming reaction that uses steam (9) and air (11) as co-reactants. Second, the carbon monoxide from the stream (12) is converted with steam into carbon dioxide in the high- and low-temperature shift reactors (HTS and LTS, respectively). Finally, the water and carbon dioxide are removed from the main stream in a water removal (WR) unit and in a ABS plant, respectively. The process steps in the ABS plant are the same as those practised in Plant A. For sake of simplicity, Fig. A2 illustrates the process flow diagram of all processes without the ABS plant. Figure A1 gives the information of the process flow diagram in the ABS plant.

The steam cycle in Plant B is different than that in Plant A. One difference is that the HRSG in Plant B is supplemented by a firing section (SF), where 6.3% of the hydrogen produced in the hydrogen production plant is burnt. The new configuration is needed because of the extra heat requirement in the PRE and ATR. Another difference is that the steam cycle in Plant B takes the advantage of the high exergy content of ATR (12), HTS (14), and LTS (17) products through a heat exchange network. The network consists of three heat exchangers, HE1, HE2, and HE4. The remaining heat exchangers (i.e., HE3 and HE5) are used to exchange heat between fuel (22) and steam (15). The saturated steam (30) obtained in the steam cycle of Plant B is superheated in the HRSG, and then it is expanded in the ST. Before it is burnt in the gas-turbine combustor, the CO_2-cleaned H_2-rich gas (22) is compressed to 12.4 bar in a fuel compressor (FC) in order to fulfil the pressure specification required by the gas turbines used.

Table A2: Process stream data (stream number, mass flow rate (m), molecular weight (MW), molar composition (x_i)) for Plant B. For stream number, readers are referred to Fig. A2.

No	m	MW	x_i (mole %)						
	(kg/s)		H_2	CO	CO_2	$C_{1,2^+}$	H_2O	O_2	N_2
1	20.1	19.67			5.34	92.00	0.01		2.65
2, 3	655.7	28.90			0.03		0.64	20.74	78.59
4, 5, 43	649.2	27.37			0.90		13.28	11.06	74.84
6, 7	51.7	18.62			1.96	33.75	63.31		0.97
8, 9	51.7	17.47	7.85	0.08	4.85	33.03	53.27		0.91
10, 11	79.7	28.90			0.03		0.64	20.74	78.59
12, 13	131.5	18.58	31.39	10.27	5.53	0.18	21.89		30.83
14-16	131.5	18.58	38.23	3.43	12.37	0.08	14.96		30.83
17-19	131.5	18.58	41.20	0.46	15.34	0.08	11.99		30.83
20	116.4	18.58	46.75	0.53	17.41	0.21	0.14		34.98
21	7.3	13.94	55.43	0.62	2.06	0.25	0.16		41.47
22, 23	73.2	13.94	55.43	0.62	2.06	0.25	0.16		41.47
24, 29	81.4	18.02					100.00		
25, 26	67.3	18.02					100.00		
27, 28	14.0	18.02					100.00		
30, 32	98.6	18.02					100.00		
33, 34	125.2	18.02					100.00		
36, 39	113.0	18.02					100.00		
37, 38	6443.0	18.02					100.00		
34 bis	8.6	18.02					100.00		
31, 41	31.7	18.02					100.00		
44, 47[a]	743.7	31.09			1.85		86.93		
45, 46[b]	700.5	30.79			0.14		88.64		
48, 49	43.5	43.95			99.79		0.21		
50	43.2	43.97			99.94		0.06		

[a]The streams contain also MEA with a molar concentration of 11.22%.

[b]The streams contain also MEA with a molar concentration of 11.22%.

Table A3. Data for selected process streams (stream number, temperature (T), pressure (p), chemical (E^{chem}) and total exergy (E^{tot})) for Plants A and B. For stream number, readers are referred to Figs. A1 and A2.

No	Plant A				Plant B			
	T (^{0}C)	p (bar)	E^{chem} (MW)	E^{tot} (MW)	T (^{0}C)	p (bar)	E^{chem} (MW)	E^{tot} (MW)
1	4	16.7	789.8	800.9	4	16.7	852.7	859.2
2	8	1.0	0.0	0.0	8	1.0	0.0	0.0
3	379	16.3	0.0	236.9	377	15.6	0.0	204.4
4	1328	15.5	18.2	805.6	1250	15.4	15.8	771.5
5	602	1.0	18.2	241.7	614	1.0	15.7	225.2
6					257	16.6	867.8	892.6
7					500	16.1	867.8	909.7
8					440	15.6	868.0	906.5
9					598	15.1	868.0	920.2
10					377	15.6	0.0	28.3
11					598	15.1	0.0	40.2
12					900	14.2	729.6	887.7
13					350	13.8	729.6	798.1
14					429	13.4	716.7	795.7
15					311	13.0	716.7	779.9
16					200	12.6	716.7	767.7
17					237	12.2	712.2	766.2
18					130	11.8	712.2	756.5
19					25	11.7	712.2	747.6
21	96	1.0	18.1	19.2	25	10.1	72.1	82.1
23					87	19.5	696.0	733.2
24					163	121.5	49.3	63.6
26					325	121.5	40.7	77.7
28					325	121.0	8.4	16.1
30					501	111.1	59.7	151.0
31	559	121.9	41.2	146.7	436	16.7	19.2	40.6
32	366	33.1	41.2	112.1	313	29.2	59.7	116.5
33	560	30.0	47.7	150.0	501	26.6	75.9	117.7
34	304	4.5	43.6	125.0	274	4.2	68.5	106.0
34 bis	145	4.5	4.0	48.9	274	4.2	4.7	7.3
36	24	0.0	54.0	54.0	24	0.0	68.5	68.5
37	8	1.0	0.0	0.0	8	1.0	0.0	0.0
38	21	1.0	0.0	4.0	21	1.0	0.0	7.6
39	24	0.4	54.0	55.0	24	0.0	70.7	70.7

Table A3 (continuation).

No	Plant A				Plant B			
	T (^{0}C)	p (bar)	E^{chem} (MW)	E^{tot} (MW)	T (^{0}C)	p (bar)	E^{chem} (MW)	E^{tot} (MW)
41	15	3.4	0.1	4.1	15	3.4	0.1	8.8
42					91	122.0	0.1	7.1
43	88	1.0	4.0	4.3	83	1.0	8.1	8.3
44	54	1.0	32.4	32.4	54	1.0	57.6	57.6
45	113	1.0	48.5	48.5	113	1.0	55.5	55.5
46	96	1.0	48.5	48.5	96	1.0	55.5	55.5
47	90	1.0	32.4	32.4	90	1.0	57.6	57.6
48	38	1.4	18.8	18.9	38	8.5	19.8	24.8
50	20	1.2	18.3	18.5	20	8.4	19.4	24.4

A3. Boundary conditions for Plants A and B

A pipeline-quality natural gas of a temperature of 4^0C and a pressure of 170 bar, is extracted from a Norwegian offshore gas reservoir, which has a molar composition (in mole %) of methane: 83.94, ethane: 4.87, propane: 2.12, butane: 0.77, pentane: 0.23, hexane: 0.07, carbon dioxide: 5.34, nitrogen: 2.65, and water: 0.01. This gas was chosen as the fossil fuel resource in both power plants. For this resource, we calculated a chemical exergy of 43.35 MJ/kg natural gas. After is extracted from the reservoir, the natural gas is first transported by pipelines and then expanded in a fuel expander. The expander is used to drop the gas pressure from 170 bar to 16.7 bar.

The group contribution method (Szargut et al. 1988) was used to estimate the chemical exergy content of the mono-ethanolamine molecule in liquid phase. A value of 1.54 kJ/kmol mono-ethanolamine was used.

The state conditions of the air used in the power plants were set to a temperature of 8^0C, a pressure of 1.01 bar, a relative humidity of 60%, and a molar composition (in mole %) of nitrogen: 77.58, oxygen: 20.82, argon: 0.93, CO_2: 0.03, and water: 0.64. The cooling seawater was assumed to be available at 8^0C, which was the temperature at 50-100 m sea depth in southern Norway. The rise of the cooling seawater temperature was assumed to be 13^0C, while the condenser temperature was set to be 24^0C.

The state-of-the-art gas turbine, a GE 9351FA gas turbine from General Electric (GE), was used in both power plants. Carbon dioxide compression was

accomplished using a three-stage inter-cooler compressor and a subsequent pump. Each stage of compression performed with an isentropic efficiency of 70%, 80% and 85%, respectively. The heat exchangers for inter-cooling were modelled with a pressure drop of 3%.

In our models and simulations, we assumed that all chemical reactors, the CO_2 absorption tower, and the amine regeneration column are operated at equilibrium. Water and steam properties were formulated by the IAPWS - industrial formulation for the thermodynamic properties of water and steam - (Wagner 2000). A pressure drop of 3% was assumed in each of the following equipments: pre-reformer, high- and low-temperature shift reactors, and in each of the heat exchangers (HE1-H5), and one of 6% in the auto-thermal reformer, the CO_2 absorption tower, and the amine regeneration column.

Appendix B: Process descriptions, stream data and assumptions for Options C and D

B1. Process description and stream data for Option C

Figure B1 shows the process flow diagram for Option C. Tables B1 and B2 give the process stream data for this option when it is combined with Plant A and Plant B, respectively. In Option C, the CO_2 captured (50) in Plant A or B is converted via photosynthesis to biomass (52) by means of a marine microalgae cultivation system. From dewatering by centrifugation a dry biomass (53) and a liquid residue (55) are obtained. The dry biomass is converted via biomass anaerobic digestion to biogas (54) (Legrand 1993) at a temperature of 17^0C and the atmospheric pressure. The biogas obtained is a gas mixture of 50 wt.% methane and 50 wt.% CO_2. Apart from the biogas, a solid residue is recuperated at the bottom of digester. The biogas is processed by means of a pressure swing adsorption (PSA) on molecular sieve carbon (Kapoor and Yang 1989), in order to obtain a methane-rich gas (58). We called this gas the synthetic gas (58), and we assumed that it has a pressure of 20 bar and contains a mixture of 90 wt.% methane and 10 wt.% $C0_2$. At this state, the synthetic gas is disposed in a depleted gas reservoir. In our study, we assumed that the carbon content of the CO_2 captured in Plants A and B is integrally converted into the carbon of biomass. This conversion is carried out in the marine microalgae cultivation system, which consists of several 1000 ha-ponds. Each pond is build from 20 ha-modules (Legrand 1993). Each module is fed by a CO_2-air mixture gas (1:10 wt%). Using these assumptions, and the figure of an average dry-biomass yield of 15 g dry-biomass per m^2 per day (Goldman 1979), we calculated that a total marine area of 6100 ha and 6500 ha per year

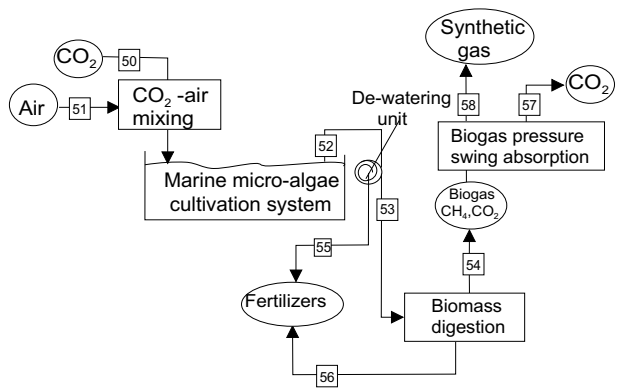

Figure B1. Process flow diagram for Option C.

is required to trap all carbon from the CO_2 captured in Plant A and Plant B, respectively.

The following reaction was used to calculate the conversion of CO_2 into biomass (Beker 1994):

$$106CO_2 + 236H_2O + 16NH_4^+ + HPO_4^{2-} = C_{106}H_{181}O_{45}N_{16}P + 118O_2 + 171H_2O + 14H^+$$

Using this reaction, one can calculate that an amount of 1.55 kg O_2 per kg dry-biomass can be released in the natural environment. In addition, a biomass chemical formula of ($C_{106}H_{181}O_{45}N_{16}P$) was used to find the biomass elemental composition. We calculated that the biomass yield of a moisture content of 90 wt% has the following elemental composition (in mass % ash-free dry-matter) of carbon: 52.4, hydrogen: 7.4, oxygen: 29.7, nitrogen: 9.2, and phosphorus: 1.3.

For the calculation of the digestion conversion potential of biomass into methane, we use the estimation provided by Legrand (1993) that 350 ml of methane at standard pressure (1.01 bar) and temperature (25^0C) are formed when one gram of chemical oxygen demand (COD) is converted to biogas (Legrand 1993). The ratio between COD and volatile solids (VS) of free-ash dry-biomass was set to 1.2. At this ratio, 350 ml x 1.2 = 420 ml methane results from the conversion of one dry-gram of biomass.

The other product from the PSA process is a CO_2-enriched waste gas stream. We assumed that this stream is recirculated into the marine micro-algae cultivation system after dilution with air. However, this was not consider in our calculation. The other products from the biomass dewatering unit and from the biomass anaerobic digestion process are a liquid and solid residue, respectively. They correspond to the streams 55 and 56, respectively, in Fig. B1. We named these residues as the liquid and solid fertiliser, respectively, because they contain biodegradable hydrocarbons and micro-elements which are valuable resources for the marine microalgae growing process and in forestry.

B2. Process description and stream data for Option D

In Option D, the CO_2 recovered from power plants is first compressed and then disposed. In our study, the compression of CO_2 was modelled by three compressors with cooling and water flashing after each compressor. The compressor-

outlet pressures were 4 bar, 15 bar and 60 bar, respectively. After each compressor, the flow was cooled to 20^0C and some condensed water was flashed off. After the third compressor, the stream containing CO_2 was cooled to liquid state and pumped to a pressure of 200 bar. This liquid is disposed in a depleted gas reservoir. The following characteristics were assumed for the depleted reservoir: a depth of 1000 m, a pressure of 145 bar, and a temperature of 60^0C.

B3. The assumptions done in Options C and D

The boundary conditions applied to Plants A and B (see Appendix A) were also used to perform the calculations of Options C and D. Per year, 365 days were considered as operation time for the power plants and Option D, while for Option C only 180 days (12 hours per day) were used as the active photosynthesis period for the microalgae cultivation under outdoor conditions, between April and September. The location of the power plants was chosen in southern Norway (60^o latitude). At this location, an annual global solar radiation on the horizontal surface of about 970 kWh/m^2 was assumed (Wild et al. 1998). Only half of this amount of radiation (ranged between 400 and 700 nm) is used for photosynthesis. This radiation is called photosynthetic active radiation (PAR = 485 kWh/m^2). From this PAR only 5% of it is converted in chemical exergy of biomass (Bisio and Bisio 1998). We used this figure to calculate the solar-based renewable exergy input for Option C in combination with Plants A and B. In addition, we assumed that the ratio of the exergy flux to the total energy flux of solar radiation is 0.93 (Petela 1964), and that the exergy content of the seawater used as marine microalgae growing medium is zero. The chemical exergy of the biomass was calculated using the following relation (Szargut et al. 1988):

$$E^{\text{chem}}_{\text{biomass}} = (LHV + L_w z_w)\beta + E^{\text{chem}}_w z_w \qquad \text{(B-2)}$$

where LHV is the lower heating value (LHV = 17.5 MJ/kg dry biomass), L_w is the latent enthalpy of evaporation of water (L_w = 2.44 MJ/kg water), z_w is the water content of biomass, β is the correction coefficient (ζ = 0.92 for streams with a 90 wt.% dry-biomass composition (Szargut et al. 1988)), and E^{chem}_w is the specific chemical exergy of liquid water (E^{chem}_w = 0.05 MJ/kg). Using Eq. (B-2), we calculated that the specific chemical exergy of biomass with a 90 wt.% dry matter is 16.3 MJ/kg.

Table B3 gives the chemical and total exergy of each steam in Option C when it is combined with Plant A or B. Tables B4 and B5 give the balances for the

total and carbon mass, and the exergy balances for Option C when Plant A and B, respectively, is combined. The exergy needs to support all processes in Option C are sustained by the power plants in question. We assumed that the exergies subtracted from power plats are in the form of electric power. Table B6 gives the exergy amounts that are needed for CO_2 abatement in Plants A and B.

Table B1. Process stream data (stream number, mass flow rate (m), molecular weight (MW), mass composition (c_i)) for Option C when Plant A is used. For stream number, readers are referred to Fig. B1.

No	m	MW	c_i (wt.%)					
	(kg/s)	(kg/kmol)	CO_2	CH_4	H_2O	O_2	N_2	Solid
50	48.8	43.9	99.9		0.01			
51	488.0	28.9	0.03		1.57	20.8	77.6	
52	254.4	20.6			90.0			10.0
53	28.2	169.0			10.0			90.0
54	19.7	23.3	50.0	50.0				
55	226.2	19.8			99.9			0.1
56	8.5	59.9			70.5			29.5
57	9.8	40.5	95.5	4.5				
58	9.8	17.1	10.0	90.0				

Table B2. Process stream data (stream number, mass flow rate (m), molecular weight (MW), mass composition (c_i)) for Option C when Plant B is used. For stream number, readers are referred to Fig. B1.

No	m	MW	c_i (wt.%)					
	(kg/s)	(kg/kmol)	CO_2	CH_4	H_2O	O_2	N_2	Solid
50	50.5	43.9	99.9		0.01			
51	505.0	28.9	0.03		1.57	20.8	77.6	
52	263.2	20.6			90.0			10.0
53	29.1	169.0			10.0			90.0
54	20.4	23.3	50.0	50.0				
55	234.1	19.8			99.9			0.1
56	8.8	59.9			70.5			29.5
57	10.2	40.5	95.5	4.5				
58	10.2	17.1	10.0	90.0				

Table B3. Exergy data for process streams (stream number, mass flow rate (m) specific chemical exergy (E^{chem}) and total exergy (E^{tot})) for Option C when Plant A and Plant B are used. For stream number, readers are referred to Fig. B1.

No	Plant A			Plant B		
	m (kg/ s)	E^{chem} (MJ/ kg)	E^{tot} (MW)	m (kg/ s)	E^{chem} (MJ/ kg)	E^{tot} (MW)
50	48.8	22.45	22.4	50.5	22.7	22.7
51	488.0	0.00	0.0	505.0	0.0	0.0
52	254.4	1.90	483.4	263.2	1.9	500.2
53	28.2	16.3	459.6	29.1	16.3	475.6
54	19.7	23.4	461.0	20.4	23.4	477.4
55	226.2	0.1	22.6	234.1	0.1	22.5
56	8.5	0.02	0.17	8.8	0.02	0.18
57	9.8	2.3	22.5	10.2	2.3	23.3
58	9.9	46.7	456.6	10.2	46.7	476.4

Table B4. Input (in) and output (out) mass flow rate (m), carbon mass flow rate (m_C), and exergy (E) for Plant A in combination with Option C. For steam number, reader are referred to Fig. B1. Exergy loss (E_{loss}) is calculated as E_{in} - E_{out}. SG is synthetic gas.

Process/stream	m_{in}	$m_{C,in}$	E_{in}	m_{out}	$m_{C,out}$	E_{out}	E_{loss}
CO_2-air mixing							
CO_2 (50)	48.8	12.2	23.6				
Air (51)	488.0	0.06	0.0				
CO_2+air				536.8	12.2	16.6	
Total	536.8	12.2	23.6	536.8	12.2	16.6	6.6
Algae growth							
CO_2+air	536.8	12.2	16.6				
Seawater	4419.4		5.0				
Exhaust gases	810.0	1.01	9.4				
Sunlight			761.6				
Biomass (52)				254.4	12.40	489.4	
Air				488.0	0.06	0.0	
Seawater				4213.8		0.0	
Exhaust gases				810.0	1.01	2.0	
Total	5766.2	13.17	792.6	5766.2	13.17	491.4	301.2
De-watering							
Biomass (52)	254.4	12.4	489.4				
Electric-power			42.3				
Biomass (53)				28.2	12.0	488.0	
Fertiliser (55)				226.2	0.4	0.2	
Total	254.4	12.4	531.7	254.4	12.4	488.2	43.5
Digestion							
Biomass (53)	28.2	12.0	488.0				
Steam	147.8		34.0				
Electric-power			3.7				
Biogas (54)				19.7	9.1	462.0	
Fertiliser (56)				8.5	2.9	22.8	
Condensate				147.8		34.4	
Total	176.0	12.0	525.7	176.0	12.0	519.2	6.5
SG processing							
Biogas (54)	19.7	9.1	462.0				
Electric-power			20.0				
CO_2 (57)				9.8	2.1	4.4	
SG (58)				9.9	7.0	456.6	
Total	19.7	9.1	482.0	19.7	9.1	461.0	21.0

Table B5. Input (in) and output (out) mass flow rate (m), carbon mass flow rate (m_C), and exergy (E) for Plant B in combination with Option C. For steam number, reader are referred to Fig. B1. Exergy loss (E_{loss}) is calculated as E_{in} - E_{out}. SG is synthetic gas.

Process/stream	m_{in}	$m_{C,in}$	E_{in}	m_{out}	$m_{C,out}$	E_{out}	E_{loss}
CO_2-air mixing							
CO_2 (50)	50.5	13.6	24.4				
Air (51)	505.0	0.1	0.0				
CO_2+air				555.5	13.7	17.4	
Total	555.5	13.7	24.4	555.5	13.7	17.4	7.0
Algae growth							
CO_2+air	555.5	13.7	17.4				
Warm seawater	4825.0		4.1				
Exhaust gases	890.0	1.1	3.9				
Sunlight			808.4				
Biomass (52)				280.0	13.7	516.5	
Air				505.0	0.0	0.0	
Seawater				4595.5		0.0	
Exhaust gases				890.0	1.1	2.0	
Total	6270.5	14.8	833.8	6270.5	14.8	518.5	315.3
De-watering							
Biomass (52)	280.0	13.7	516.5				
Electric-power			49.2				
Biomass (53)				29.7	13.5	520.2	
Fertiliser (55)				250.3	0.2	0.5	
Total	280.0	13.7	565.7	280.0	13.7	520.7	45.0
Digestion							
Biomass (53)	29.7	13.5	520.0				
Steam	152.9		45.0				
Electric-power			6.2				
Biogas (54)				22.1	10.5	488.0	
Fertiliser (56)				7.6	3.0	30.0	
Condensate				152.9		46.0	
Total	182.6	13.5	571.2	182.6	13.5	564.0	7.2
SG processing							
Biogas (54)	22.1	10.5	488.0				
Electric-power			21.0				
CO_2 (57)				12.0	3.3	5.2	
SG (58)				10.1	7.2	476.4	
Total	22.1	10.5	509.0	22.1	10.5	481.6	27.4

Table B6. Exergy needs (in MW) for abatement of CO_2 from Plant A (A) and Plant B (B) in their combination with Option C (A+C and B+C, respectively) and Option D (A+D and B+D, respectively).

Process	A+C	B+C	A+D	B+D
CO_2 to biomass conversion	42.3	49.0	-	-
Biomass digestion	3.7	6.2	-	-
Biogas processing	20.0	20.0	-	-
CO_2 sequestration	-	-	86.8	132.8
Total	66.0	75.2	86.8	132.8

Appendix C: Process descriptions, inventory data and assumptions for Scenarios Z, L and H

This appendix contains thirteen sections (C1-C13), which describe the components of the system in Scenarios Z, L and H. Chapter 4 gives the description of the system and it specifies which process steps are part of the system in which scenario. The inventory data on mass and exergy bases are also given for every component in the narrow and wide system boundaries (see Chapter 4). The equations used for exergy calculation are presented.

The following appendices correspond to the following components of the system in Scenarios Z, L and H:

1. Appendix C1 for the woodyard (W);
2. Appendices C2-C3 for the thermo-mechanical pulping plant (TMP);
3. Appendices C4-C5 for the paper making plant (PMP);
4. Appendix C6 for the de-inking plant (DIP);
5. Appendices C7-C9 for the boiler house plant (BHP) and the natural gas-fired combined cycle power plant (NG PP);
6. Appendix C10 for the wastewater treatment plant (WWTP);
7. Appendix C11 for the wastepaper treatment plant (WPTP);
8. Appendix C12 for the municipal waste incineration plant (MWIP);
9. Appendix C13 for the transportation network (T).

In the following, the equations for exergy calculation of water- and wood-type streams are presented.

For the water-type streams (freshwater, wire water, process water and wastewater), with a temperature different than the average annual environmental temperature (assumed in this study to be $T_0 = 285$ K), the exergy content due to the heat was calculated as

$$E_{water}^{thermal} = Q(1 - \frac{T_0}{T - T_0} ln(\frac{T}{T_0})) \tag{C-1}$$

where

$$Q = mc_p(T - T_0) \tag{C-2}$$

Here, Q is the thermal energy flow of water/wastewater (in kW), m is the mass flow rate of water/wastewater (in kg/s), and c_p is the specific heat capacity of water/wastewater (in J/K kg).

For the wood-type materials, with a mass ratio $2.67 > \frac{O}{C} > 0.667$, the chemical exergy was calculated by (Kotas 1985)

$$E_{\text{wood-type materials}}^{\text{chem}} = LHV_{wood}\psi + WL\psi \quad \text{[kJ/kg wood]} \tag{C-3}$$

where W is the mass fraction of moisture in the wood-type material and L is the enthalpy of evaporation of water at the standard temperature ($T_0 = 293$ K).

The coefficient ψ is calculated by (Kotas 1985):

$$\psi = \frac{1.0438 + 0.1882\frac{H}{C} - 0.2509(1 + 0.7256\frac{H}{C}) + 0.0383\frac{N}{C}}{1 - 0.3035\frac{O}{C}} \quad [-] \tag{C-4}$$

where H/C is the atomic ratio between the hydrogen and carbon in the wood-type material, N/C is the atomic ratio between the nitrogen and carbon in the wood-type material, and O/C is the atomic ratio between the oxygen and carbon in the wood-type material. Because of lack of sufficient data, the effect of sulphur was not taken into account in Eq. (C-4). Also, the exergy of the ash contained in the fuel was neglected.

C1 The woodyard (W)

The woodyard (W) at Norske Skog's mill receives and stores the softwood (Norwegian spruce, *Picea abies*), bark and wood chips that are purchased from the forestry. The logs are partially debarked at the woodyard and partially at the thermo-mechanical pulping plant I (TMP I). The bark obtained at the woodyard and that purchased from the forestry are sent to the boiler house

plant (BHP). The amount of electricity and thermal energy needed for the processes in the woodyard are obtained from natural gas-fired power plant (NG PP) and boiler house plant (BP), respectively. A significant amount of freshwater per tonne of paper produced is required in the woodyard. The effluent of wastewater contains organic matter (BOD and COD), phosphorus (P_t) and nitrogen (N_t). No data was possible to obtain for the emissions into water due to the woodyard alone. These emissions are found in the input flow stream of wastewater of the wastewater treatment plant (see Table C10).

Table C1 gives the inventory data of the woodyard in Scenarios Z, L and H, for the narrow and wide system boundaries.

Table C1
Mass (M) and exergy (E) input/output inventory of the woodyard (W) in Scenarios Z, L and H, for the narrow and wide system boundaries (data are per air-dried tonne of newsprint paper), TS = total dry solids

	Scenario Z				Scenario L				Scenario H			
	Narrow		Wide		Narrow		Wide		Narrow		Wide	
Input flow description	M (t)	E (GJ)	M (t)	E (GJ)	M (t)	E (GJ)	M (t)	E (GJ)	M (t)	E (GJ)	M (t)	E (GJ)
Electricity		0.11		0.11		0.06		0.06		0.04		0.04
Steam (3.3 bar, 195 grd C)	0.15	0.09	0.15	0.09	0.12	0.07	0.12	0.07	0.03	0.02	0.03	0.02
Softwood from forestry (47 %TS)	1.24	14.88	1.24	14.88	0.98	11.70	0.98	11.70	0.09	1.08	0.09	1.08
Bark from forestry (39.5 %TS)	0.19	1.10	0.19	1.10	0.12	0.70	0.12	0.70	0.04	0.22	0.04	0.22
Chips from forestry (47 %TS)	0.52	5.93	0.52	5.93	0.41	4.67	0.41	4.67	0.10	1.19	0.10	1.19
Fresh water (10 grd C)	0.89	0.00	0.89	0.00	0.71	0.00	0.71	0.00	0.18	0.00	0.18	0.00
Total input for production	2.99	22.11	2.99	22.11	2.34	17.21	2.34	17.21	0.44	2.54	0.44	2.54
Total input for abatement	-	-	-	-	-	-	-	-	-	-	-	-
Output flow description												
Chips to TMP I (55 %TS)	0.18	2.02	0.18	2.02	0.15	1.61	0.15	1.61	0.00	0.00	0.00	0.00
Logs to TMP I (47 %TS)	0.89	10.15	0.89	10.15	0.64	7.30	0.64	7.30	0.05	0.57	0.05	0.57
Chips to TMP II (47 %TS)	0.81	9.26	0.81	9.26	0.65	7.41	0.65	7.41	0.16	1.85	0.16	1.85
Chips to BHP (47 %TS)	0.01	0.06	0.01	0.06	0.00	0.05	0.00	0.05	0.00	0.01	0.00	0.01
Bark to BHP (39.5 %TS)	0.01	0.10	0.01	0.10	0.01	0.08	0.01	0.08	0.00	0.02	0.00	0.02
Wastewater to WWTP (50 grd C)	1.00	0.01	1.00	0.01	0.81	0.00	0.81	0.00	0.20	0.00	0.20	0.00
Total output	2.89	21.58	2.89	21.58	2.26	16.44	2.26	16.44	0.42	2.45	0.42	2.45
Input - Output	0.10	0.53	0.10	0.53	0.08	0.77	0.08	0.77	0.02	0.09	0.02	0.09
Exergy efficiency (-)		0.9760		0.9760		0.9555		0.9555		0.9641		0.9641

C2-C3 The thermo-mechanical pulping plant (TMP)

The thermo-mechanical pulping plant (TMP) at Norske Skog's mill consists of two wood pulping facilities, termed TMP I and TMP II. The following processes are carried out here: wood handling through debarking, chips washing, dewatering, preheating, and refining, screening and thickening. The washing and screening processes are subject to a thermal pretreatment, while the disintegration and defibration processes are carried in a series of disc refiners at overpressure. After chipping and washing, the raw material is preheated with steam and then refined in a two-step refining system in which the first step is carried out at atmospheric pressure while the second step is carried out at a pressure of 4.5 bar. Part of the organic matters of the wood is dissolved in water and discarded in the process water downstream the thermo-mechanical pulping plant.

A large share (80%, in term of the heating value) of the electricity required in refiners is converted into heat in form of low-pressure steam. This steam is obtained from the wood moisture and dilution water in the refiners. Thermal energy may be recovered as steam in the refiners because of the pressured conditions undertaken here. This steam, after is cleaned through heat exchanger, is used as process steam for paper drying. After refining, the pulp is screened and cleaned through watering and dewatering processes.

Tables C2 and C3 present the inventory data of the thermo-mechanical pulping plant TMP I and TMP II, respectively, in Scenarios Z, L and H, for the narrow and wide system boundaries.

Table C2
Mass (M) and exergy (E) input/output inventory of the thermo-mechanical pulping plant TMP I in Scenarios Z, L and H, for the narrow and wide system boundaries (data are per air-dried tonne of newsprint paper), TS = total dry solids

	Scenario Z				Scenario L				Scenario H			
	Narrow scale		Wide scale		Narrow scale		Wide scale		Narrow scale		Wide scale	
Input flow description	M (t)	E (GJ)	M (t)	E (GJ)	M (t)	E (GJ)	M (t)	E (GJ)	M (t)	E (GJ)	M (t)	E (GJ)
Electricity		2.01		2.01		1.60		1.60		1.10		1.10
Warm water from PM1 and PM3 (55 grd C)	1.83	0.03	1.83	0.03	1.46	0.02	1.46	0.02	0.37	0.01	0.37	0.01
Fresh water (10 grd C)	7.17	0.00	7.17	0.00	15.00	0.00	15.00	0.00	1.43	0.00	1.43	0.00
Wirewater from PM1 and PM3 (0.5 %TS, 50 grd	3.86	0.52	3.86	0.52	3.09	0.42	3.09	0.42	0.00	0.00	0.00	0.00
Logs from woodyard (47 %TS)	0.89	10.15	0.89	10.15	0.64	7.30	0.64	7.30	0.05	0.57	0.05	0.57
Chips from woodyard (55 %TS)	0.18	2.02	0.18	2.02	0.15	1.61	0.15	1.61	0.00	0.00	0.00	0.00
Pulp from TMP II (12 %TS, 80 grd C)	0.88	2.58	0.88	2.58	0.70	2.07	0.70	2.07	0.18	0.52	0.18	0.52
Total input for production	14.81	17.30	14.81	17.30	21.05	13.02	21.05	13.02	2.03	2.20	2.03	2.20
Total input for abatment	-	-	-	-	-	-	-	-	-	-	-	-
Output flow description												
Primary pulp to PM1 (4.5 %TS, 58 grd C)	2.66	1.86	2.66	1.86	2.13	1.49	2.13	1.49	0.00	0.00	0.00	0.00
Primary pulp to PM 3 (4.5 %TS, 58 grd C)	3.39	2.37	3.39	2.37	2.71	1.90	2.71	1.90	0.00	0.00	0.00	0.00
Pulp to TMP II (4.5 %TS, 55 grd C)	7.88	8.75	7.88	8.75	5.60	7.00	5.60	7.00	1.00	1.75	1.00	1.75
Rejects (70 % TS)	0.02	0.21	0.02	0.21	0.01	0.16	0.01	0.16	0.00	0.00	0.00	0.00
Wastewater effluent and its emissions to WWTP	0.86	0.01	0.86	0.01	10.59	0.01	10.59	0.01	1.03	0.00	1.03	0.00
Bio-chemical matter (BOD7), in kg and MJ	6.96	0.22	6.96	0.22	5.57	0.17	5.57	0.17	1.39	0.04	1.39	0.04
Chemical matter (COD), in kg and MJ	18.00	0.65	18.00	0.65	14.40	0.52	14.40	0.52	3.60	0.13	3.60	0.13
Total nitrogen (Nt), in g and J	36.00	6.80	36.00	6.80	28.80	5.44	28.80	5.44	7.20	1.36	7.20	1.36
Total phosphorus (Pt), in g and J	9.00	0.03	9.00	0.03	7.20	0.03	7.20	0.03	1.80	0.01	1.80	0.01
Suspended solids, in g and J	0.00	0.00	0.00	0.00	0.00	0.00	0.00	0.00	0.00	0.00	0.00	0.00
Total output	14.80	13.20	14.80	13.20	21.04	10.56	21.04	10.56	2.03	1.75	2.03	1.75
Input - Output	0.00	4.10	0.00	4.10	0.00	2.46	0.00	2.46	0.00	0.44	0.00	0.44
Exergy efficiency (-)		0.7629		0.7629		0.8109		0.8109		0.7983		0.7983

Table C3
Mass (M) and exergy (E) input/output inventory of the thermo-mechanical pulping plant TMP II in Scenarios Z, L and H, for the narrow and wide system boundaries (data are per air-dried tonne of newsprint paper), TS = total dry solids

	Scenario Z				Scenario L				Scenario H			
	Narrow scale		Wide scale		Narrow scale		Wide scale		Narrow scale		Wide scale	
Input flow description	M (t)	E (GJ)	M (t)	E (GJ)	M (t)	E (GJ)	M (t)	E (GJ)	M (t)	E (GJ)	M (t)	E (GJ)
Electricity		2.01		2.01		1.60		1.60		0.10		0.10
Steam (15 bar, 185 grd C)	0.15	0.13	0.15	0.13	0.12	0.10	0.12	0.10	0.03	0.03	0.03	0.03
Fresh water (10 grd C)	6.12	0.00	6.12	0.00	4.90	0.00	4.90	0.00	1.22	0.00	1.22	0.00
Wirewater from paper mill (100 grd C)	0.85	0.05	0.85	0.05	0.68	0.04	0.68	0.04	0.17	0.01	0.17	0.01
Condensate from paper mill (60 grd C)	10.57	0.25	10.57	0.25	8.45	0.20	8.45	0.20	2.11	0.05	2.11	0.05
Condensate from steam recovery (60 grd C)	11.47	0.28	11.47	0.28	9.18	0.22	9.18	0.22	2.29	0.06	2.29	0.06
Pulp from pulping plant TMP I (4.5 %TS, 55 grd	7.88	8.75	7.88	8.75	5.60	7.00	5.60	7.00	1.00	1.75	1.00	1.75
Chips from woodyard (47 %TS)	0.81	9.26	0.81	9.26	0.65	7.41	0.65	7.41	0.16	1.85	0.16	1.85
Total input for production	37.86	20.72	37.86	20.72	29.58	16.58	29.58	16.58	7.00	3.84	7.00	3.84
Total input for abatement	-	-	-	-	-	-	-	-	-	-	-	-
Output flow description												
Steam (3.3 bar, 195 grd C)	0.85	0.51	0.85	0.51	0.68	0.41	0.68	0.41	0.17	0.10	0.17	0.10
Primary pulp to TMP I (12%TS, 80 grd C)	0.88	2.58	0.88	2.58	0.70	2.07	0.70	2.07	0.18	0.52	0.18	0.52
Primary pulp to PM2 (30 %TS, 60 grd C)	2.10	12.69	2.10	12.69	1.58	9.48	1.58	9.48	0.33	1.98	0.33	1.98
Condensate from steam recovery (85 grd C)	11.47	0.49	11.47	0.49	9.18	0.39	9.18	0.39	2.29	0.10	2.29	0.10
Process water to PM 1 and PM 3 (55 grd C)	3.23	0.06	3.23	0.06	2.59	0.05	2.59	0.05	0.65	0.01	0.65	0.01
Process water to boiler house plant (55 grd C)	0.60	0.01	0.60	0.01	0.48	0.01	0.48	0.01	0.12	0.00	0.12	0.00
Process water discharded (40 grd C)	2.28	0.02	2.28	0.02	1.83	0.02	1.83	0.02	0.46	0.00	0.46	0.00
Wastewater effluent and its emissions to WWTP	16.33	0.33	16.33	0.33	12.46	0.25	12.46	0.25	2.78	0.06	2.78	0.06
Bio-chemical matter (BOD7), in kg and MJ	16.24	0.50	16.24	0.50	12.99	0.40	12.99	0.40	3.25	0.10	3.25	0.10
Chemical matter (COD), in kg and MJ	42.00	1.51	42.00	1.51	33.60	1.21	33.60	1.21	8.40	0.30	8.40	0.30
Total nitrogen, in g and J	84.00	15.88	84.00	15.88	67.20	12.70	67.20	12.70	16.80	3.18	16.80	3.18
Total phosphorus, in g and J	21.00	0.08	21.00	0.08	16.80	0.06	16.80	0.06	4.20	0.02	4.20	0.02
Suspended solids, in g and J	0.00	0.00	0.00	0.00	0.00	0.00	0.00	0.00	0.00	0.00	0.00	0.00
Total output	37.76	16.70	37.76	16.70	29.50	12.67	29.50	12.67	6.98	2.77	6.98	2.77
Input - Output	0.10	4.03	0.10	4.03	0.08	3.91	0.08	3.91	0.02	1.07	0.02	1.07
Exergy efficiency (-)		0.8057		0.8057		0.8057		0.8057		0.7219		0.7219

C4-C5 The paper making plant (PMP)

The paper making plant (PMP) at Norske Skog's mill consists of three paper drying machines, termed PM1, PM2 and PM3. The following process units are part of the paper machines: a stock preparation unit, a head box (where the suspension of fibres is introduced to the wire and forms a uniform dispersion of fibres across the total width of the wire belt), a wire section (where the water from the paper web is drained to around 88% moisture content), a pressure section (were the water of the paper web is removed by pressing down to about 45%), a drying section (where the paper sheet moisture is removed by heating the web with drying cylinders), a reeler (where the paper sheet is rolled).

The paper drying process is carried out using steam heated cylinders enclosed in a closed hood. In the drying section the paper web is dried to the final dry content of 90 wt.%. Almost all the thermal energy used for drying ends up in the hood exhaust air. The temperature of the exhaust air is 55^0C and the humidity is 0.14 kg H_2O/kg dry air. A small part (13 wt.%) of the moisture is driven off to the atmosphere. The remaining part is passed through a heat recovery system consisting of several heat exchangers. The heat recovery system was not taken into account in the calculation. We assumed that the thermal energy of the hood exhaust air is released into the atmosphere without a preliminary treatment with thermal energy recovery.

Tables C4 and C5 present the inventory data of the paper making plants in Scenarios Z, L and H, for the narrow and wide system boundaries.

Table C4
Mass (M) and exergy (E) input/output inventory of the paper making plant (PM1 and PM3),
in Scenarios Z, L and H, for the narrow and wide system boundaries (data are per air-dried tonne of newsprint), TS = total dry solids

	Scenario Z				Scenario L				Scenario H			
	Narrow scale		Wide scale		Narrow scale		Wide scale		Narrow scale		Wide scale	
Input flow description	M (t)	E (GJ)	M (t)	E (GJ)	M (t)	E (GJ)	M (t)	E (GJ)	M (t)	E (GJ)	M (t)	E (GJ)
Electricity		1.18		1.18		0.94		0.94		0.00		0.00
Steam (3.3 bar, 195 grd C)	3.50	2.28	3.50	2.28	2.80	1.82	2.80	1.82	0.00	0.00	0.00	0.00
Warm water from TMP II (52 grd C)	3.02	0.05	3.02	0.05	2.42	0.04	2.42	0.04	0.00	0.00	0.00	0.00
Primary pulp from TMP I to PM1 (4.5% TS, 58 grd C)	2.66	1.86	2.66	1.86	2.13	1.49	2.13	1.49	0.00	0.00	0.00	0.00
Primary pulp from TMP I to PM3 (4.5% TS, 58 grd C)	3.39	2.37	3.39	2.37	2.71	1.90	2.71	1.90	0.00	0.00	0.00	0.00
Suphate cellulose (5%TS, 50 grd C)	0.01	0.01	0.01	0.01	0.01	0.00	0.01	0.00	0.00	0.00	0.00	0.00
Air for drying (2.5% water, 85 grd C)	4.00	0.30	4.00	0.30	3.20	0.24	3.20	0.24	0.00	0.00	0.00	0.00
Total input for production	16.58	8.04	16.58	8.04	13.26	6.43	13.26	6.43	0.00	0.00	0.00	0.00
Total input for abatement	-	-	-	-	-	-	-	-	-	-	-	-
Output flow description												
Newsprint paper from PM1 (91% TS)	0.13	2.23	0.13	2.23	0.11	1.78	0.11	1.78	0.00	0.00	0.00	0.00
Newsprint paper from PM3 (90% TS)	0.17	2.66	0.17	2.66	0.14	2.13	0.14	2.13	0.00	0.00	0.00	0.00
Condensate from PM1, PM3 (105 grd C)	3.50	0.21	3.50	0.21	2.80	0.17	2.80	0.17	0.00	0.00	0.00	0.00
Exhaust air from drying section (13 wt.% water, 55 grd C)	4.79	0.26	4.79	0.26	3.83	0.21	3.83	0.21	0.00	0.00	0.00	0.00
Process water for recirculation (50 grd C)	0.30	0.00	0.30	0.00	0.24	0.00	0.24	0.00	0.00	0.00	0.00	0.00
Wirewater to TMP I (0.5% TS, 50 grd C)	3.86	0.52	3.86	0.52	3.09	0.42	3.09	0.42	0.00	0.00	0.00	0.00
Process water to WWTP (50 grd C)	3.82	0.07	3.82	0.07	3.06	0.06	3.06	0.06	0.00	0.00	0.00	0.00
Total output	16.57	5.96	16.57	5.96	13.26	4.77	13.26	4.77	0.00	0.00	0.00	0.00
Input - Output	0.00	2.08	0.00	2.08	0.00	1.66	0.00	1.66	0.00	0.00	0.00	0.00
Exergy efficiency (-)		0.7418		0.7418		0.7418		0.7418		-		-

Table C5
Mass (M) and exergy (E) input/output inventory of the paper making plant (PM 2) in Scenarios Z, L and H,
for the narrow and wide system boundary (data are per air-dried tonne of newsprint paper), TS = total dry solids

	Scenario Z				Scenario L				Scenario H			
	Narrow scale		Wide scale		Narrow scale		Wide scale		Narrow scale		Wide scale	
Input flow description	M (t)	E (GJ)	M (t)	E (GJ)	M (t)	E (GJ)	M (t)	E (GJ)	M (t)	E (GJ)	M (t)	E (GJ)
Electricity		1.62		1.62		1.60		1.60		1.80		1.80
Steam (3.3 bar, 195 grd C)	3.18	2.07	3.18	2.07	3.50	2.27	3.50	2.27	3.82	2.48	3.82	2.48
Warm water from TMP II (52 grd C)	3.71	0.06	3.71	0.06	4.08	0.07	4.08	0.07	5.00	0.08	5.00	0.08
Primary pulp from TMP II (30 %TS)	2.10	12.69	2.10	12.69	1.58	9.48	1.58	9.48	0.33	1.98	0.33	1.98
Secondary pulp from DIP (30 %TS)	0.00	0.00	0.00	0.00	0.67	4.03	0.67	4.03	2.69	16.13	2.69	16.13
Air for drying (2.5 % water, 85 grd C)	9.50	0.53	9.50	0.53	11.00	0.62	11.00	0.62	12.00	0.67	12.00	0.67
Total input for production	18.49	16.97	18.49	16.97	20.84	18.07	20.84	18.07	23.84	23.14	23.84	23.14
Total input for abatement	-	-	-	-	-	-	-	-	-	-	-	-
Output flow description												
Newsprint paper (90.5 %TS)	0.70	11.87	0.70	11.87	0.75	9.49	0.75	9.49	1.00	16.95	1.00	16.95
Condensate from PM2 (105 grd C)	3.18	2.07	3.18	2.07	3.50	2.27	3.50	2.27	3.82	2.48	3.82	2.48
Exhaust air from drying section (13 wt.% water, 55 grd C)	10.65	0.01	10.65	0.01	12.32	0.01	12.32	0.01	13.47	0.01	13.47	0.01
Wirewater to TMP I (50 grd C)	3.96	0.20	3.96	0.20	4.26	0.21	4.26	0.21	5.55	0.28	5.55	0.28
Total output	18.49	14.14	18.49	14.14	20.83	11.99	20.83	11.99	23.84	19.72	23.84	19.72
Input - Output	0.00	2.83	0.00	2.83	0.00	6.08	0.00	6.08	0.00	3.42	0.00	3.42
Exergy efficiency (-)		0.8334		0.8334		0.8334		0.8334		0.8523		0.8523

C6 The de-inking plant (DIP)

In this section the de-inking plant at Norske Skog's mill is presented. The mass and exergy input/output inventory data of this plant are given in Table C6.

The following process steps are carried out in the de-inking plant: re-pulping of recovered paper (where the recovered paper is put into an equipment producing pulp together with hot water and pulped with mechanical and hydraulic agitation resulting into secondary fibres), mechanical removal of impurities (where secondary fibres are separated from impurities in screen-type equipment with different dimensions of screen opening and various types of hydro-cyclones), ink removal by flotation (where ink items are dispersed by means of chemicals such as hydrogen peroxide, sodium hydroxide and sodium silicate in dispersers, and separated from fibre slurry by means of two-stage flotation). After de-inking the secondary pulp obtained is thickened and washed using sieve belt presses.

In our study we assumed that the secondary pulp consists of a 50:50 mixture of newspapers and magazines. The ink and other impurities are found in the wastewater effluent or in the sludge that is sent to the boiler house plant for burning purpose.

Table C6 presents the inventory data of the de-inking plant in Scenarios Z, L and H, for the narrow and wide system boundaries.

Table C6
Mass (M) and exergy (E) input/output inventory of the de-inking plant (DIP) in Scenarios Z, L and H, for the narrow and wide system boundaries (data are per air-dried tonne of newsprint paper), TS = total dry solids

	Scenario L				Scenario H			
	Narrow scale		Wide scale		Narrow scale		Wide scale	
Input flow description	M (t)	E (GJ)	M (t)	E (GJ)	M (t)	E (GJ)	M (t)	E (GJ)
Electricity for deinking, screening, bleaching		0.40		0.40		0.86		0.86
Recycled paper (90 %TS)	0.24	4.07	0.24	4.07	1.04	17.59	1.04	17.59
Steam (1.5 bar, 120 grd C)	0.20	0.03	0.20	0.03	0.80	0.03	0.80	0.03
Process water (30 grd C)	8.45	0.08	8.45	0.08	9.82	0.10	9.82	0.10
Chemicals for repulping, flotation, bleaching								
Hydrogen peroxide (30%), in kg and MJ	5.00	11.50	5.00	11.50	20.00	46.00	20.00	46.00
Sodium hydroxide (98% TS), in kg and MJ	2.40	3.23	2.40	3.23	9.60	12.91	9.60	12.91
Sodium silicate (98% TS), in kg and MJ	5.00	2.70	5.00	2.70	20.00	10.80	20.00	10.80
Total input for production	-	-	-	-	-	-	-	-
Total input for abatement	8.90	4.60	8.90	4.60	11.71	18.66	11.71	18.66
Output flow description								
Secondary pulp to PM2 (30% TS, 20 grd C)	0.67	4.03	0.67	4.03	2.69	16.13	2.69	16.13
Rejects to BHP (70% TS)	0.03	0.35	0.03	0.35	0.10	1.26	0.10	1.26
Sludge to BHP (60% TS)	0.00	0.02	0.00	0.02	0.07	0.76	0.07	0.76
Wastewater effluent and its components to WWTP	8.20	0.08	8.20	0.08	8.85	0.09	8.85	0.09
Bio-chemical matter (BOD7), in kg and MJ	1.66	0.05	1.66	0.05	6.64	0.21	6.64	0.21
Chemical matter (COD), in kg and MJ	4.20	0.15	4.20	0.15	16.80	0.60	16.80	0.60
Total nitrogen, in g and kJ	0.02	0.00	0.02	0.00	0.06	0.01	0.06	0.01
Total phosphorus, in g and kJ	0.00	0.00	0.00	0.00	0.00	0.00	0.00	0.00
Suspended solids	0.02	0.00	0.02	0.00	0.09	0.00	0.14	0.00
Total output	8.90	4.48	8.90	4.48	11.71	18.23	11.71	18.23
Input - Output	0.00	0.12	0.00	0.12	0.00	0.43	0.00	0.43
Exergy efficiency (-)		0.9749		0.9749		0.9772		0.9772

C7-C9 The boiler house plant (BHP) and the natural gas-fired combined cycle power plant (NGPP)

In this section the boiler house plant (BHP) and the natural gas-fired combined cycle power plant (NGPP) are presented. The mass and exergy input/output inventory data for these plants alone and together are given in Tables C7-C8 and Table C9, respectively.

At Norske Skog's mill, the amount of thermal energy needed to manufacture newspaper is produced by three types of boilers: (1) two bark/wood waste boilers of a 50 and 36 MW capacity, respectively (the first boiler has a fluidised bed, while the latter one has a moving grit); (2) one electric boiler of a 40 MW capacity, (3) and one oil boiler of a 25 MW capacity. The boiler house plant has a back-pressure steam turbine, which can generate electricity from the high pressure supra-saturated steam (55 bar, 450^0C) obtained in the boilers. Today, this steam turbine is not operated. This is the reason why our study does not considered it for the calculations.

Table C7 gives the inventory data of the boiler house plant in Scenarios Z, L and H, for the narrow and wide system boundaries.

The natural gas-fired combined cycle power plant which is taken as the facility for electricity generation is under project at Norske Skog's mill. The project has been proposed to be constructed in the next 10 years. Its technical details are yet not known. Therefore, the inventory data of the NG PP was obtained from Chapter 3 and Appendix A. There was assumed that the amount of electricity needed for the paper production, wastewater and wastepaper treatment and wastepaper incineration is obtained from the NG PP.

Table C8 gives the inventory data of the natural gas-fired combined cycle power plant in Scenarios Z, L and H, for the narrow and wide system boundaries.

Table C9 summarises the results obtained in Tables C7 and C8 in order to obtain the data for the energy conversion sector in the system.

Table C7
Mass (M) and exergy (E) input/output inventory of the boilerhouse plant (BHP) in Scenarios Z, L and H, for the narrow and wide system boundaries (data are per air-dried tonne of newsprint paper), TS = total dry solids

	Scenario Z				Scenario L				Scenario H			
	Narrow scale		Wide scale		Narrow scale		Wide scale		Narrow scale		Wide scale	
Input flow description	M (t)	E (GJ)	M (t)	E (GJ)	M (t)	E (GJ)	M (t)	E (GJ)	M (t)	E (GJ)	M (t)	E (GJ)
Cooling water (10 grd C)	0.03	0.00	0.03	0.00	0.03	0.00	0.03	0.00	0.03	0.00	0.03	0.00
Condensate (1.2 bar, 95 grd C)	8.84	0.44	8.84	0.44	8.24	0.41	8.24	0.41	5.05	0.25	4.69	0.23
Bark from woodyard (39.5% TS)	0.01	0.10	0.01	0.10	0.01	0.08	0.01	0.08	0.00	0.02	0.00	0.02
Wood wastes from forestry (70% TS)	0.04	0.16	0.04	0.16	0.07	0.28	0.07	0.28	0.07	0.28	0.07	0.28
Rejects from TMP I (70% TS)	0.02	0.21	0.02	0.21	0.00	0.04	0.00	0.04	0.00	0.00	0.00	0.00
Sludge from WWTP (25% TS)	0.01	0.00	0.01	0.00	0.00	0.00	0.00	0.00	0.00	0.00	0.00	0.00
Sludge from DIP (60% TS)	0.00	0.00	0.00	0.00	0.00	0.02	0.00	0.02	0.07	0.76	0.07	0.76
Oil purchased from market	0.00	0.06	0.00	0.06	0.00	0.10	0.00	0.10	0.10	4.14	0.10	4.14
Electricity from the natural gas-fired power plant		35.00		35.00		30.00		30.00		13.00		13.00
Air	0.90	0.00	0.90	0.00	1.11	0.00	1.11	0.00	2.29	0.00	2.29	0.00
Oxygen	0.21	0.03	0.21	0.03	0.25	0.03	0.25	0.03	0.53	0.07	0.53	0.07
Nitrogen	0.69	0.02	0.69	0.02	0.85	0.02	0.85	0.02	1.76	0.05	1.76	0.05
Total input for production	9.83	35.96	9.83	35.96	9.47	30.93	9.46	30.93	7.62	18.44	7.25	18.42
Total input for abatement	-	-	-	-	-	-	-	-	-	-	-	-
Output flow description												
Cooling water effluent (18 grd C)	0.03	0.00	0.03	0.00	0.03	0.00	0.03	0.00	0.03	0.00	0.03	0.00
Steam (55 bar, 450 grd)	8.84	7.51	8.84	7.51	8.24	7.00	8.24	7.00	5.05	4.30	4.69	3.99
Ash (99% TS)	0.06	0.00	0.06	0.00	0.07	0.00	0.07	0.00	0.15	0.01	0.15	0.01
Exhaust air and its components (140 grd C)	0.91	0.04	0.91	0.04	1.12	0.04	1.12	0.04	2.38	0.10	2.38	0.10
Oxygen	0.02	0.00	0.07	0.01	0.08	0.01	0.08	0.01	0.52	0.06	0.52	0.06
Nitrogen	0.69	0.02	0.69	0.02	0.85	0.02	0.85	0.02	1.76	0.05	1.76	0.05
Carbon dioxide	0.04	0.02	0.04	0.02	0.05	0.02	0.05	0.02	0.09	0.04	0.09	0.04
Nitrogen monoxide	0.00	0.00	0.00	0.00	0.00	0.00	0.00	0.00	0.00	0.00	0.00	0.00
Carbon monoxide	0.15	1.48	0.15	1.48	0.14	1.38	0.14	1.38	0.00	0.00	0.00	0.00
Hydrocarbons	0.01	0.09	0.01	0.09	0.00	0.08	0.00	0.08	0.00	0.00	0.00	0.00
Particulates	0.00	0.00	0.00	0.00	0.00	0.00	0.00	0.00	0.00	0.00	0.00	0.00
Total output	9.83	7.55	9.83	7.55	9.47	7.05	9.47	7.05	7.61	4.40	7.25	4.09
Input - Output	0.00	28.41	0.00	28.41	0.00	23.88	0.00	23.88	0.00	14.04	0.00	14.33
Exergy efficiency (-)		0.2100		0.2100		0.2280		0.2280		0.2386		0.2220

Table C8
Mass (M) and exergy (E) input/output inventory of the natural gas-fired power plant (NG PP) in Scenarios Z, L and H, for the narrow and wide system boundaries (data are per air-dried tonne of newsprint paper)

	Scenario Z				Scenario L				Scenario H			
	Narrow scale		Wide scale		Narrow scale		Wide scale		Narrow scale		Wide scale	
Input flow description	M (t)	E (GJ)	M (t)	E (GJ)	M (t)	E (GJ)	M (t)	E (GJ)	M (t)	E (GJ)	M (t)	E (GJ)
Natural gas	1.97	85.58	1.98	85.66	1.73	74.83	1.73	75.06	0.88	37.95	0.88	38.16
Air	16.78	0.00	16.80	0.00	14.67	0.00	14.72	0.00	7.44	0.00	7.48	0.00
Oxygen	3.86	0.48	3.86	0.48	3.37	0.42	3.39	0.42	1.71	0.21	1.72	0.21
Nitrogen	12.92	0.33	12.93	0.33	11.30	0.29	11.33	0.29	5.73	0.15	5.76	0.15
Cooling water (10 grd C)	24.48	0.00	24.50	0.00	21.40	0.00	21.47	0.00	10.86	0.00	10.91	0.00
Condensate									0.00	0.00	0.00	0.00
Total input	43.24	85.58	43.27	85.66	37.80	74.83	37.92	75.06	19.17	37.95	19.28	38.16
Output flow description												
Electricity		41.94		41.97		36.67		36.78		18.60		18.70
Cooling water effluent (18 grd C)	24.48	0.05	24.50	0.05	21.40	0.04	21.47	0.04	10.86	0.02	10.91	0.02
Exhaust air and its components (80 grd C)	18.76	0.56	18.77	0.56	16.40	0.49	16.45	0.49	8.32	0.25	8.36	0.25
Oxygen	0.38	0.05	0.38	0.05	0.37	0.05	0.37	0.05	0.22	0.03	0.22	0.03
Nitrogen	12.92	0.33	12.93	0.33	11.30	0.29	11.33	0.29	5.73	0.15	5.76	0.15
Carbon dioxide	5.54	2.50	5.54	2.50	4.84	2.18	4.85	2.19	2.45	1.11	2.47	1.11
Nitrogen monoxide	0.01	0.00	0.01	0.00	0.01	0.00	0.01	0.00	0.00	0.00	0.00	0.00
Carbon monoxide	0.01	0.08	0.01	0.08	0.01	0.07	0.01	0.07	0.00	0.04	0.00	0.04
Hydrocarbons	0.00	0.02	0.00	0.02	0.00	0.02	0.00	0.02	0.00	0.01	0.00	0.01
Particulates	0.03	0.00	0.03	0.00	0.03	0.00	0.03	0.00	0.01	0.00	0.01	0.00
Total output	43.24	42.55	43.27	42.58	37.80	37.20	37.92	37.32	19.17	18.87	19.28	18.97
Input - Output	0.00	43.04	0.00	43.07	0.00	37.63	0.00	37.74	0.00	19.09	0.00	19.19
Exergy efficiency (-)		0.4971		0.4971		0.4971		0.4971		0.4971		0.4971

Table C9
Mass (M) and exergy (E) input/output inventory of the BHP and the NG PP in Scenarios Z, L and H,
for the narrow and wide system boundaries (data are per air-dried tonne of newsprint paper), TS = total dry solids

	Scenario Z				Scenario H				Scenario H			
	Narrow scale		Wide scale		Narrow scale		Wide scale		Narrow scale		Wide scale	
Input flow description	M (t)	E (GJ)	M (t)	E (GJ)	M (t)	E (GJ)	M (t)	E (GJ)	M (t)	E (GJ)	M (t)	E (GJ)
Natural gas	1.97	85.58	1.98	85.66	1.73	74.83	1.73	75.06	0.88	37.95	0.88	38.16
Bark from woodyard (39.5 %TS)	0.01	0.10	0.01	0.10	0.01	0.08	0.01	0.08	0.00	0.02	0.00	0.02
Woodwaste purchased from forestry (70% TS	0.04	0.16	0.04	0.16	0.07	0.28	0.07	0.28	0.07	0.28	0.07	0.28
Rejects from TMP I and II (70% TS)	0.02	0.21	0.02	0.21	0.00	0.04	0.00	0.04	0.00	0.00	0.00	0.00
Paperwaste rest and other wastes (40% TS)	0.00	0.06	0.00	0.06	0.00	0.10	0.00	0.10	0.10	4.14	0.10	4.14
Oil	0.00	0.06	0.00	0.06	0.00	0.10	0.00	0.10	0.10	4.14	0.10	4.14
Air	17.68	0.00	17.69	0.00	15.78	0.00	15.82	0.00	9.73	0.00	9.77	0.00
Nitrogen	13.61	0.35	13.62	0.35	12.15	0.31	12.18	0.31	7.49	0.19	7.52	0.19
Oxygen	4.07	0.50	4.07	0.50	3.63	0.45	3.64	0.45	2.24	0.28	2.25	0.28
Cooling water	24.51	0.00	24.53	0.00	21.44	0.00	21.50	0.00	10.88	0.00	10.94	0.00
Condensate	8.84	0.44	8.84	0.44	8.24	0.41	8.24	0.41	5.05	0.25	4.69	0.23
Total input	53.06	86.61	53.10	86.68	47.27	75.85	47.38	76.08	26.79	46.78	26.55	46.96
Output flow description												
Electricity		41.94		41.97		36.67		36.78		18.60		18.70
Cooling water effluent (18 grd C)	24.51	0.05	24.53	0.05	21.44	0.04	21.50	0.04	10.88	0.02	10.94	0.02
Steam (15 bar, 185 grd C)	8.84	7.51	8.84	7.51	8.24	7.00	8.24	7.00	5.05	4.30	4.69	3.99
Exhaust air and its components (110 grd C)	19.66	0.60	19.68	0.60	17.52	0.54	17.57	0.54	10.70	0.34	10.77	0.35
Oxygen	3.88	0.48	3.93	0.49	3.45	0.43	3.47	0.43	2.23	0.28	2.24	0.28
Nitrogen	13.61	0.35	13.62	0.35	12.15	0.31	12.18	0.31	7.49	0.19	7.52	0.19
Carbon dioxide	5.57	2.51	5.58	2.52	4.89	2.20	4.90	2.21	2.55	1.15	2.56	1.16
Nitrogen monoxide	0.01	0.00	0.01	0.00	0.01	0.00	0.01	0.00	0.00	0.00	0.00	0.00
Carbon monoxide	0.16	1.56	0.16	1.56	0.15	1.45	0.15	1.45	0.00	0.04	0.00	0.04
Hydrocarbons	0.01	0.11	0.01	0.11	0.01	0.10	0.01	0.10	0.00	0.01	0.00	0.01
Particulates	0.03	0.00	0.03	0.00	0.03	0.00	0.03	0.00	0.01	0.00	0.01	0.00
Ash	0.06	0.00	0.06	0.00	0.07	0.00	0.07	0.00	0.15	0.01	0.15	0.01
Total output	53.06	50.10	53.10	50.14	47.27	44.26	47.39	44.37	26.79	23.27	26.55	23.06
Input - Output	0.00	36.51	0.00	36.54	0.00	31.60	-0.01	31.71	0.00	23.51	0.00	23.90
Exergy efficiency (-)		0.5658		0.5658		0.5703		0.5701		0.4840		0.4780

C10 The wastewater treatment plant (WWTP)

In this section the process description of wastewater treatment plant (WWTP) is presented. The assumptions and the formula for the exergy calculation of the chemicals and emissions that are part of the wastewater composition are also given. The inventory data of this plant in Scenarios Z, L and H are presented in Table C10. These data were collected from the wastewater treatment facility at Norske Skog's mill.

The following assumptions and simplifications were used for the calculation of exergy of input and output material flows: (1) the water was considered as a fluid containing components of thermal exergy (heat) and chemical exergy (organic matter represented by COD and BOD, phosphorus (P_t) and nitrogen (N_t)), (2) the exergy content of clean water and uncontaminated nutrients is not estimated. (3) The exergy embodied in buildings and the exergy needed for plant maintenance are excluded from the exergy calculations. (4) The system boundary of WWTP is drawn around the plant.

The wastewater that comes from the woodyard, thermo-mechanical pulping plant, and paper making plant has a temperature of 52^0C. This temperature is different from the average annual environmental temperature ($T_0 = 12^0$C). This means that the exergy content of the wastewater, due to its heat content, is different from zero. The thermal exergy content ($E^{thermal}_{wastewater}$) of wastewater was calculated as:

$$E^{thermal}_{wastewater} = Q(1 - \frac{T_0}{T - T_0} ln(\frac{T}{T_0})) \qquad \text{(C10-1)}$$

where

$$Q = mc_p(T - T_0) \qquad \text{(C10-2)}$$

Here, Q is the thermal energy flow of wastewater (in kW), m is the mass flow rate of wastewater (in kg/s), and c_p is the specific heat capacity of water (in J/K kg).

The temperature change of wastewater when it passes through the treatment plant is small. It was assumed that the exergy loss due heat exchange between wastewater and hot water is insignificant. In addition, it was assumed that the exergy demand for raising the air temperature in the buildings is also insignificant. However, the air in the buildings of the treatment plant can be cooled down due to water evaporation. This means that the thermal energy for heating the buildings can be important, and also, the exergy loss related to

the production, distribution and exchange of thermal energy. There are also exergy losses when the treated wastewater is released into the water reservoir. These exergy losses were not considered in the study.

Exergy of organic matter. Tai and anf T. Goda (1986) showed that the standard chemical exergy of organic matter in wastewater can be estimated by (Hellström 1997):

$$E_{organic\ matter} = 13.7\ TOD \quad [\text{kJ/l}] \qquad \text{(C10-3)}$$

where TOD is the theoretical oxygen demand of wastewater. Hellström (1997) obtained a value of 13.6 kJ/g for the chemical exergy of the chemical oxygen demand (COD) matter, and a value of 31 kJ/g for the chemical exergy of the biochemical oxygen demand (BOD) matter. The contribution of the dilution of COD and BOD matter into pure water was not considered for the calculation of the exergy of wastewater. The exergy content of wastewater was calculated considering only the temperature contribution, see Eq. C10-1.

Exergy of phosphorus and nitrogen. It was assumed that all nitrogen exists as ammonium (NH_4^+) and all phosphorus as phosphate ions ($HPO_4{}^{2-}$). The standard chemical exergy of ammonium is 322.1 kJ/mole and for $HOP_4{}^{2-}$ is 134.1 kJ/mole (Szargut et al. 1988).

Exergy of chemicals. Two main chemicals and one auxiliary material are utilised at the WWTP. They are the lime (CaO) and the AVT (8 wt.% aluminium as $Al_2(SO_4)-3x(14\text{-}16)\ H_2O$ and 0.7 wt.% iron as $Fe_2(SO_4)_3x9\ H_2O$), and the organic polymers, respectively. The chemical exergies of these chemicals were collected from Szargut et al. (1988).

Organic polymers are typically classified as long-chain organic molecules with molecular weights between 10^4 and 10^10. The exergy content of organic polymers is highly correlated to the amount of oxygen, nitrogen and sulphur in the molecules. Szargut et al. (1988) gave the values of standard chemical exergy for several organic compounds. In this study, the chemical exergies of the organic polymers were estimated to be the same (40 kJ/g polymer).

Exergy of sludge. We assumed that the removed phosphorus is precipitated with Ca^{2+}or Al^{3+} and the remaining chemicals form hydroxides and carbonates. The chemical exergies of these chemicals were calculated from Szargut et al. (1988). The following chemical exergies were obtained: 60 kJ/g for $Ca_3(PO_4)_2$, 123 kJ/g for $AlPO_4$, 10 kJ/g for $CaCO_3$, 126 kJ/g for $Al(OH)_3$,

and 45 kJ/g for $Fe(OH)_3$.

The organic matter in sludge was assumed to be present as cellulose ($C_{12}H_{24}O_{12}$) or as cell tissue ($C_5H_7NO_2$) (Hellström 1997). The chemical exergy of cellulose is 8.7 kJ/g (Szargut et al. 1988), while that of cell tissue is 36.26 kJ/g (Hellström 1997).

Table C10 gives the inventory data of the wastewater treatment plant in Scenarios Z, L and H, for the narrow and wide system boundaries.

Table C10
Mass (M) and exergy (E) input/output inventory of the wastewater treatment plant (WWTP) in Scenarios Z, L and H, for the narrow and wide system boundaries (data are per air-dried tonne of newsprint paper), BOD = biological oxygen demand, COD = chemical oxygen demand, TS = total dry solids

	Scenario Z				Scenario L				Scenario H			
	Narrow scale		Wide scale		Narrow scale		Wide scale		Narrow scale		Wide scale	
Input flow description	M (kg)	E (MJ)	M (kg)	E (MJ)	M (kg)	E (MJ)	M (kg)	E (MJ)	M (kg)	E (MJ)	M (kg)	E (MJ)
Electricity		18.05		18.05		28.80		28.80		8.66		8.66
Steam (1.2 bar, 110 grd C)	20.26	4.66	20.26	4.66	32.33	7.44	32.33	7.44	9.72	2.24	9.72	2.24
Wastewater (50 grd C)	22010.00	11.89	22010.00	11.89	35120.00	18.96	35120.00	18.96	10560.00	5.70	10560.00	5.70
Biological matters (BOD7)	23.20	0.72	23.20	0.72	20.22	0.63	20.22	0.63	11.28	0.35	11.28	0.35
Organic matter (COD)	60.00	2.16	60.00	2.16	52.20	1.88	52.20	1.88	28.80	1.04	28.80	1.04
Total nitrogen	120.00	22.68	120.00	22.68	96.02	18.15	96.02	18.15	24.06	4.55	24.06	4.55
Total phosphorus	30.00	0.11	30.00	0.11	24.00	0.09	24.00	0.09	6.00	0.02	6.00	0.02
Suspended solids	0.00	0.00	0.00	0.00	0.02	0.00	0.02	0.00	0.09	0.00	0.09	0.00
Auxiliary materials:												
Calcium oxide (90 %TS)	3.48	0.01	3.48	0.01	2.92	0.01	2.78	0.01	0.70	0.00	0.70	0.00
Aluminium sulphate	0.70	0.00	0.70	0.00	0.59	0.00	0.56	0.00	0.14	0.00	0.14	0.00
Ferric sulphate	0.92	0.00	0.92	0.00	0.78	0.00	0.74	0.00	0.18	0.00	0.18	0.00
Ferro sulphate	0.26	0.00	0.26	2.38	0.22	2.00	0.21	1.90	0.05	0.48	0.05	0.48
Polymer	0.00	0.00	0.01	0.00	0.00	0.00	0.01	0.00	0.00	0.00	0.00	0.00
Total input for production	-	-	-	-	-	-	-	-	-	-	-	-
Total input for abatement	22035.63	34.60	22035.65	36.98	35156.84	57.20	35156.64	57.11	10570.80	17.07	10570.80	17.07
Output flow description												
Treated, discarded wastewater	22030.26	3.75	21529.82	3.75	24703.13	4.20	24703.14	4.20	10569.72	1.80	10569.72	1.80
Biological materials (BOD7)	4.01	0.12	4.01	0.12	3.37	0.10	3.21	0.10	0.80	0.02	0.80	0.02
Organic materials (COD)	13.50	0.49	13.50	0.49	11.34	0.41	10.80	0.39	2.70	0.10	2.70	0.10
Total nitrogen	0.16	0.03	0.16	0.03	0.13	0.03	0.13	0.02	0.03	0.01	0.03	0.01
Total phosphorus	0.02	0.00	0.02	0.00	0.01	0.00	0.01	0.00	0.00	0.00	0.00	0.00
Suspended solids	2.63	0.01	2.63	0.01	2.21	0.00	2.10	0.00	0.53	0.00	0.53	0.00
Sludge to boiler house (25%TS)	5.37	0.21	5.37	0.21	4.51	0.14	4.29	0.13	1.07	0.03	1.07	0.03
Precipitates	1.05	0.00	1.05	0.00	0.88	0.00	0.84	0.00	0.21	0.00	0.21	0.00
Calcium phosphate	0.39	0.00	0.39	0.00	0.32	0.00	0.31	0.00	0.08	0.00	0.08	0.00
Aluminium phosphate	0.15	0.00	0.15	0.00	0.13	0.00	0.12	0.00	0.03	0.00	0.03	0.00
Calcium carbonate	0.32	0.00	0.32	0.00	0.27	0.00	0.25	0.00	0.06	0.00	0.06	0.00
Aluminium hydroxide	0.18	0.00	0.18	0.00	0.15	0.00	0.14	0.00	0.04	0.00	0.04	0.00
Ferro oxide	0.02	0.00	0.02	0.00	0.01	0.00	0.01	0.00	0.00	0.00	0.00	0.00
Other organic matter	4.32	0.11	4.33	0.11	3.62	0.09	3.46	0.09	0.86	0.02	0.87	0.02
Cell tissue	1.36	0.00	1.36	0.00	1.15	0.00	1.09	0.00	0.27	0.00	0.27	0.00
Cellulose	2.95	0.11	2.95	0.11	2.48	0.09	2.36	0.09	0.59	0.02	0.59	0.02
Total output	22035.63	3.96	21535.19	3.96	24707.64	4.34	24707.43	4.33	10570.79	1.83	10570.80	1.83
Input - Output	0.00	30.64	500.46	33.02	10449.21	52.87	10449.21	52.78	0.00	15.24	0.00	15.24
Exergy efficiency (-)		0.1144		0.1071		0.0759		0.0759		0.1072		0.1072

C11 The wastepaper treatment plant (WPTP)

In this section a process description of the wastepaper treatment plant is first presented. Then, the inventory data for this plant in Scenarios Z, L and H are given in Table C11.

The wastepaper treatment plant (WPTP) consists of sorting and bales pressing of the wastepaper collected from the households in Trondheim. Wastepaper, delivered by garbage trucks, is dumped on the tipping floor of the storage building where any non-paper item is removed. Then, the wastepaper is sent to a magnetic separation, and finally, to a manual screening. The electricity demand for this plant is supplied by the natural gas-fired power plant located at Norske Skog's mill (see Appendix C8).

Table C11 gives the inventory data of the wastepaper treatment plant in Scenarios Z, L and H, for the narrow and wide system boundaries.

Table C11
Mass (M) and exergy (E) input/output inventory of the wastepaper treatment plant (WPTP) in Scenarios Z, L and H for the narrow and wide system boundaries (data are per air-dried tonne of wastepaper)

	Scenario Z				Scenario S				Scenario M			
	Narrow scale		Wide scale		Narrow scale		Wide scale		Narrow scale		Wide scale	
	Mass (t)	E (GJ)	M (t)	E (GJ)	Mass (t)	E (GJ)	M (t)	E (GJ)	Mass (t)	E (GJ)	M (t)	E (GJ)
Input flow description												
Electricity	0.00	0.00		0.00	0.00	0.00		0.08	0.00	0.00		0.08
Diesel fuel	0.00	0.00	0.00	0.00	0.00	0.00	0.00	0.01	0.00	0.00	0.00	0.01
Wastepaper	0.00	0.00	0.00	0.00	0.00	0.00	0.20	3.39	0.00	0.00	0.80	13.56
Process water	0.00	0.00	0.00	0.00	0.00	0.00	0.09	0.00	0.00	0.00	0.09	0.00
Ferrous wire	0.00	0.00	0.00	0.00	0.00	0.00	0.00	0.00	0.00	0.00	0.00	0.00
Polimer	0.00	0.00	0.00	0.00	0.00	0.00	0.00	0.06	0.00	0.00	0.00	0.06
Total input for abatement			0.00	0.00	0.00	0.00	0.29	3.55	0.00	0.00	0.89	13.72
Output flow description	0.00	0.00			0.00	0.00			0.00	0.00		
Wastewater	0.00	0.00	0.00	0.00	0.00	0.00	0.09	0.00	0.00	0.00	0.09	0.00
Wastepaper bails	0.00	0.00	0.00	0.08	0.00	0.00	0.20	3.45	0.00	0.00	0.80	13.62
Ferrous material	0.00	0.00	0.00	0.00	0.00	0.00	0.00	0.00	0.00	0.00	0.00	0.00
Solid residues	0.00	0.00	0.00	0.00	0.00	0.00	0.00	0.00	0.00	0.00	0.00	0.00
Total output	0.00	0.00	0.00	0.00	0.00	0.00	0.29	3.45	0.00	0.00	0.89	13.62
Input - Output	0.00	0.00	0.00	0.00	0.00	0.00	0.00	0.09	0.00	0.00	0.00	0.09
Exergy efficiency (-)		-		-		-		0.9738		-		0.9932

C12 The municipal waste incineration plant (MWIP)

In this section, a process description of the municipal waste incineration plant is presented. The inventory data for this plant in Scenarios Z, L and H are also given in Table C12.

The facility of municipal waste incineration consists of three sections: combustion, thermal energy recovery and flue gas treatment. The combustion section has three parallel lines, each with a capacity of 22 tonne per hour. One line is for incineration of wastepaper, while the other two are for mass combustion of food waste and other household and industrial wastes. The combustion section for wastepaper is characterised by a mobile grate consisting of a series of alternate fixed and mobile bars where the wastepaper fuel undergoes combustion. The grate is cooled by water since the lower heating value of wastepaper is higher than that of the mixed wastes (17 vs. 8.8 MJ/kg). The furnace is divided in three zones: the feeding zone, the central zone (where combustion takes place), and the final zone (where the ashes are discarded). In the combustion zone the alternate movement of bars allows to have a good mixing of waste that is exposed to flame radiation. The grate is inclined by 10^o in order to ensure a continuous movement of the waste. The combustion process is controlled by taking into account: the steam mass flow, the oxygen and carbon monoxide concentrations in the flue gas, the combustion temperature and flame length over the grate. The flue gas acid treatment is done by a semi dry scrubber, which consists of a fabric filter for removing fly ashes and a selective catalytic reduction unit for removal of nitrogen oxides and organic micro-pollutants. The scrubber uses a lime solution in water that is sprayed counter currently with hot flue gas. The water is totally vaporised, which means that no water effluent treatment is necessary.

Table C12 gives the inventory data of the municipal waste incineration plant in Scenarios Z, L and H, for the narrow and wide system boundaries.

Table C12
Mass (M) and exergy (E) input/output inventory of the municipal waste incineration palnt (MWIP) in Scenarios Z, L and H for the narrow and wide system boundaries
(data are per air-dried tonne of wastepaper), TS = total dry solids

	Scenario Z		Scenario L		Scenario H	
	Wide scale		Wide scale		Wide scale	
	M (t)	E (GJ)	M (t)	E (GJ)	M (t)	E (GJ)
Input flow description						
Electricity		0.04		0.03		0.01
Wastepaper	1.00	16.95	0.80	13.56	0.20	3.39
Air	7.60	0.00	6.08	0.00	1.52	0.00
Oxygen	1.75	0.22	1.40	0.17	0.35	0.04
Nitrogen	5.78	0.15	4.62	0.12	1.16	0.03
Condensate (1.2 bar, 95 grd C)	17.12	0.14	13.70	0.11	3.42	0.03
Process water	0.16	0.00	0.13	0.00	0.03	0.00
Ash conditioning water	0.02	0.00	0.01	0.00	0.00	0.00
Calcium oxide (90% TS)	0.03	0.05	0.02	0.04	0.01	0.01
Sodium silicate (30% TS)	0.00	0.00	0.00	0.00	0.00	0.00
Activated carbon	0.00	0.01	0.00	0.01	0.00	0.00
Calcium hydroxide (30% TS)	0.00	0.01	0.00	0.00	0.00	0.00
Cement	0.00	0.00	0.00	0.00	0.00	0.00
Urea	0.00	0.03	0.00	0.03	0.00	0.01
Total input for production	-	-	-	-	-	-
Total input for abatement	25.93	17.22	20.75	13.78	5.19	3.44
Output flow description						
Thermal energy (sat. steam, 10 bar)	17.12	5.14	13.70	4.11	3.42	1.03
Exhaust air and its components (116 grd C)	8.29	0.15	6.70	0.12	1.67	0.03
Oxygen	0.12	0.01	0.09	0.01	0.02	0.00
Nitrogen	5.78	0.15	4.62	0.12	1.16	0.03
Carbon dioxide	1.52	0.70	1.21	0.56	0.30	0.14
Nitrogen oxide	0.80	0.98	0.64	0.78	0.16	0.20
Carbon monoxide	0.01	0.10	0.08	0.78	0.02	0.20
Hydrocarbons	0.06	0.98	0.05	0.78	0.01	0.20
Particulates	0.01	0.01	0.01	0.01	0.00	0.00
Wastewater effluent	0.16	0.00	0.13	0.00	0.03	0.00
Filter dusts	0.09	0.06	0.07	0.05	0.02	0.01
Ash	0.27	0.00	0.15	0.00	0.04	0.00
Total output	25.93	5.35	20.74	4.28	5.19	1.07
Input - Output	0.00	11.87	0.00	9.49	0.00	2.37
Exergy efficiency (-)		0.3109		0.3109		0.3109

C13 The transportation network (T)

In this section the distances for the transportation of paper and wastepaper are presented. The inventory data of the transportation in Scenarios Z, L and H are given in Table C13.

It was assumed that the configuration of transportation network is the same in each scenario. Waste paper source sorting of the waste paper was assumed only in the case of wastepaper recycling, and not in the case of waste paper incineration.

On-site the Norske Skog's mill (narrow system boundary), a transport distance of 0.5 km per tonne newsprint paper produced was assumed. For the wide system boundary, the transportation network starts when the newsprint paper is transported from the Norske Skog's mill to Trondheim. The following steps in the transportation network were considered:

1. From Norske Skog's mill to Trondheim, the transport distance is 80 km, plus 80 km empty return. This transport is done with diesel trucks of a 20 tonnes capacity.

2. From the collection point close to the households in Trondheim to the wastepaper treatment plant (WPTP) in Melhus, the transport distance is 8 km, plus 8 km empty return. This transport is done by garbage trucks with a 10 tonnes capacity.

3. From the collection point to the municipal wastepaper incineration plant (MWIP), the transport distance is 10 km, plus 10 km empty return. This transport is done by diesel trucks of a 20 ton capacity.

Data on the resource use and emissions related to the transport network by means of medium-sized diesel trucks (20 ton) were taken from Beer (2000). The author claimed that the amount of exergy spent in such trucks is 0.134 MJ diesel exergy per kg of paper or waste paper per km transport distance (Beer 2000). The chemical exergy of the diesel fuel with an assumed ratios of H/C = 1.89, O/C = 0.8, and S/C = 0.47, was calculated as (Kotas 1985):

$$E_{diesel}^{\text{chem}} = LHV_{diesel}\psi + 9417S \quad \text{[kJ/kg diesel]} \tag{C13-1}$$

where

$$\psi = 1.0401 + 0.1728\frac{H}{C} + 0.0432\frac{O}{C} + 0.2169\frac{S}{C}(1 - 2.0629\frac{H}{C}) \quad [-] \tag{C13-2}$$

and

$$LHV_{diesel} = 42.7 \quad \text{[kJ/kg diesel]} \tag{C13-3}$$

The following life-cycle emissions for one GJ diesel exergy were calculated by Beer (2000): 83 kg carbon dioxide, 0.14 kg hydrocarbons, 1.044 kg nitrogen monoxide, 0.27 kg carbon monoxide, 0.011 kg particulate matters (Beer 2000).

Data on internal combustion engine exergy conversion efficiency estimate were taken from Ayres (2002). In this work, an exergy conversion efficiency of 8.5% was calculated for a fuel-air 4-cycle truck engine that is operated at a speed of 2000 rpm and an average compression ratio of 8. The efficiency value was obtained after subtraction of internal engine friction losses, transmission losses, the penalty for variable loads in stop-start urban driving, and the losses introduced by lighting, heating and air conditioning.

Table C13 gives the inventory data of the transportation network in Scenarios Z, L and H, for the narrow and wide boundaries.

Table C13
Mass (M) and exergy (E) input/output inventory of the transportation network (T) in Scenarios Z, L and H for the narrow and wide system boundaries (data are per air-dried tonne of newsprint)

	Scenario Z				Scenario L				Scenario H			
	Narrow scale		Wide scale		Narrow scale		Wide scale		Narrow scale		Wide scale	
Input flow description	M (t)	E (GJ)	M (t)	E (GJ)	M (t)	E (GJ)	M (t)	E (GJ)	M (t)	E (GJ)	M (t)	E (GJ)
Total transportation distance	0.01		186		0.01		184.8		0.01		181.21	
Diesel fuel	0.00	0.01	2.73	116.52	0.00	0.01	2.71	115.77	0.00	0.01	2.66	113.51
Air	0.00	0.00	40.11	0.00	0.00	0.00	39.85	0.00	0.00	0.00	39.08	0.00
Oxygen	0.00	0.00	9.23	1.14	0.00	0.00	9.17	1.14	0.00	0.00	8.99	1.11
Nitrogen	0.00	0.00	30.89	0.79	0.00	0.00	30.29	0.78	0.00	0.00	29.70	0.76
Total input for production	-	-	-	-	-	-	-	-	-	-	-	-
Total input for abatement	0.00	0.01	42.84	116.52	0.00	0.01	42.57	115.77	0.00	0.01	41.74	113.51
Output flow description												
Internal combustion engine work		0.00		9.32		0.00		9.26		0.00		9.08
Exhaust air and its components (120 grd C)	0.00	0.00	40.11	1.60	0.00	0.00	39.85	1.59	0.00	0.00	39.08	1.56
Oxygen	0.01	0.00	2.27	0.28	0.01	0.00	2.65	0.33	0.01	0.00	2.6	0.32
Nitrogen	0.00	0.00	30.89	0.79	0.00	0.00	30.29	0.78	0.00	0.00	29.70	0.76
Carbon dioxide	0.00	0.00	8.95	4.04	0.00	0.00	8.89	4.01	0.00	0.00	8.72	3.93
Nitrogen monoxide	0.00	0.00	0.09	0.00	0.00	0.00	0.09	0.00	0.00	0.00	0.09	0.00
Carbon monoxide	0.00	0.00	0.55	5.40	0.00	0.00	0.55	5.37	0.00	0.00	0.54	4.78
Hydrocarbons	0.00	0.00	0.10	1.58	0.00	0.00	0.10	1.57	0.00	0.00	0.09	1.54
Soot	0.00	0.00	2.73	0.00	0.00	0.00	2.71	0.00	0.00	0.00	2.66	0.00
Total output	0.00	0.00	42.84	10.93	0.00	0.00	42.57	10.86	0.00	0.00	41.74	10.64
Input - Output	0.00	0.01	0.00	105.59	0.00	0.01	0.00	104.91	0.00	0.01	0.00	102.87
Exergy efficiency (-)		0.0938		0.0938		0.0947		0.0938		0.0938		0.0938

Appendix D: The thermodynamic relations used in the model of paper drying process

The enthalpy and entropy changes for water between the states in the paper sheet and the air near to the paper sheet surface, are

$$\Delta H = \Delta_{\mathrm{sor}} H + \Delta_{\mathrm{vap}} H + \int_{T_p}^{T_{\mathrm{air}}} C_{p,\mathrm{H_2O}}^{\text{in air}}\, dT \tag{D-1}$$

and

$$\begin{aligned} \Delta S \;=\; & -\frac{\Delta_{\mathrm{sor}} H}{T_p} - \frac{R}{M_{\mathrm{H_2O}}} ln(\Theta(w, T_p)) + \frac{\Delta_{\mathrm{vap}} H}{T_p} \\ & -\frac{R}{M_{\mathrm{H_2O}}} ln\left(\frac{p_{\mathrm{H_2O}}^{\text{in air}}}{p^*}\right) + \int_{T_p}^{T_{\mathrm{air}}} \frac{C_{p,\mathrm{H_2O}}^{\text{in air}}}{T}\, dT. \end{aligned} \tag{D-2}$$

The sorption enthalpy of liquid water to paper is

$$\Delta_{\mathrm{sor}} H = -R \frac{\partial ln \Theta(w, T_p)}{\partial (1/T_p)}. \tag{D-3}$$

The desorption isotherm of paper (Prahl 1968) is

$$\Theta(w, T_p) = \frac{p_{\mathrm{p}}^*}{p^*} = \exp(\beta_1 T_p - \beta_2), \tag{D-4}$$

where β_1 and β_2 were determined by Karlsson and Soininen (1982)

$$\beta_1 = \exp(-15.03w - 1.37\sqrt{w} - 3.14), \tag{D-5}$$

$$\beta_2 = \exp(-13.53w - 2.90\sqrt{w} + 2.9). \tag{D-6}$$

Using Clausius-Clapeyron's relation, the evaporation enthalpy is

$$\Delta_{\mathrm{vap}} H = -R \frac{\partial ln(p^*/p^{\ominus})}{\partial (1/T_p)}, \tag{D-7}$$

where the equilibrium vapour pressure was given by Pakowski et al. (1991) as

$$p^*(T_p) = 0.133 \times 10^3 \exp(18.303 - \frac{3816.44}{T_p - 46.13}). \quad \text{(D-8)}$$

The heat capacity of paper is taken as

$$C_{p,p} = C_{p,\mathrm{dry}-p} + wC_{p,\mathrm{H_2O}}, \quad \text{(D-9)}$$

where $C_{p,\mathrm{dry}-p}$ is the specific heat capacity of dry paper. Wilhelmsson et al. (1994) suggested that the heat capacity of newsprint is 1256 J/K kg.

Appendix E: The heat transfer coefficients used in the model of paper drying process

The heat transfer coefficients between cylinder and paper were calculated with a relation given by Rhodius and Gottsching (1979)

$$h_{\mathrm{cyl}-p} = 1556.6w + 52.87. \tag{E-1}$$

The heat transfer coefficients between the paper sheet and air were calculated from the following relations given by Incropera and Witt (1985). When the paper sheet is located between two cylinders, the heat transfer coefficient is

$$h_{p-\mathrm{air}} = \frac{\kappa}{D_{\mathrm{cyl}}} \left\{ 0.3 + \frac{0.62 Re_D^{1/2} Pr^{1/3}}{\left[1 + \left(\frac{0.4}{Pr}\right)^{2/3}\right]^{1/4}} \left[1 + \left(\frac{Re_D}{282000}\right)^{5/8}\right]^{4/5} \right\}. \tag{E-2}$$

When the paper sheet is in contact with cylinder, the heat transfer coefficient is

$$h_{p-\mathrm{air}} = \frac{\kappa}{l} \left(0.664 Re_l^{1/2} Pr^{1/3}\right) \tag{E-3}$$

when $Re_l < 5 \times 10^5$, and it is

$$h_{p-\mathrm{air}} = \frac{\kappa}{l} Pr^{1/3} \left(0.037 Re_l^{4/5} - 871\right) \tag{E-4}$$

when $Re_l > 5 \times 10^5$.

The Reynolds and Prandtl numbers were determined by

$$Re_D = \frac{v\ D_{cyl}}{\nu} \qquad Re_l = \frac{v\ l}{\nu} \qquad Pr = \frac{C_p \mu}{\kappa}. \tag{E-5}$$

All physical properties of the gas phase (C_p, κ, μ and ν) are calculated at the film temperature (average of T_{air} and T_p).